

**ANALYSIS OF MICE CARRYING HUMAN *GMAO1* MUTATIONS AS A MODEL TO STUDY  
ASSOCIATED MOVEMENT DISORDERS**

By

Cassandra Lynn Larrivee

A THESIS

Submitted to  
Michigan State University  
in partial fulfillment of the requirements  
for the degree of

Comparative Medicine and Integrative Biology—Master of Science

2019

## ABSTRACT

### ANALYSIS OF MICE CARRYING HUMAN *GNAO1* MUTATIONS AS A MODEL TO STUDY ASSOCIATED MOVEMENT DISORDERS

By

Cassandra Lynn Larrivee

Due to the increased availability of genetic screening, patients with idiopathic epilepsy and movement disorders are being identified with mutations in the *GNAO1* gene. The *GNAO1* gene encodes a heterotrimeric G protein subunit,  $G\alpha_o$ , abundantly found within the brain. Patients with *de novo* mutations in *GNAO1* specifically may have early onset seizure disorders and/or involuntary movements. These two phenotypes were later classified as early infantile epileptic encephalopathy (EIEE17) and neurodevelopmental delay with involuntary movements (NEDIM) respectively. Previous work in our lab uncovered a pattern between the *in vitro* function of mutations and the type of disorder observed in patients. Loss-of-function mutations associated with EIEE17 while gain-of-function mutations or proteins with essentially normal function were seen in NEDIM. To determine whether this pattern could be replicated *in vivo*, heterozygous mutant mice were created using CRISPR/Cas9. Here we report the first mouse models of *GNAO1* disorders, *Gnao1*<sup>+/*G203R*</sup> and *Gnao1*<sup>+/*R209H*</sup>. Using a variety of behavioral battery tests including open field, rotarod and digigait, we were able to show distinct behavioral patterns between the mutant mice. Using these models we began to explore preclinical drug repurposing and neural mechanisms.

## ACKNOWLEDGEMENTS

I had a wonderful mentor in Dr. Richard Neubig, for whom I owe my deepest appreciation. His guidance was supportive, inspiring and ever-present. He always encouraged and challenged me to think past my limits, making me a stronger scientist.

This project was made possible in large part to Huijie Feng and Jefferey Leipprandt; However, all the members of Neubig lab at one point or another helped me on my way. To all of you – thank you.

Thanks to Dr. Nara Parameswaran, Dr. Brian Schutte, and Dr. Florian Kagerer each of whom served as my professors and as my committee members. Their expertise challenged me and extended my own knowledge base. Their input was invaluable and essential to this project and my own academics.

Within my department of Comparative Medicine and Integrative Biology, Dr. Vilma Yuzbasiyan-Gurkan and Dimity Palazzola supported and aided me every step of the way. They were an anchor during my time in graduate school, I always knew I had a team of amazing women on my side.

## TABLE OF CONTENTS

LIST OF TABLES.....	v
LIST OF FIGURES.....	vi
KEY TO ABBREVIATIONS.....	viii
CHAPTER 1: INTRODUCTION.....	1
Background of GNAO1 research .....	2
EIEE17 .....	6
NEDIM.....	7
Genetics of GNAO1 .....	8
Statement of Purpose.....	9
CHAPTER 2: MOUSE MODELS OF <i>GNAO1</i> -ASSOCIATED MOVEMENT DISORDER: ALLELE- AND SEX-SPECIFIC DIFFERENCES IN PHENOTYPES .....	11
Statement of Contribution.....	12
Abstract.....	13
Introduction .....	15
Materials and Methods.....	18
Results.....	29
Discussion .....	43
CHAPTER 3: BEHAVIORAL ASSESSMENT OF MICE WITH A COMMON GNAO1 MOVEMENT DISORDER VARIANT R209H .....	48
Statement of Contribution.....	49
Abstract.....	50
Introduction .....	51
Materials and Methods.....	54
Results.....	63
Discussion .....	74
CHAPTER 4: CONCLUSIONS AND FUTURE DIRECTIONS .....	77
APPENDICES.....	81
APPENDIX A: Chapter 2.....	82
APPENDIX B: Chapter 3.....	94
REFERENCES .....	96

## LIST OF TABLES

Table 2-1. Location, sequence and genotyping of gRNA targets in <i>Gnao1</i> locus.....	20
Table 2-2. Scoring scale for postural and motor abnormalities .....	25
Table 2-3. GNAO1 G203R patient classification .....	40
Table 3-1. Location and sequence of gRNA and ssODN template for CRISPR-Cas targeting <i>Gnao1</i> locus; primers and genotyping method for <i>Gnao1</i> <sup>+/R209H</sup> mice .....	55
Table 3-2. GNAO1 R209H patient classification .....	71
Supplemental Table 2-1. Gait analysis parameters Male <i>Gnao1</i> G203R mutants.....	88
Supplemental Table 2-2. Gait analysis parameters Female <i>Gnao1</i> G203R mutants .....	89
Supplemental Table 2-3. Gait analysis parameters Male <i>Gnao1</i> G184S mutants .....	90
Supplemental Table 2-4. Gait analysis parameters Female <i>Gnao1</i> G184S mutants.....	91
Supplemental Table 2-5. Benchmarking off-target list for <i>Gnao1</i> G203 gRNA .....	92

## LIST OF FIGURES

Figure 1-1. Functions of $G\alpha_o$ protein.....	3
Figure 1-2. Conformational changes of GPCR.....	4
Figure 1-3. GNAO1 allelic variants .....	5
Figure 2-1. Development of $Gnao1^{+/G203R}$ mouse model .....	19
Figure 2-2. The timeline for utilizing animals in this study .....	22
Figure 2-3. Female $Gnao1^{+/G184S}$ mice and male $Gnao1^{+/G203R}$ mice show reduced time on RotaRod and reduced grip strength.....	31
Figure 2-4. $G184S$ mutant mice showed reduced activities in Open Field Test but $G203R$ mutants do not .....	33
Figure 2-5. DigiGait Imaging System reveals sex-specific gait abnormalities in $Gnao1^{+/G184S}$ mice and $Gnao1^{+/G203R}$ mice.....	36
Figure 2-6. $Gnao1^{+/G203R}$ male mice have an enhanced Pentylentetrazol (PTZ) Kindling response .....	38
Figure 2-7. Induction of abnormal movements and postures by oxotremorine .....	39
Figure 2-8. Treatment with trihexyphenidyl on $Gnao1^{+/G203R}$ mice .....	41
Figure 2-9. Brain neurotransmitter analysis of $Gnao1^{+/G203R}$ mice .....	42
Figure 3-1. Targeting of the mouse $Gnao1$ locus.....	55
Figure 3-2. $Gnao1^{+/R209H}$ exhibited a developmental delay during the negative geotaxis assessment .....	64
Figure 3-3. $Gnao1^{+/R209H}$ shows significant hyperactivity and reduced time in center in the open field arena .....	66
Figure 3-4. Male and Female $Gnao1^{+/R209H}$ mice shows gait abnormalities in different tests on the DigiGait imaging system .....	68

Figure 3-5. *Gnao1*<sup>+/R209H</sup> mice do not have an enhanced Pentylentetrazol (PTZ) kindling response ..... 69

Figure 3-6. Risperidone treatments decreases hyperkinetic movements in *Gnao1*<sup>+/R209H</sup> ..... 72

Figure 3-7. Western blot shows no statistical difference in Gα<sub>o</sub> protein between *Gnao1*<sup>+/R209H</sup> and WT mice ..... 73

Supplemental Figure 2-1. RotaRod test was conducted with 5 training sessions and 1 test session over two consecutive days..... 83

Supplemental Figure 2-2. Time spent at the center in the Open Field Tests ..... 84

Supplemental Figure 2-3. RotaRod learning curve was collected in 10 consecutive tests with a 5-min break between each test ..... 85

Supplemental Figure 2-4. False discovery rate (FDR) calculation probed through all the parameters given by DigiGait in *Gnao1*<sup>+G184S</sup> mice ..... 86

Supplemental Figure 2-5. False discovery rate (FDR) calculation probed through all the parameters given by DigiGait in *Gnao1*<sup>+G203R</sup> mice ..... 87

Supplemental Figure 2-6. GABA and glutamate show no significant differences between *Gnao1*<sup>+/R209H</sup> and wildtype littermates..... 93

Supplemental Figure 3-1. WT and *Gnao1*<sup>+/R209H</sup> mice show no difference in percent suppression of locomotion after oxotremorine treatment ..... 95

## KEY TO ABBREVIATIONS

5-HT 5-Hydroxytryptamine

AC Adenylyl Cyclase

cAMP Cyclic adenosine monophosphate

DA Dopamine

DSB Double strand DNA break

EEG Electroencephalogram

EIEE17 Early infantile epileptic encephalopathy

GABA Gamma-Aminobutyric acid

GDP Guanine diphosphate

GNAO1 Guanine nucleotide-binding protein, alpha-activating activity polypeptide O

GOF Gain-of-function

GPCR G-protein coupled receptor

GTP guanine triphosphate

GWAS Genome wide association studies

HET Heterozygous

HPLC High performance liquid chromatography

LOF Loss-of-function

NE Norepinephrine

NEDIM Neurodevelopmental disorder with involuntary movements

OXO Oxotremorine

PAM Protospacer adjacent motif

PTX pertussis toxin

PTZ Pentylenetetrazol

RGS regulators of g-proteins

ssODN Single stranded oligodeoxynucleotide

THP Trihexyphenidyl

WT Wildtype

## CHAPTER 1: INTRODUCTION

## Background of *GNAO1* research

Two neurological conditions, epilepsy and movement disorders, have both been linked to mutations within the brain abundant protein  $G\alpha_o$  [1, 2]. The  $G\alpha_o$  protein belongs to the  $G_i/G_o$  subfamily of  $G\alpha$  proteins. Within the  $\alpha$  family there are roughly 21 subunits, and can be grouped by the  $G\alpha_{i/o}$  family as well as  $G\alpha_s$ ,  $G\alpha_{12/13}$  and  $G\alpha_q$ . Encoded by the *GNAO1* gene, the function of  $G\alpha_o$  is widely characterized by its inhibition of adenylyl cyclase preventing production cyclic adenosine monophosphate (cAMP) and its sensitivity to pertussis toxin (PTX).  $G\alpha_o$  was first identified in 1984 when researchers [3, 4] were looking to isolate  $G\alpha_i$  from the brain instead finding another inhibitory  $G\alpha$  protein, naming  $G\alpha_o$  for "other".

$G\alpha$  proteins are well known for their coupling to G-protein coupled receptors (GPCR) to aid in eliciting intercellular effects.  $G\alpha_o$  couples to a wide range of GPCRs including,  $GABA_B$  receptors,  $\alpha_2$ -adrenergic receptors, and  $D_2$  dopamine receptors. Activation of these receptors leads to a decrease in cAMP as mentioned above, through  $G\alpha_o$ . However,  $G\alpha_o$  signal transduction can also function to inhibit sodium and calcium ion channels, as well as activating potassium channels (Figure 1-1) [5, 6]. These functions lead to a decrease in neuronal excitability and allow receptors coupled to  $G\alpha_o$  to regulate release of neurotransmitters, as well as other functions.

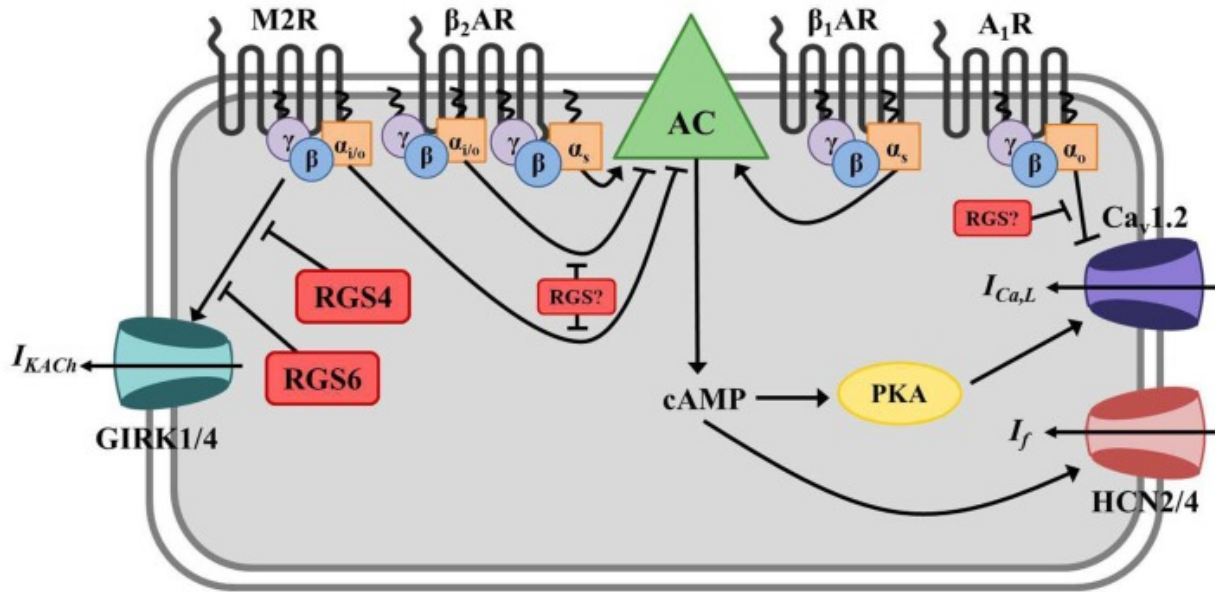


**Figure 1-1. Functions of  $G\alpha_o$  protein**  $G\alpha_o$  proteins canonically function to inhibit adenylyl cyclase in producing cAMP. The  $G\alpha_o$  and  $\beta\gamma$  dimer the associated by dimer complex also can also activate potassium channels and inhibit activation of calcium channels. [7] (*reproduced with permission under the Creative Commons Attribution License*).

$G\alpha_o$  can only cause its effects in its active state when it is bound to guanine triphosphate (GTP). During basal conditions the  $G\alpha$  subunit is bound to guanine diphosphate (GDP), and to a  $\beta\gamma$  dimer, composing the heterotrimeric G-protein. After receptor activation when  $G\alpha$  proteins are bound to GTP, it continues signal transduction, but once GTP is hydrolyzed back to GDP, the receptor is inactivated. This can happen spontaneously through intrinsic activity of the  $G\alpha$  protein or by specialized GTP accelerating proteins (GAPs) known as regulators of G-proteins (RGS). RGS proteins can bind to  $G\alpha$  proteins, stimulate GTP hydrolysis to GDP which will cause inactivation and the re-association of the  $G\alpha$  to the  $\beta\gamma$  dimer (Figure 1-2).

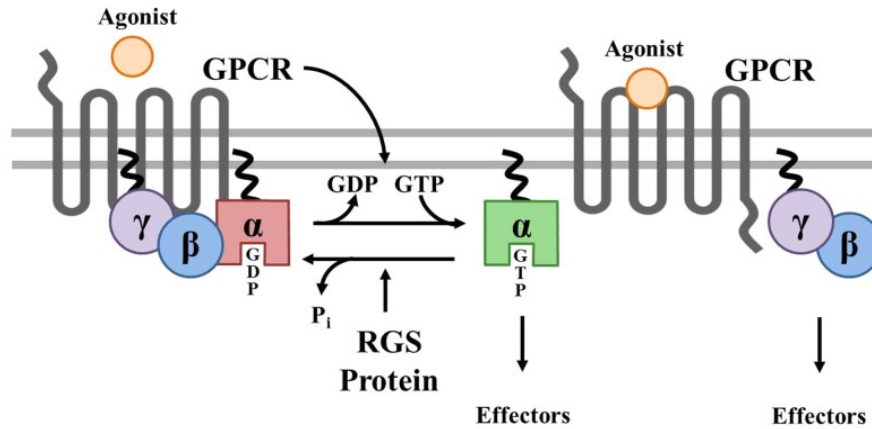


**Figure 1-2. Conformational changes of GPCR** Activation of GPCR cause conformational change of the heterotrimeric G-protein. The  $\alpha$  protein dissociates from the  $\beta\gamma$  dimer, both subunits can then bring about effector functions until GTP is hydrolyzed to GDP by either intrinsic GTPase activity or by RGS proteins. [7] (reproduced with permission under the Creative Commons Attribution License).

To assess the role of  $G\alpha_o$ , early studies mutated  $G\alpha$  proteins with a G184S point mutation which rendered  $G\alpha_o$  insensitive to RGS proteins causing prolonged activation [8, 9]. After 2013, Nakamura et. al established a link between *GNAO1* and cases of early onset epilepsy[10] researchers realized their G184S GOF mouse model could be used to study *GNAO1* associated disorders including early infantile epileptic encephalopathy (EIEE17). Consistent with patient symptomology they were able to show heterozygous G184S mice were more sensitized to pentylenetetrazol (PTZ) kindling studies [11]. PTZ is a  $GABA_A$  agonist, and in high doses it can cause a convulsion but in lower frequent doses it causes an electrophysiological change in the brain decreasing the threshold of excitability, making it a model for epileptogenesis [12]. While the *Gnao1*<sup>+/G184S</sup> mouse model showed kindling sensitivity correlative with the epilepsy observed in patients, this specific *GNAO1* G184S variant has not been seen any patients, which is why recent research has focused specifically on patient variant models.

In the past five years the number of pathological variants within *GNAO1* have accumulated, to date there are 78 published cases[13-16] and 34 different variants (Figure 1-1.) While the variants were initially identified in children with early onset epilepsy[10] further reports discussed presence of developmental delay and movement disorders[17, 18] expanding the phenotype of *GNAO1* mutations. It was later uncovered that certain variants more commonly associated to epilepsy while others linked to movement disorders[19]. This was largely dependent on functionality of the *GNAO1* protein  $G\alpha_o$ .

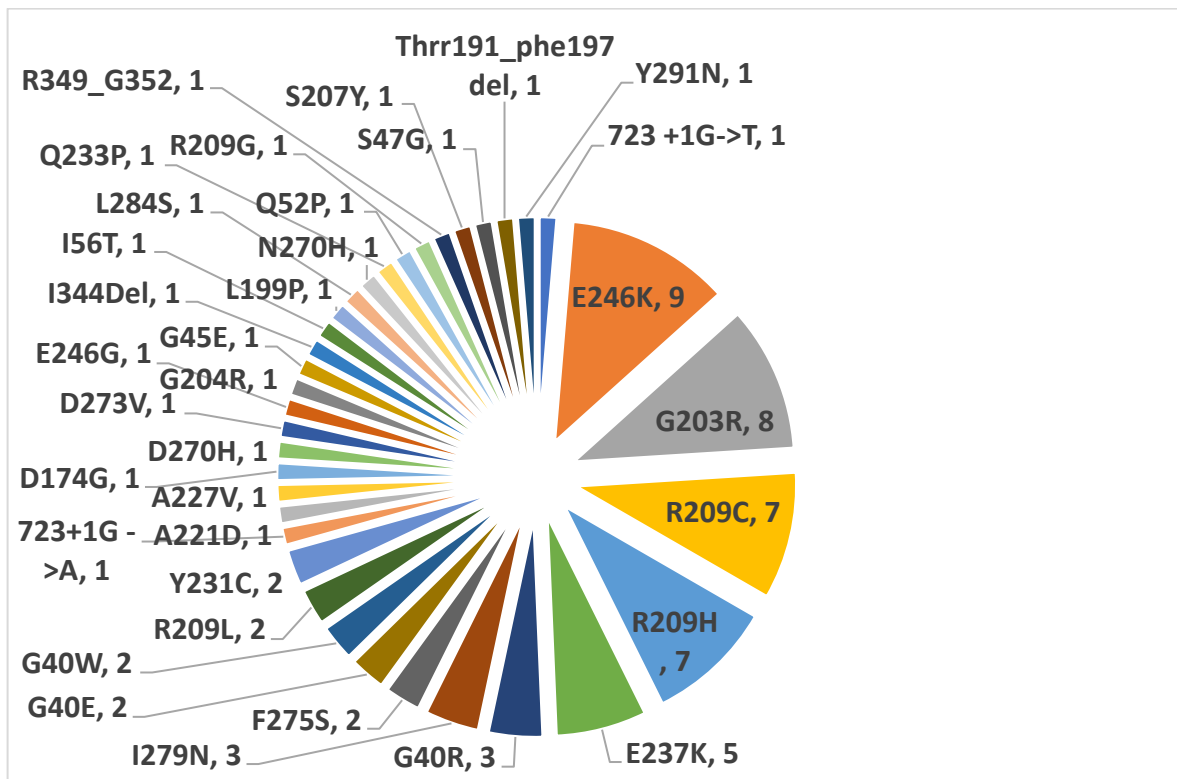


**Figure 1-3. *GNAO1* allelic variants** To date there are 34 different causative variants that have been found within *GNAO1*. Many of the variants occur infrequently, presenting in only one or two patients, a few of the variants are found more frequently. Some of the mutation hotspots include; E246K, G203R, R209 (C,H) and E237K.

## EIEE17

Epilepsy is the one of the common neurological conditions in the United States [20], characterized by multiple unpredictable seizures that may or may not be visible through electrical recording of the brain. Severity and types of seizures range between cases. Early infantile epileptic encephalopathy is a severe form of epilepsy categorized by tonic seizures that occur early in life, with the presence of observable EEG abnormalities. There is a wide range of genetic heterogeneity within EIEE, with over 50 different associated etiologies [21]. While many of the associated genes are only linked with the epilepsy syndrome, mutations in a few causative genes, including *GNAO1*, give rise to multiple syndromes. The *CACNA1A* gene, which encodes a subunit of a voltage gated P-type calcium channel, not only causes EIEE but is also linked to ataxia, a motor disorder characterized by spells of imbalance and a loss in coordination [22]. Possibly not surprising is that the regulation of P-type voltage gated calcium channels is also a role of  $G\alpha_o$  proteins[6]. As calcium plays a vital role in the release of neurotransmitters and mutations in both genes cause epilepsy and a movement disorder it is likely that a causative mechanism behind one or both of the phenotypes is neurotransmitter release.

Large scale sequencing efforts in patients with epilepsy have identified several other mutations within *GNAO1*. Cell based assays then classified the known mutations in terms of  $G\alpha_o$  protein ability to inhibit cAMP through adenylyl cyclase [19]. They found a correlation that those mutations with a decreased amount of cAMP inhibition, classified as a loss-of-function (LOF) mutations, were more commonly seen in patients with EIEE17. They also showed that mutations

with an increased amount of cAMP inhibition, gain-of-function (GOF) mutations, associated with the patients who had neurodevelopmental disorder with involuntary movements (NEDIM) [19].

## NEDIM

While some patients present with both epilepsy and movement disorders [17] those with mutations classified as GOF more commonly presented with neurodevelopmental disorder with involuntary movements (NEDIM). In addition to the presentation of involuntary movement disorders, patients with *GNAO1* mutations also present with hypotonia – low muscle tone -- and developmental delay [23]. This consistent grouping of symptoms in *GNAO1* patients is what lead to the classification of NEDIM. While NEDIM is a blanket name for presence the of movement disorders, there are more detailed clinical profiles of the movement abnormalities displayed in patients. Commonly seen disorders include chorea, athetosis, dystonia and dyskinesias [24]. Each of which explain a specific type of involuntary movement. From the Greek word for “dance” chorea is classified by brief and abrupt movements that seem to flow between body parts. Athetosis involves slow involuntary writhing movements. Dystonia involves sustained muscle contractions that can lead to repetitive or twisting movements. However, diagnosing movement disorders is quite complex as they often present together or with other comorbidities, such as epilepsy. Making genetic analysis an invaluable tool for determining etiologies.

The *GNAO1* GOF correlation with NEDIM is consistent with other rare monogenic disorders that disrupt cAMP. For example, a mutation in the gene that encodes an adenylyl cyclase, *ADCY5*, has been linked to dyskinesia. Mutations in *ADCY5* have also been found to

increase cAMP [25], similar to GOF mutations in GNAO1. Mutations in *GPR88*, and *GNAL* are also genes involved in regulation of cAMP that cause movement disorders [26].

Movement is largely controlled by areas of the brain including the basal ganglia and the cerebellum, motor pathways largely involve the synaptic transition between these areas of the brain and the cortex. As  $G\alpha_o$  is widely abundant in these regions [1] it is likely these regions may be mechanistically important within the pathophysiology of GNAO1 associated movement disorders.

### **Genetics of *GNAO1***

There are now roughly 35 published variants of GNAO1, most of which are *de novo* missense mutations. While many of the mutations only have been found in one or two patients, there are a few mutational hotspots, these include G203R, R209C, and R209H (Figure 1-1). The high frequency of Arg<sup>209</sup> mutations (R209C and R209H) and G203R are not surprising when we look at the specific base changes and the surrounding sequence. R209C and R209H mutations are due to 625 cytosine to thymine transitions (C >T) and 626 guanine to adenine (G > A) transitions respectively. The genetic sequence at these sites show a cytosine followed by a guanine (CpG dinucleotide). It is well known that sequences that mutate at a higher rate are CpG dinucleotides because cytosine is vulnerable to methylation and subsequent deamination resulting in a transitional mutation of C >T [27]. In the case of R209H mutation it is the complementary strand transition from C >T, which will result in a G -T mismatch at site 626 of *GNAO1*. DNA repair mechanisms will then change the guanine to an adenine resulting in the G>A

transition we observe in the R209H mutation. The G203R base change is a c. 607 G >A, at position at 606 is a cytosine, therefore we again observe another CpG dinucleotide.

Moreover, DNA methylation has also been linked to other neurological conditions such as Huntington's, and Rett syndrome [28] both of which have phenotypic similarities to GNAO1. All of the *GNAO1* mutations are *de novo*, implying a germ cell (sperm or egg) mutation in one of the parents. Research has found a link between *de novo* mutations and age of fathers, possibly due to the fact that sperm cells generate high levels of mutation [29-31]. While such correlations may not be directly useful to treatments as CpG mutations may not be preventable, research is being done on possible epigenetic therapies such as preventing DNA demethylation [28, 32]. Further, this information might be useful for parents of patients with GNAO1 mutations considering having more children. *De novo* mutations in general are not preventable, however, it is possible to test for germ-cell mutations within sperm cells themselves. Therefore, fathers who have a child with a *GNAO1* mutation might consider genetic testing to assess for possible germ-line mutations that could be passed onto to any future offspring.

### **Statement of Purpose**

Clinically, scientists and physicians are able to correlate the presence of EIEE17 and NEDIM with mutations in the *GNAO1* gene. While we are starting to understand the etiology, quality of life for these patients is still quite low. Both seizure disorders and involuntary movements are difficult to control and impair daily tasks. While there are a wide variety of therapeutic options, patients must try many different agents before they show some

improvement, many still do not have their symptoms completely under control [24, 33]. The work in this thesis looks primarily at the use of animal models as a means to understand the *GNAO1* mutations. Using the phenotype-genotype correlation we begin to assess different variants in a CRISPR/Cas9 mouse model to assess their predictive nature. From there this work is able to study the models and assess outcome to pharmacological treatments in an allele-specific personalized medicine approach.

**CHAPTER 2: MOUSE MODELS OF *GNAO1*-ASSOCIATED MOVEMENT DISORDER: ALLELE- AND SEX-SPECIFIC DIFFERENCES IN PHENOTYPES**

Reprinted and adapted with permission under the Creative Commons Attribution License

## Statement of Contribution

My role in the following chapter first published in PLoS ONE on 2019 January 25 was the following. I planned, performed and analyzed, open field, and rotarod studies for both of the *Gnao1*<sup>+/*G184S*</sup> and *Gnao1*<sup>+/*G203R*</sup> animal models. I performed all initial data analysis for these experiments and wrote up my experimental protocols that would be used in writing the paper. I also performed some additional experiments that were not in the initial publication. These include; neurotransmitter analysis and testing the effects of oxotremorine and trihexyphenidyl on the *Gnao1*<sup>+/*G203R*</sup> model. The didigait, grip strength and kindling studies were done by Huijie Feng. Genotyping and breeding of mice was done by Jefferey Leipprandt. Elena Demireva and Huirong Xie at the MSU transgenic core generated the mutant mouse models with CRISPR/cas9 technology.

## Abstract

Infants and children with dominant *de novo* mutations in *GNAO1* exhibit movement disorders, epilepsy, or both. Children with loss-of-function (LOF) mutations exhibit Epileptiform Encephalopathy 17 (EIEE17). Gain-of-function (GOF) mutations or those with normal function are found in patients with Neurodevelopmental Disorder with Involuntary Movements (NEDIM). There is no animal model with a human mutant *GNAO1* allele.

Here we develop a mouse model carrying a human *GNAO1* mutation (G203R) and determine whether the clinical features of patients with this *GNAO1* mutation, which includes both epilepsy and movement disorder, would be evident in the mouse model.

A mouse *Gnao1* knock-in GOF mutation (G203R) was created by CRISPR/Cas9 methods. The resulting offspring and littermate controls were subjected to a battery of behavioral tests. A previously reported GOF mutant mouse knock-in (*Gnao1*<sup>+/<sup>G184S</sup></sup>), which has not been found in patients, was also studied for comparison. We also tested the effects of multiple pharmacologic agents on the *Gnao1*<sup>+/<sup>G203R</sup></sup> mouse model.

*Gnao1*<sup>+/<sup>G203R</sup></sup> mutant mice are viable and gain weight comparably to controls. Homozygotes are non-viable. Grip strength was decreased in both males and females. Male *Gnao1*<sup>+/<sup>G203R</sup></sup> mice were strongly affected in movement assays (RotaRod and DigiGait) while females were not. Male *Gnao1*<sup>+/<sup>G203R</sup></sup> mice also showed enhanced seizure propensity in the pentylenetetrazole kindling test. Movement phenotype in the *Gnao1*<sup>+/<sup>G203R</sup></sup> model was exacerbated after administration of oxotremorine, a cholinergic agonist. However, treatment with a cholinergic antagonist did not alleviate motor impairment. Mice with a G184S GOF knock-

in also showed movement-related behavioral phenotypes but females were more strongly affected than males.

*Gnao1*<sup>+/G203R</sup> mice phenocopy children with heterozygous *GNAO1* G203R mutations, showing both movement disorder and a relatively mild epilepsy pattern. This mouse model should be useful in mechanistic and preclinical studies of *GNAO1*-related movement disorders.

## Introduction

Neurodevelopmental Disorder with Involuntary Movements (NEDIM) is a newly defined neurological disorder associated with mutations in *GNAO1*. It is characterized by “hypotonia, delayed psychomotor development, and infantile or childhood onset of hyperkinetic involuntary movements” (OMIM 617493). NEDIM is monogenetic and associated with GOF mutations in *GNAO1* [19]. The *GNAO1* gene has also been associated with early infantile epileptic encephalopathy 17 (EIEE17; OMIM 615473). However, 36% of patients showed both epilepsy and movement disorder phenotypes (G40R, G45R, S47G, I56T, T191\_F197del, L199P, G203R, R209C, A227V, Y231C and E246G) [34].

*GNAO1* encodes  $G\alpha_o$ , the most abundant membrane protein in the mammalian central nervous system[35].  $G\alpha_o$  is the  $\alpha$ -subunit of the  $G_o$  protein, a member of the  $G_{i/o}$  family of heterotrimeric G proteins.  $G_{i/o}$  proteins couple to many important G protein-coupled-receptors (GPCRs) involved in movement control like GABA<sub>B</sub>, dopamine D<sub>2</sub>, adenosine A<sub>1</sub> and adrenergic  $\alpha_{2A}$  receptor [35-38]. Upon activation,  $G\alpha_o$  and  $G\beta\gamma$  separate from each other and modulate separate downstream signaling pathways.  $G\alpha_o$  mediates inhibition of cyclic AMP (cAMP), and  $G\beta\gamma$  mediates inhibition of cAMP and N-type calcium channels and activation of G-protein activated inward rectifying potassium channels (GIRK channels)[36].  $G_o$  is expressed mainly in the central nervous system and it regulates neurotransmitter release by modulating intracellular calcium concentrations in pre-synaptic cells [37]. It has also been suggested that  $G_o$  plays a role in neurodevelopmental processes like neurite outgrowth and axon guidance [38, 39].

Consequently,  $G_o$  is an important modulator of neurological functions. In this report we began to assess differences in neurotransmitter levels within the brains of *Gnao1*<sup>+/G203R</sup> mice.

Previously, we defined a functional genotype-phenotype correlation for *GNAO1* [19]. GOF mutations are found in patients with movement disorders, while loss-of-function (LOF) mutations are associated with epilepsy [19]. An updated mechanistic review of this genotype-phenotype correlation was recently published [34]. The experimental study of mutant alleles, however, was done with human *GNAO1* mutations expressed in HET293T cells, which lack a complex physiological content. Therefore, it would be important to see whether mouse models with *GNAO1* mutations would share clinical characteristics of the human patients. Such a result would verify the previously reported genotype-phenotype correlation and would provide a preclinical testing model for possible new therapeutics. Previously, we studied heterozygous *Gnao1*<sup>+/G184S</sup> mice carrying a human-engineered GOF mutation (G184S). This mutation blocks the binding of the regulation of G protein signaling (RGS) proteins and results in GOF [8, 40]. Those mice showed heightened sensitization to pentylenetetrazol (PTZ) kindling and had an elevated frequency of interictal epileptiform discharges on EEG [41]. In this report, we tested whether the *Gnao1*<sup>+/G184S</sup> mice also exhibit movement disorders. The G184S is a GOF mutation but has not been found in human.

G203R is a GOF mutation that is one of the more common *GNAO1* mutations found clinically [10, 17, 33, 42, 43]. Most patients with this mutation exhibit both seizures and movement disorders [10, 17, 33, 42, 43]. We wanted to develop a mouse model with that mutation (*Gnao1*<sup>+/G203R</sup>) to see if it replicated the clinical phenotype of *GNAO1* G203R-associated

neurological disorders. If so, it would be a valuable tool to understand neural mechanisms underlying the complex phenotypic spectrum of patients with *GNAO1* mutations.

In this report, we show that mice carrying two  $G\alpha_o$  GOF mutations *Gnao1*<sup>+/<sup>G203R</sup> and *Gnao1*<sup>+/<sup>G184S have sex-specific motor impairment and seizures. We show that motor impairment can be extenuated with a nonselective cholinergic agonist. These two mouse models present the possibility of studying *GNAO1*-associated neurological defects in animal models.</sup></sup></sup>

## Materials and Methods

### ***Animals***

Animal studies were performed in accordance with the Guide for the Care and Use of Laboratory Animals established by the National Institutes of Health. All experimental protocols and personnel were approved and trained by the Michigan State University Institutional Animal Care and Use Committee. Mice were housed on a 12-h light/dark cycle and had free access to food and water. They were studied between 8-12 weeks old.

### ***Generation of *Gnao1* mutant mice***

*Gnao1*<sup>+/*G184S*</sup> mutant mice were generated as previously described [8, 9, 11, 19] and used as N10 or greater backcross on the C57BL/6J background.

*Gnao1*<sup>*G203R*</sup> mutant mice were generated using CRISPR/Cas9 genome editing on the C57BL/6NCrl strain. gRNA targets within exon 6 of the *Gnao1* locus (ENSMUSG00000031748) were used to generate the G203R mutation (Fig 2-1A). Synthetic single-stranded DNA oligonucleotides (ssODN) were used as repair templates carrying the desired mutation and short homology arms (Table 2-1). CRISPR reagents were delivered as ribonucleoprotein (RNP) complexes. RNPs were assembled in vitro using wild-type *S.p.* Cas9 Nuclease 3NLS protein, and synthetic tracrRNA and crRNA (Integrated DNA Technologies, Inc.). TracrRNA and crRNA were denatured at 95°C for 5 min and cooled to room temperature in order to form RNA hybrids, which were incubated with Cas9 protein for 5 min at 37°C. RNPs and ssODN templates were electroporated into C57BL/6NCrl zygotes as described previously [44], using a Genome Editor

electroporator (GEB15, BEX CO, LTD). C57BL/6NCRl embryos were implanted into pseudo-pregnant foster dams. Founders were genotyped by PCR (Table 2-1) followed by T7 endonuclease I assay (M0302, New England BioLabs) and validated by Sanger sequencing.

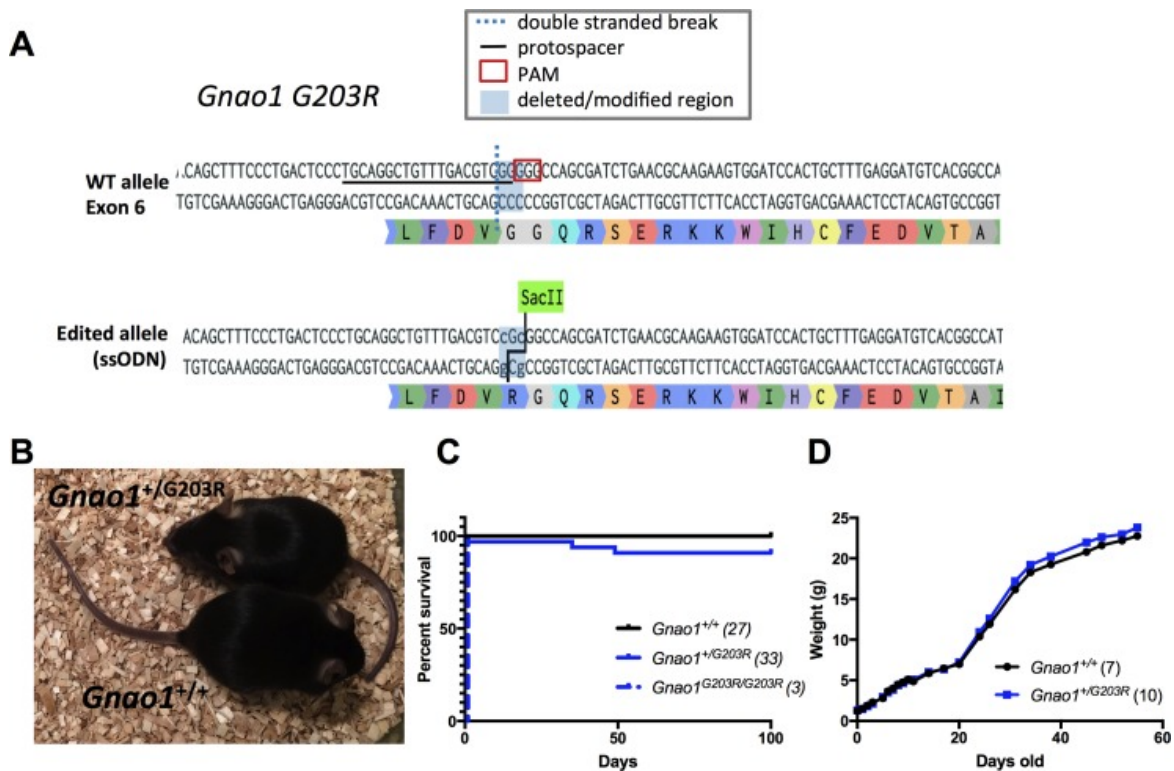


**Figure 2-1. Development of *Gnao1*<sup>+/G203R</sup> mouse model** (A) Targeting of the *Gnao1* locus. The location of the gRNA target protospacer and the PAM, and double stranded breaks following Cas9 cleavage are indicated on the WT allele. Deleted or modified sequences are highlighted in blue. The resulting edited allele sequence and translation are presented along with the sequences used as references for ssODN synthesis. (B) Heterozygous *Gnao1*<sup>+/G203R</sup> mutant mice are largely normal in size and behavior. Photo comparing mutant mouse with its littermate control is shown. (C) *Gnao1*<sup>+/G203R</sup> mice have a relatively normal survival; while homozygous *Gnao1*<sup>G203R/G203R</sup> mice die perinatally (P0-P1). (D) *Gnao1*<sup>+/G203R</sup> mice develop normally and gain weight similarly to their WT littermate controls.

**Table 2-1. Location, sequence and genotyping of gRNA targets in *Gnao1* locus**

<i>Gnao1</i> G203R	
DSB location	chr 8: 93,950,314
gRNA target	5' TGCAGGCTGTTTGACGTCGG GGG 3' (+)
ssODN	5' ATGGCCGTGACATCCTCAAAGCAGTGGATCCAC TTCTTGCGTTCAGATCGCTGGCC <b>GCG</b> GACGTCAAA CAGTTTGCAGGGAGTCAGGGAAAGCTGT 3'
PCR primers	Fwd: 5' GACAGGTGTCACAGGGGATG 3' Rev: 5' TCCTAGCCAAGACCCCAACT 3' PCR product = 462bp
Genotyping	SacII site created by G203R mutation

The likelihood of an off-target site being edited is very low. Based on the number and position of mismatches, several predictive algorithms were used to assign guide specificity scores from 0 to 100 (100=best) to rank gRNAs by specificity with respect to off-target modifications occurring [45-47]. The gRNA target used for this experiment has a specificity score of 94, which is the highest seen in over 40 similar targeting experiments done by the MSU Transgenic and Genomic Editing Facility. This greatly reduces the probability of off-target edits. After examining the off-target lists (S5 Table), we did not identify any off-target loci with less than 3 mismatches or with an off-target binding score > 0.5 which we deem as thresholds for further validation. We also did not identify any off-target loci with significant scores that were on the same chromosome and would be less likely to be removed from the genome after breeding of several generations. Furthermore, the RNP (ribonucleoprotein) approach that we employed to deliver CRISPR reagents to mouse embryos further lowers the risk of off-target events [48].

Nevertheless, we directly validated several predicted off-target loci for the G203 gRNA target (TGCAGGCTGTTTGACGTCGG GGG) that occur within coding regions. One potential off-target site

with 4 mismatches and a score of 0.52 was validated for locus ENSMUSG00000041390. We also analyzed two other off-target candidates with 4 mismatches ENSMUSG00000086805 and ENSMUSG00000097637 and scores of 0.15 and 0.069 respectively. They were predicted to occur on the same chromosome (chr 8) as *Gnao1*. To test these 3 off-target candidates, DNA from WT and founder animals was analyzed by PCR and sequencing and we found that no off-target effects had occurred for all 3 off-target loci analyzed (see Supplemental Materials).

gRNA target – 20bp protospacer and PAM sequences are listed, strand orientation indicated by (+) or (-). Sequence of ssODN used as repair template is listed. For G203R, mutated codon is highlighted in bold. DSB – double stranded break. PAM – protospacer adjacent motif.

### **Genotyping and Breeding**

Heterozygous *Gnao1*<sup>+/G203R</sup> mutant founder mice were crossed against C57BL/6J mice to generate *Gnao1*<sup>+/G203R</sup> heterozygotes (N1 backcross). Further breeding was done to produce N2 backcross heterozygotes while male and female N1 heterozygotes were crossed to produce homozygous *Gnao1*<sup>G203R/G203R</sup> mutants. Studies were done on N1 or N2 G203R heterozygotes with comparisons to littermate controls.

All mice had ears clipped before weaning. DNA was extracted from earclips by an alkaline lysis method [49]. The G203R allele of  $G\alpha_o$  was identified by Sac II digests (wt 462 Bp and G203R 320 & 140Bp) of genomic PCR products generated with primers (Fwd 5' GACAGGTGTCACAGGGGATG 3'; Rev 5' TCCTAGCCAAGACCCCAACT 3'). Reaction conditions were: 0.8µl template, 4µl 5x Promega PCR buffer, 0.4µl 10mM dNTPs, 1µl 10µM Forward Primer, 1µl 10µM Reverse Primer, 0.2µl Promega GoTaq and 12.6 µl DNase free water (Promega catalog #

M3005, Madison WI). Samples were denatured for 4 minutes at 95 °C then underwent 32 cycles of PCR (95 °C for 30 seconds, 60°C for 30 seconds, and 72 °C for 30 seconds) followed by a final extension (7 minutes at 72°C). After PCR, samples were incubated with Sac II restriction enzyme for 2 hrs.

### **Behavioral Studies**

Researchers conducting behavioral experiments were blinded until the data analysis was completed. Before each experiment, mice were acclimated in the testing room for at least 10 min. The timeline of behavioral protocols is described in Figure 2-2. Two female experimenters conducted all behavioral studies.

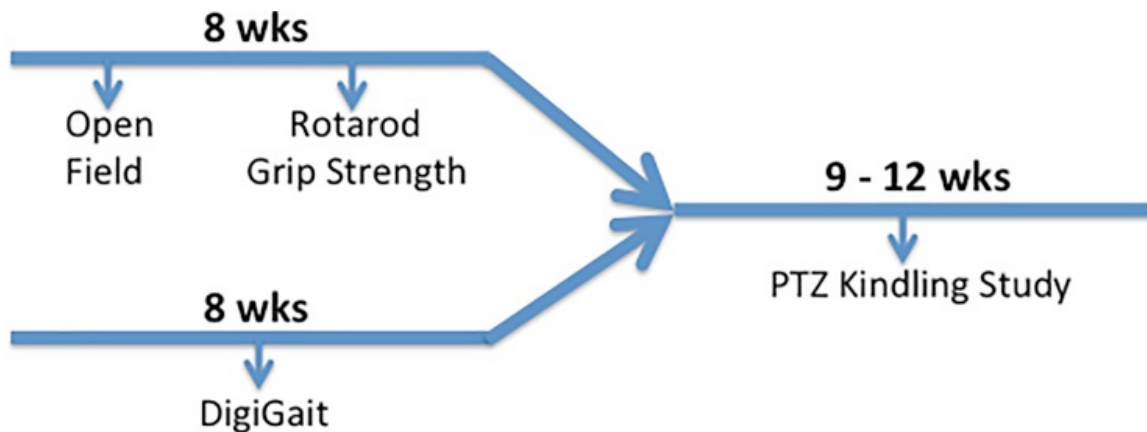


**Figure 2-2. The timeline for utilizing animals in this study** Open field, Rotarod and Grip strength tests were performed on the same group of 8-week-old animals in this as showed above. DigiGait tests were done on naïve 8-week-old animals. After completion of the motor behavior studies, animals were used for the PTZ kindling study.

### ***Open Field***

The Open Field test was conducted in a Fusion VersaMax 42 cm x 42 cm x 30 cm arenas (Omnitech Electronics, Inc., Columbus, OH). Mice and their littermate controls were placed in the arena for 30 minutes to observe spontaneous activities. Using the Fusion Software, distance traveled (cm) was evaluated for novel (first 10 minutes), sustained (10-30 minutes), and total (0-30 minutes) activity. Center Time was also measured. Center Time was defined as the time spent in the center portion (20.32cm x 20.32cm) of the Open Field cage.

### ***RotaRod***

Motor skills were assessed using an Economex accelerating RotaRod (Columbus Instruments, Columbus, OH). The entire training and testing protocol took two days. On day 1, mice were trained for three 2-minute sessions, with a 10-minute rest between each training period. During the first two sessions, the RotaRod was maintained at a constant speed of 5 rpm. In the third training session, the rod was started at 5 rpm and accelerated at 0.1 rpm/sec for 2 minutes. On day 2, mice were trained with two more accelerating sessions for 2 minutes each with a 10-minute break in between. The final test session was 5 minutes long, starting at 5 rpm then accelerating to 35 rpm (0.1 rpm/sec). For all training and test trials, the time to fall off the rod was recorded. RotaRod learning curves were done on a separate group of mice with 10 tests in one day with a 5-min rest between each test. The learning rate of each group of animals was calculated as described [50].

### ***Grip Strength***

Mouse grip strength data was collected following a protocol adapted from Deacon et al [51] using seven home-made weights (10, 18, 26, 34, 42, 49, 57 grams). Briefly, the mouse was held by the middle/base of the tail and lowered to grasp a weight. A total of three seconds was allowed for the mouse to hold the weight with its forepaws and to lift the weight until it was clear of the bench. Three trials were done starting with the 10 g weight to permit the mice to lift the weights with a 10-second rest between each trial. If the mouse successfully held a weight for 3 seconds, the next heavier weight was given; otherwise the maximum time/weight achieved was recorded. A final total score was calculated based on the heaviest weight the mouse was able to lift up and the time that it held it [51]. The final score was normalized to the body weight of each mouse, which was measured before the trial.

### ***DigiGait***

Mouse gait data were collected using a DigiGait Imaging System (Mouse Specifics, Inc., Framingham, MA) [52]. The test is used for assessment of locomotion as well as the integrity of the cerebellum and muscle tone/equilibrium [53]. Briefly, after acclimation, mice were allowed to walk on a motorized transparent treadmill belt. A high-speed video camera was mounted below to capture the paw prints on the belt. Each paw image was treated as a paw area and its position recorded relative to the belt. Seven speeds (18, 20, 22, 25, 28, 32 and 36 cm/s) were tested per animal with a 5-minute rest between each speed. An average of 4-6 s of video was saved for each mouse, which is sufficient for the analysis of gait behaviors in mice [53]. For each speed, left & right paws were averaged for each animal while fore and hind paws were evaluated

separately. Stride length was normalized to animal body length. We eliminated data points at speed 36 cm/s since many mice cannot run at that speed, which increased the variability.

**Tests of Oxotremorine on Motor Behavior**

Male 8-12 week old mice *Gnao1*<sup>+/*G203R*</sup> and *Gnao1*<sup>+/*+*</sup> littermates were allowed to habituate in the testing room for ten minutes. Mice were then treated with a single intraperitoneal (IP) dose of either 0.1mg/kg oxotremorine methiodide (Cayman Chemical) dissolved in DI water, or vehicle control. After twenty minutes they were evaluated for postural abnormalities every ten minutes using a scoring scale [54] (Table 2-2)

**Table 2-2. Scoring scale for postural and motor abnormalities**

Scoring scale
0. Normal Motor behavior
1. No gait changes, but slowed movement
2. Mild impairments: slow walk, occasional postural abnormalities
3. Moderate impairment: frequent abnormal postures, limited ambulation
4. Severe impairment: sustained abnormal postures with no ambulation or upright position

### ***Tests of Trihexyphenidyl Treatment***

We tested the effects of trihexyphenidyl treatment on *Gnao1*<sup>+/*G203R*</sup> mice using our rotarod protocol. Male 8-12 week old mice *Gnao1*<sup>+/*G203R*</sup> and *Gnao1*<sup>+/*+*</sup> littermates were allowed to habituate in the testing room for ten minutes. On day one, mice were trained on the accelerating rotarod as normal. On day two mice, were then treated with a single intraperitoneal (IP) dose of either 5 mg/kg or 10 mg/kg trihexyphenidyl (Cayman Chemical) dissolved in DI water, or vehicle control. Ten minutes following injection mice were tested using the day 2 rotarod protocol. The third test on day two was analyzed.

### ***PTZ Kindling Susceptibility***

A PTZ kindling protocol was performed as described before [11] to assess epileptogenesis. Briefly, PTZ (40 mg/kg, i.p. in 5 mg/ml) was administered every other day starting at 8 weeks of age. Mice were monitored and scored for 30 minutes for signs of behavioral seizures as described [11, 55, 56]. Kindling is defined as death or the onset of a tonic-clonic seizure on two consecutive treatment days. The number of injections for each mouse to reach the kindled state was reported in survival curves. This experiment lasted up to 4 weeks with a maximum of 12 doses. Each animal in the study was checked every day for health and seizure development.

Animals were humanely euthanized with CO<sub>2</sub> immediately after kindling or after 12 PTZ injections and observation. In total, 40 animals were used for this study, among which 27 died of tonic-clonic seizures and 13 were euthanized after 12 doses of PTZ injections.

### ***Brain Neurotransmitter Analysis***

*Gnao1*<sup>+/*G203R*</sup> Mice and their control littermates, ages 8-12 weeks old, were euthanized. Immediately following brain tissue was dissected and left hemisphere was collected, flash frozen until stored in -80 until samples were processed for HPLC.

### ***High-Performance Liquid Chromatography***

Measurements of monoamines was followed as described here [57]. Striatum and Cerebellum tissue was homogenized in 4 times volume of 0.1 M perchloric acid, centrifuged and then filtered through a 30 kDa tube. To analyze the filtrates, we used a HPLC system with a Coulochem III electrochemical detector set at -300 mV (Thermo Fisher Scientific; Waltham, MA, USA). Analytes were separated at 35°C on a HR-80 reverse-phase column (Thermo Fisher Scientific) with Cat-A-Phase II (Thermo Fisher Scientific), a mobile phase with a flow rate of 1.1 mL min<sup>-1</sup>. Standards were run every 5th sample to confirm peak location on the chromatogram. The limit of detection for NE, DA, DOPA was 0.1 ng mL<sup>-1</sup> for DA, and 0.5 ng mL<sup>-1</sup> for 5-HT. HPLC data are reported as the mean ± SEM monoamine content in each tissue normalized to initial weight of sample.

### ***Amino Acid Neurotransmitters***

Amino acids were measured as their OPA/BME derivatives according to [58, 59]. OPA/BME stock solutions were prepared by dissolving 27mg OPA in 1 mL methanol, then 5µl of BME and 9 mL tetraborate buffer were then added. To make the working OPA/BME derivatizing reagent 2.5mL of the stock OPA/BME derivatizing reagent was mixed with 7.5mL Tetraborate

buffer. 50ul of the working reagent was combined with 20-25ul tissue extract which was deproteinized in 0.1M perchloric acid 1:10 (wet weight : acid). Stock solutions for amino acid standards were prepared in 50% for a level of 1mg/ml. Derivatization was performed by the 542 autosampler using the 4- line method. Line 1 contained 30ul from reagent, line 2 mix 4 cycles with 30ul line 3 wait 1 min line 4 End. We used a Waters Xterra MS Column. Mobile phase consisted of 100mM Disodium Hydrogen phosphate; 20% methanol; 3.5% acetonitrile and a mobile phase flow rate 0.6mL/min at 30°C. Injection of 20ul in partial loop mode with 17ul flush volume. The detector used Model 5600A. HPLC data are reported as the mean  $\pm$  SEM amino acid content in each tissue normalized to initial weight of sample.

### ***Data Analysis***

All data was analyzed using GraphPad Prism 7.0 (GraphPad; La Jolla, CA). Data are presented as mean  $\pm$  SEM and a p value less than 0.05 was considered significant. All statistical tests are detailed in Figure Legends. Multiple comparison correction of the dataset from DigiGait was performed via a false discovery rate (FDR) correction at a threshold value of 0.01 in an R environment using the psych package.

## Results

### ***Gnao1<sup>+/G203R</sup> mice showed normal viability and growth.***

Genotypes of offspring of *Gnao1<sup>+/G203R</sup>* x WT crosses (N1 - C57BL/6NCrI x C57BL/6J) were observed at the expected frequency (29 WT and 27 heterozygous). All three homozygous mice from *Gnao1<sup>+/G203R</sup>* x *Gnao1<sup>+/G203R</sup>* crosses died by P1. The small numbers of offspring observed from these crosses so far, however, were not significantly different from expected frequencies (4 wt, 14 het, and 3 homozygous). Heterozygous *Gnao1<sup>+/G203R</sup>* mice did not show any growth abnormalities compared to *Gnao1<sup>+/+</sup>* mice (Figure 2-1B & 2-1D) and they had relatively normal survival. There were two spontaneous deaths (~5-7 weeks) seen for *Gnao1<sup>+/G203R</sup>* mice out of 33 (Fig 2-1C). This is reminiscent of the spontaneous deaths seen previously with the *Gnao1<sup>+/G184S</sup>* GOF mutant mice [11]. *Gnao1<sup>+/G203R</sup>* mice did not exhibit any obvious spontaneous seizures or abnormal movements.

### ***Female Gnao1<sup>+/G184S</sup> and male Gnao1<sup>+/G203R</sup> mice show impaired motor coordination and reduced grip strength.***

Since GOF alleles of *GNAO1* in children result primarily in movement disorder, we tested motor coordination in two mouse lines. One carried an engineered GOF mutant G184S, designed to block RGS protein binding [8, 40, 54]. The other is the G203R GOF mutant, which has been seen in at least 7 children (1, 2). First, we used a two-day training and testing procedure on the RotaRod (Figure 2-3A & B). *Gnao1<sup>+/G184S</sup>* and *Gnao1<sup>+/G203R</sup>* mice were compared to their same-sex littermate controls. Female *Gnao1<sup>+/G184S</sup>* mice exhibited a reduced retention time on the

accelerating RotaRod (unpaired t-test,  $p < 0.001$ , Figure 2-3A) while male mice remained unaffected. In contrast, male *Gnao1*<sup>+/<sup>G203R</sup> mice exhibited reduced time to stay on the rotating rod (unpaired t-test,  $p < 0.05$ , Figure 2-3B) while female *Gnao1*<sup>+/<sup>G203R</sup> mice did not show any abnormalities. Results from all the RotaRod training and testing sessions are shown in S1 Fig. Neither *Gnao1*<sup>+/<sup>G184S</sup> nor *Gnao1*<sup>+/<sup>G203R</sup> mice showed a significant difference in learning rate on RotaRod (S3 Fig), suggesting that the differences we observed in the RotaRod study were due to movement deficits rather than learning difficulties.</sup></sup></sup></sup>

Grip strength was assessed as described [51]. This test is widely done in combination with the RotaRod motor coordination test. This may be relevant to the hypotonia, seen in many *GNAO1* patients [14-18, 23, 33, 60-67]. Similar to the RotaRod results, female *Gnao1*<sup>+/<sup>G184S</sup> mice also showed reduced forepaw grip strength compared to their littermate controls (unpaired Student's t-test,  $p < 0.05$ , Figure 2-3C) while males did not exhibit a significant difference (Figure 2-3C). In contrast, both male and female *Gnao1*<sup>+/<sup>G203R</sup> mice displayed reduced forepaw grip strength (unpaired t-test,  $p < 0.05$ , Figure 2-3D).</sup></sup>

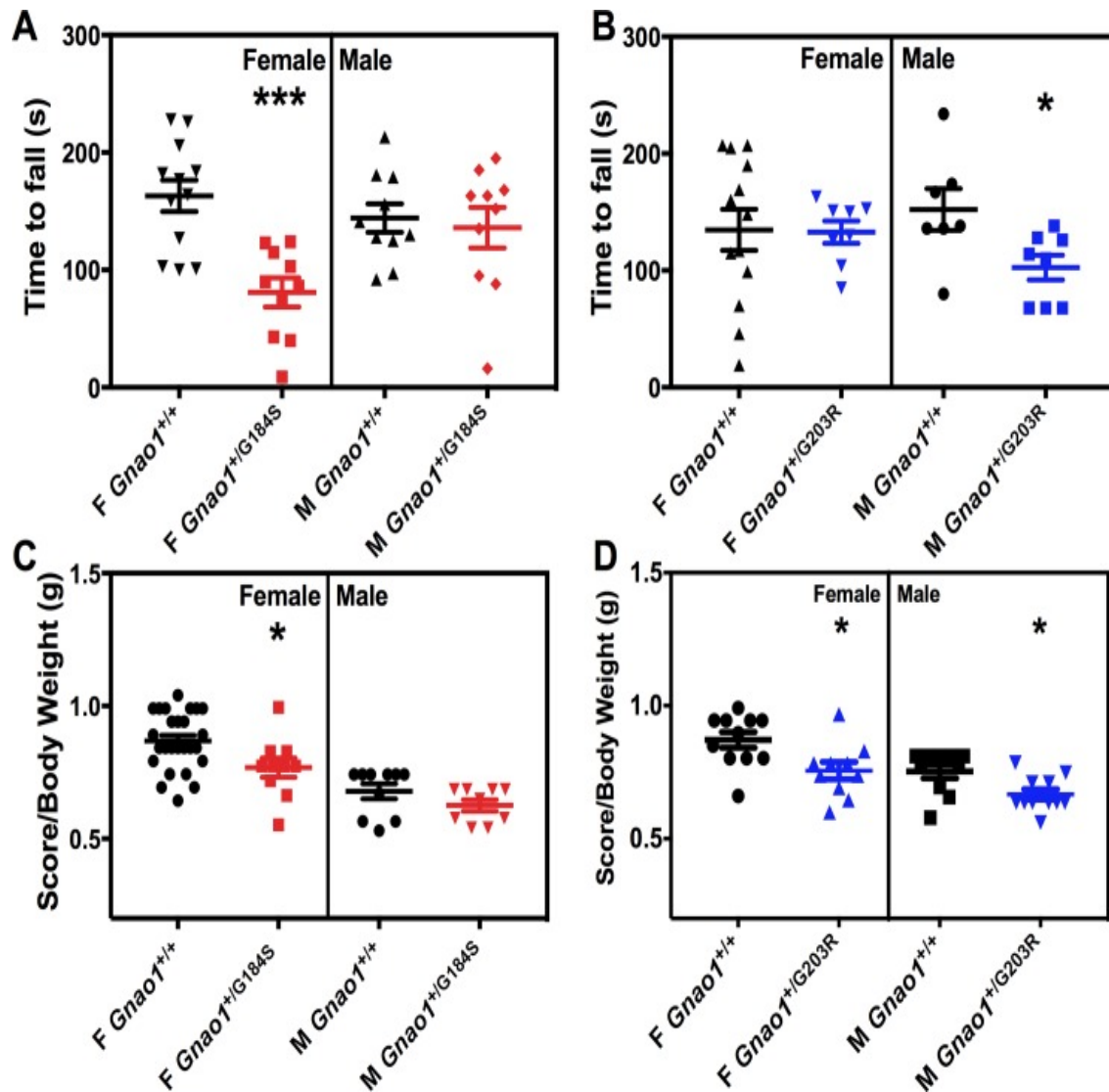


**Figure 2-3. Female *Gnao1*<sup>+/G184S</sup> mice and male *Gnao1*<sup>+/G203R</sup> mice show reduced time on RotaRod and reduced grip strength (A&B) Quantification of RotaRod studies. (A) Female *Gnao1*<sup>+/G184S</sup> mice lose the ability to stay on a RotaRod (unpaired t-test; \*\*\*p<0.001), while male *Gnao1*<sup>+/G184S</sup> mice appeared unaffected. (B) Male *Gnao1*<sup>+/G203R</sup> also showed reduced motor coordination on RotaRod (unpaired t-test, \*p<0.01). (C&D) Quantification of grip strength results. Scores for each mouse were normalized to body weight. (C) Female *Gnao1*<sup>+/G184S</sup> mice are less capable of lifting weights compared to their *Gnao1*<sup>+/+</sup> siblings (unpaired t-test, \*p<0.05). (D) Both male and female *Gnao1*<sup>+/G203R</sup> mice showed reduced ability to hold weights (unpaired t-test, \*p<0.05). Data are shown as mean  $\pm$  SEM.**

***Gnao1<sup>+/G184S</sup> mice show reduced activity in the open field arena.***

The open field test provides simultaneous measurements of locomotion, exploration and surrogates of anxiety. It is a useful tool to assess locomotive impairment in rodents [68], however, environmental salience may reduce the impact of the motor impairment on behaviors [69]. Therefore, we divided the 30-min open field measurements into two periods, with the first 10 minutes assessing activity in a novel environment and the 10-30 minute period designated as sustained activity (Figure 2-4C & 2-4D). The novelty measurement showed a significant difference between *Gnao1<sup>+/G184S</sup>* mice and their littermate controls for both male and female mice (2-way ANOVA,  $p < 0.01$  for female,  $p < 0.05$  for male, Figure 2-4C). Female, but not male, *Gnao1<sup>+/G184S</sup>* mice showed reduced activity in the sustained phase of open field testing (Figure 2-4C, 2-way ANOVA, \* $p < 0.05$ , \*\* $p < 0.01$ , \*\*\*\* $p < 0.0001$ ). Both male and female *Gnao1<sup>+/G184S</sup>* mice also showed reduced total activity (2-way ANOVA,  $p < 0.001$ , Fig 4A & 4C). Neither male nor female *Gnao1<sup>+/G203R</sup>* mice performed differently in the open field arena compared to their littermate controls (Figure 2-4B & 2-4D). No significant difference was observed in the time mice spent in the center of the arena (S2 Fig).

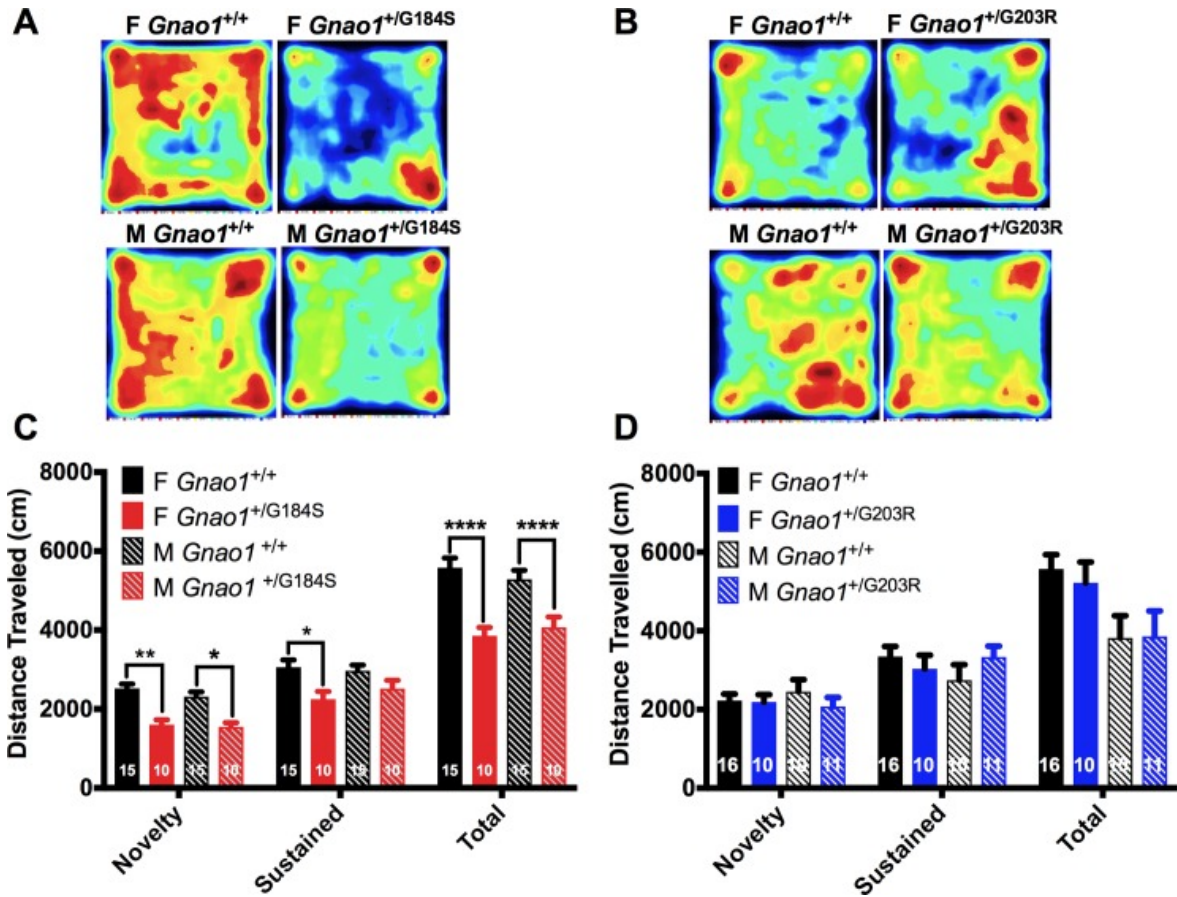


**Figure 2-4. *G184S* mutant mice showed reduced activities in Open Field Test but *G203R* mutants do not** (A&C) Female and male *Gnao1*<sup>+/G184S</sup> mice showed decreased activity in the open field test. A total of 30 min activity was recorded which was divided into a Novelty (0-10 min) and a Sustained (10-30 min) period. (A) Representative heat map of overall activity comparing *Gnao1*<sup>+/+</sup> and *Gnao1*<sup>+/G184S</sup> mice of both sexes. (C) Quantitatively, both male and female *Gnao1*<sup>+/G184S</sup> travelled less in the open field arena (2-way ANOVA; \*\*\*\**p*< 0.0001, \*\**p*<0.01, \**p*<0.05). (B & D) Neither male nor female *Gnao1*<sup>+/G203R</sup> mice showed abnormalities in the open field arena. (B) Sample heat map tracing of female and male mouse movement in open field. (D) Quantification showed no difference between *Gnao1*<sup>+/+</sup> and *Gnao1*<sup>+/G203R</sup> mice in distance traveled (cm) in the open field arena (2-way ANOVA; n.s.). Data are shown as mean ± SEM. Numbers of animals are indicated on bars.

***Female  $Gnao1^{+/G184S}$  mice and male  $Gnao1^{+/G203R}$  mice exhibit markedly abnormal gaits.***

In addition to the above behavioral tests, we also performed gait assessment on  $Gnao1^{+/G184S}$  and  $Gnao1^{+/G203R}$  mice of both sexes. Gait is frequently perturbed in rodent models of human movement disorders even when the actual movement behavior seen in the animals does not precisely phenocopy the clinical movement pattern [70, 71]. The multiple parameters assessed in DigiGait allow it to pick up subtle neuromotor defects and make it more informative than the RotaRod test.

The gait analysis largely confirmed the sex differences between the two strains in RotaRod tests. Thirty-seven parameters were measured for both front and hind limbs. Given the large number of measurements, we used false discovery rate (FDR) analysis with a Q of 1% as described in Methods to reduce the probability of Type I errors (S2-4 and S2-5 Fig, S2-1-S2-4 Tables).  $Gnao1^{+/G184S}$  female mice showed 22 significant differences ( $Q < 0.01$ ) and males showed 8 (S2-4 Fig, S2-3 and S2-4 Table). For  $Gnao1^{+/G203R}$  mice, the opposite sex pattern was seen with 27 parameters in females and 8 parameters in males showing significant differences from WT (S2-5 Fig, S2-1 and S2-2 Table). Two of the most highly significant parameters and ones that had face validity in terms of clinical observations (stride length and paw angle variability) were chosen for further analysis.

Across the range of treadmill speeds, female  $Gnao1^{+/G184S}$  mice showed significantly reduced stride length (2-way ANOVA,  $p < 0.01$ , Fig 2-5A) and increased paw angle variability (2-way ANOVA,  $p < 0.0001$ , Fig 2-5E) compared to WT littermates. Male  $Gnao1^{+/G184S}$  mice only had a difference in paw angle variability (2-way ANOVA,  $p < 0.0001$ ), not in stride length (Fig 2-5C & 2-5G). These results are consistent with the results of RotaRod and grip strength measurements in that female

*Gnao1*<sup>+/*G184S*</sup> mice showed a stronger phenotype than males. In contrast to the *Gnao1*<sup>+/*G184S*</sup> mice, male *Gnao1*<sup>+/*G203R*</sup> mice appeared to be more severely affected in gait compared to female *Gnao1*<sup>+/*G203R*</sup> mice. Male *Gnao1*<sup>+/*G203R*</sup> mice had highly significantly reduced stride length (2-way ANOVA,  $p < 0.0001$ , Fig 2-5D) and increased paw angle variability (2-way ANOVA,  $p < 0.05$ , Fig 2-4H). In contrast, female *Gnao1*<sup>+/*G203R*</sup> mice did not show any significant differences in stride length or paw angle variability (Fig 2-5B & 2-5F).

In addition to these quantitative gait abnormalities a qualitative defect was seen. A significant number of *Gnao1*<sup>+/*G203R*</sup> mice of both sexes failed to run when the belt speed exceeded 22 cm/s (Mann-Whitney test, female and male  $p < 0.05$ , Fig 2-5J). For reasons that are not clear such a difference was not seen for *Gnao1*<sup>+/*G184S*</sup> mice (Fig 2-5I).

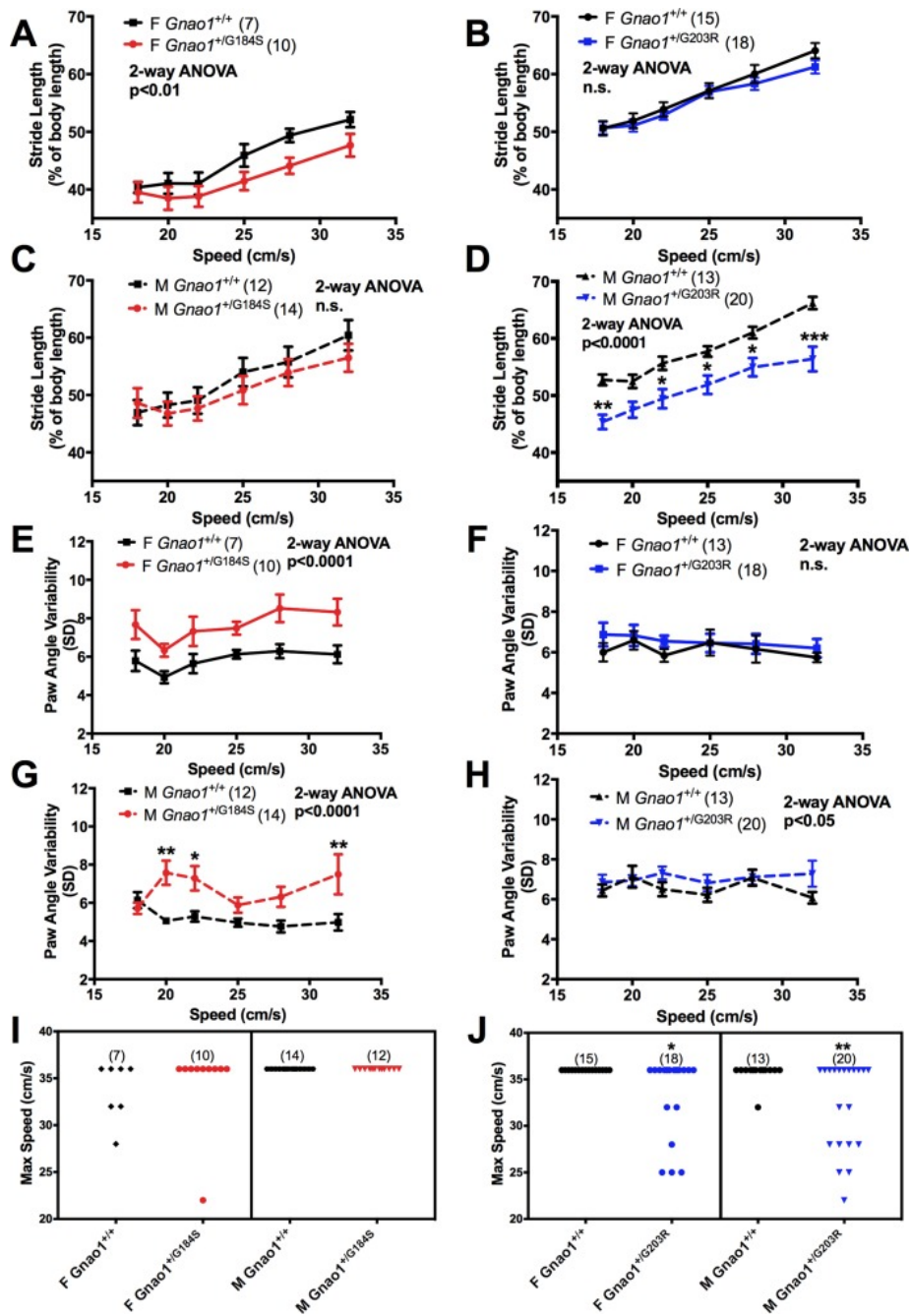


**Figure 2-5. DigiGait Imaging System reveals sex-specific gait abnormalities in *Gnao1*<sup>+/G184S</sup> mice and *Gnao1*<sup>+/G203R</sup> mice** (A-D) Female *Gnao1*<sup>+/G184S</sup> mice showed significant gait abnormalities, while female *Gnao1*<sup>+/G203R</sup> mice remain normal. (A & B) Female *Gnao1*<sup>+/G184S</sup> mice showed reduced stride length (2-way ANOVA with Bonferroni multiple comparison post-test) while female *Gnao1*<sup>+/G203R</sup> mice were not different from control (2-way ANOVA; n.s.). (C) Female *Gnao1*<sup>+/G184S</sup> mice also showed increased paw angle variability (2-way ANOVA, p<0.0001) while female *Gnao1*<sup>+/G203R</sup> mice showed normal paw angle variability. (E-H) Male *Gnao1*<sup>+/G203R</sup> and *Gnao1*<sup>+/G184S</sup> mutant mice showed distinct gait abnormalities. (E & G) Male *Gnao1*<sup>+/G184S</sup> mice

showed significantly increased paw angle variability (2-way ANOVA  $p < 0.0001$  overall with significant Bonferroni multiple comparison tests;  $**p < 0.01$  and  $*p < 0.05$ ). There was no effect on stride length. (F & H) In contrast, male *Gnao1*<sup>+/G203R</sup> mice showed markedly reduced stride length (2-way ANOVA  $p < 0.0001$  with Bonferroni multiple comparison post-test;  $***p < 0.001$ ,  $**p < 0.01$ , and  $*p < 0.05$ ) and modestly elevated paw angle variability (overall  $p < 0.05$ ). (I) *Gnao1*<sup>+/G184S</sup> mice did not show significant differences in the highest treadmill speed successfully achieved. (J) Both male and female *Gnao1*<sup>+/G203R</sup> mice showed reduced capabilities to run on a treadmill at speeds greater than 25 cm/s (Mann-Whitney test;  $*p < 0.05$ ).

**Male *Gnao1*<sup>+/G203R</sup> mice are sensitized to PTZ kindling.**

Epilepsy has been observed in 100% of patients with *GNAO1* G203R mutations [10, 17, 33, 34, 42, 43]. Also in the *Gnao1*<sup>+/G184S</sup> GOF mutant mice, we previously reported spontaneous lethality as well as increased susceptibility to kindling by the chemical anticonvulsant PTZ for both males and females [11]. Kindling is a phenomenon where a sub-convulsive stimulus, when applied repetitively and intermittently, leads to the generation of full-blown convulsions [72]. To determine if the G203R GOF mutant mice mimicked the G184S mutants and phenocopied the human epilepsy pattern of children with the G203R mutation, we assessed PTZ-induced kindling in *Gnao1*<sup>+/G203R</sup> mutant mice. As expected for C57BL/6 mice, females were more prone to kindling than male mice. Half of the mice kindled at 4 and 8-10 injections for females and males, respectively (Fig 2-6A & 2-6B). Despite the increased sensitivity of females in general, female *Gnao1*<sup>+/G203R</sup> mice did not show significantly higher sensitivity to PTZ compared to their littermate controls (Fig 2-6A). On the contrary, male *Gnao1*<sup>+/G203R</sup> mice were more sensitive to PTZ kindling than controls (Fig 2-6B, Mantel-Cox Test,  $p < 0.05$ ). Also, three spontaneous deaths were seen (two male and one female) among the 33 G203R mice observed for at least 100 days, similar to the early lethality seen in G184S mutant mice [11]. We cannot, however, attribute those deaths to seizures at this point.

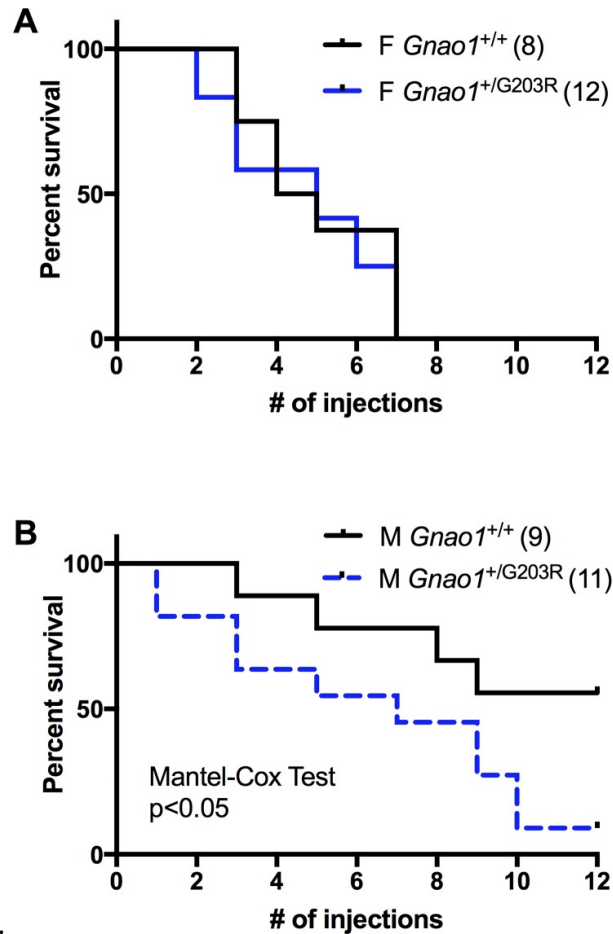


**Figure 2-6. *Gnao1*<sup>+/G203R</sup> male mice have an enhanced Pentylentetrazol (PTZ) Kindling response**  
 (A) Female *Gnao1*<sup>+/G203R</sup> mice did not show heightened sensitivity to PTZ injection. (B) Male *Gnao1*<sup>+/G203R</sup> mice developed seizures earlier than WT littermates after repeated PTZ injections (Mantel-Cox Test;  $p < 0.05$ ).

***Gnao1*<sup>+/G203R</sup> mice show increased sensitivity to oxotremorine**

*Gnao1*<sup>+/G203R</sup> mice do not display any overt movement or postural abnormality at baseline. However, previous studies used oxotremorine, a muscarinic cholinergic agonist, to induce movement abnormalities in a LOF *Gnal* model [73]. The *GNAL* gene, which is linked to dystonia, encodes  $G\alpha_{\text{olf}}$  an isoform of  $G\alpha_s$  which functions antagonistically of  $G\alpha_o$  to stimulate AC to

produce cAMP. *GNAL* LOF mutations decrease cAMP similar to GOF *GNAO1* mutations. Therefore, we reasoned that *Gnao1*<sup>+/G203R</sup> mice would display a similar phenotype. In response to 0.1 mg/kg of the cholinergic agonist oxotremorine, wildtype mice displayed some abnormal movements, characterized by slow movements and some abnormal postures. (Figure 2-7). *Gnao1*<sup>+/G203R</sup> mice also displayed higher abnormal movement scores than vehicle control groups., however, at thirty minutes post injection *Gnao1*<sup>+/G203R</sup> mice displayed a higher abnormal movement score compared to wildtype mice treated with oxotremorine. This phenotype was mainly characterized by the mouse standing vertically on hindlimbs for sustained periods of longer than >10s.

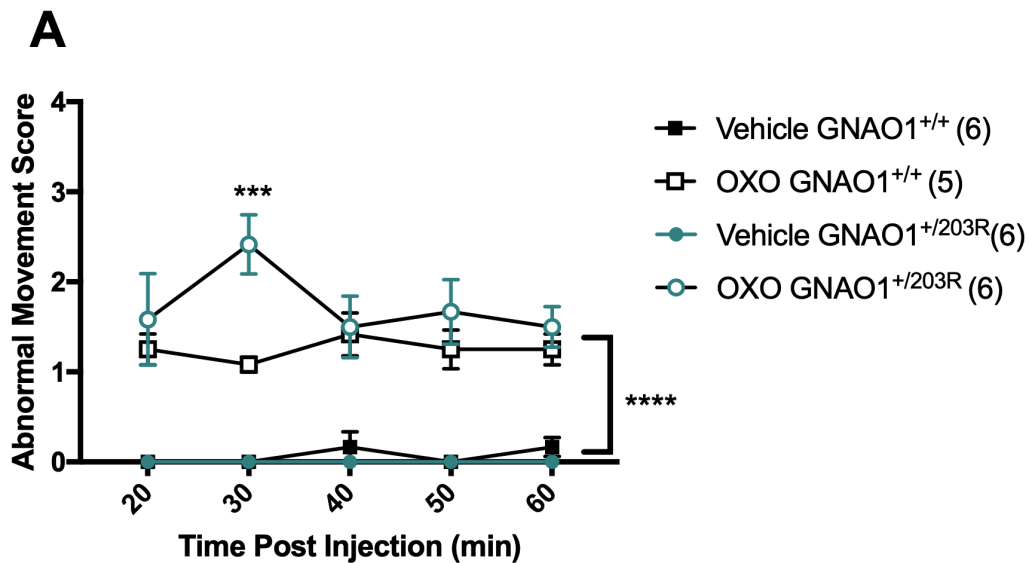


**Figure 2-7. Induction of abnormal movements and postures by oxotremorine** (A) Starting at 20 minutes following injection of cholinergic agonist, oxotremorine, behavior was scored for abnormal movements and postural differences. Oxotremorine treated WT and *Gnao1*<sup>+/G203R</sup> male mice show higher abnormal movement scores than vehicle control littermates. *Gnao1*<sup>+/G203R</sup> mice show higher sensitivity to oxotremorine at T=30 compared to WT mice. 2-Way ANOVA with Bonferonni correction: p<0.0001 \*\*\*\*, p<0.001 \*\*\*, p < 0.01\*\*, p < 0.05 \*

### ***Trihexyphenidyl treatment on movement disorders***

Patients with *GNAO1* G203R mutations have shown some benefits to oral therapeutics (Table 2-3) including trihexyphenidyl (THP), a cholinergic antagonist. As *Gnao1*<sup>+/G203R</sup> mice displayed a greater sensitivity to oxotremorine, a cholinergic agonist, we had reason to believe the *Gnao1*<sup>+/G203R</sup> motor coordination impairments displayed on the rotarod would be alleviated following administration of trihexyphenidyl. In initial pilot studies of a single 5 mg/kg or 10 mg/kg doses of THP, both WT and *Gnao1*<sup>+/G203R</sup> mice showed small but non- significant reductions in rotarod times *Gnao1*<sup>+/G203R</sup> mice (Figure 2-8.).

**Table 2-3. *GNAO1* G203R patient classification**

Patient No.	Sex	Amino Acid Change	Age of Onset	Presence of Epilepsy	Movement Disorder	Treatment for Movement Disorder	Motor Developmental Delay(MDD)/Intellectual Delay(ID)	Reference
1	F	G203R	7 mo	EE	Chorea	NA	MDD/ID	Nakamura et al (2013)
2	F	G203R	7 d	EE	Chorea	NA	MDD/ID	Saitu et al (2016)
3	M	G203R	1 mo	EE	Chorea	NA	MDD/ID	Arya et al (2017)
4	F	G203R	3 mo	WS	Dyskinesia Dystonia	L-Dopa	MDD/ID	Schorling et al (2017)
5	F	G203R	Birth	EE	Dyskinesia Dystonia	GBP,THP,BCL , BZD	MDD/ID	Schorling et al (2017)
6	F	G203R	4 mo*	EE	-	NA	MDD/ID	Xiong et al (2018)
7	F	G203R	1 d	EE	Chorea and Dystonia	Clonazepam	MDD/ID	Schirinizi et al (2018)
8	M	G203R	12 d		Dyskinesia	TBZ, BZD, PB, Lorazepam	MDD/ID	Schirinizi et al (2018)

\* at 12 months patient developed a pulmonary infection and died

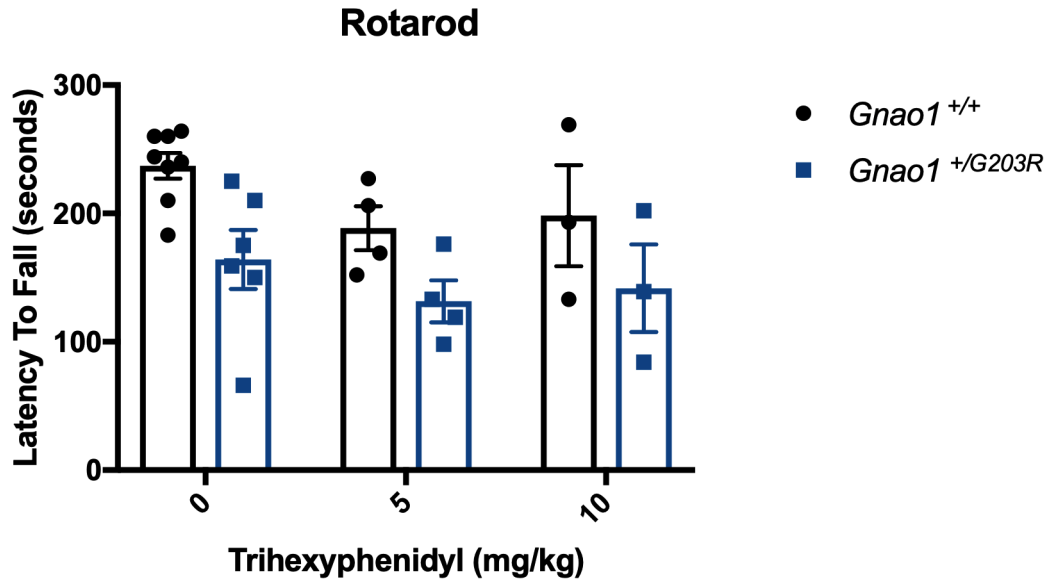


**Figure 2-8. Treatment with trihexyphenidyl on *Gnao1*<sup>+/G203R</sup> mice** Thirty minutes following injection of cholinergic antagonist, trihexyphenidyl, motor coordination was assessed on the accelerating rotarod. Trihexyphenidyl treatment showed no alleviation of motor abnormalities on the rotarod. 2-Way Anova: non-significant

### ***Neurotransmitter levels***

GNAO1 functions to regulate neurotransmitter release through multiple mechanisms[19]. Certain neurotransmitters, such as glutamate and  $\gamma$ -aminobutyric acid (GABA), and dopamine are shown to play a direct role in regulating movement control [74]. We reasoned that *Gnao1*<sup>+/R209H</sup> would show differences in neurotransmitter levels. To test this, we analyzed the left hemisphere of the brains of *Gnao1*<sup>+/G203R</sup> mice for catecholamine and amino acid neurotransmitter levels via HPLC. The amino acid neurotransmitters GABA and glutamate showed no significant differences between mutant and wildtype mice in either group (Figure 2-6A and Supplemental Figure 2-6). Compared to wildtype mice we also saw no significant differences between L-3,4-

dihydroxyphenylalanine (DOPA), dopamine, and 5-HT. However, there was a significant increase in the amount of norepinephrine within the brains of *Gnao1*<sup>+/*G203R*</sup> mice (Figure 2-8).

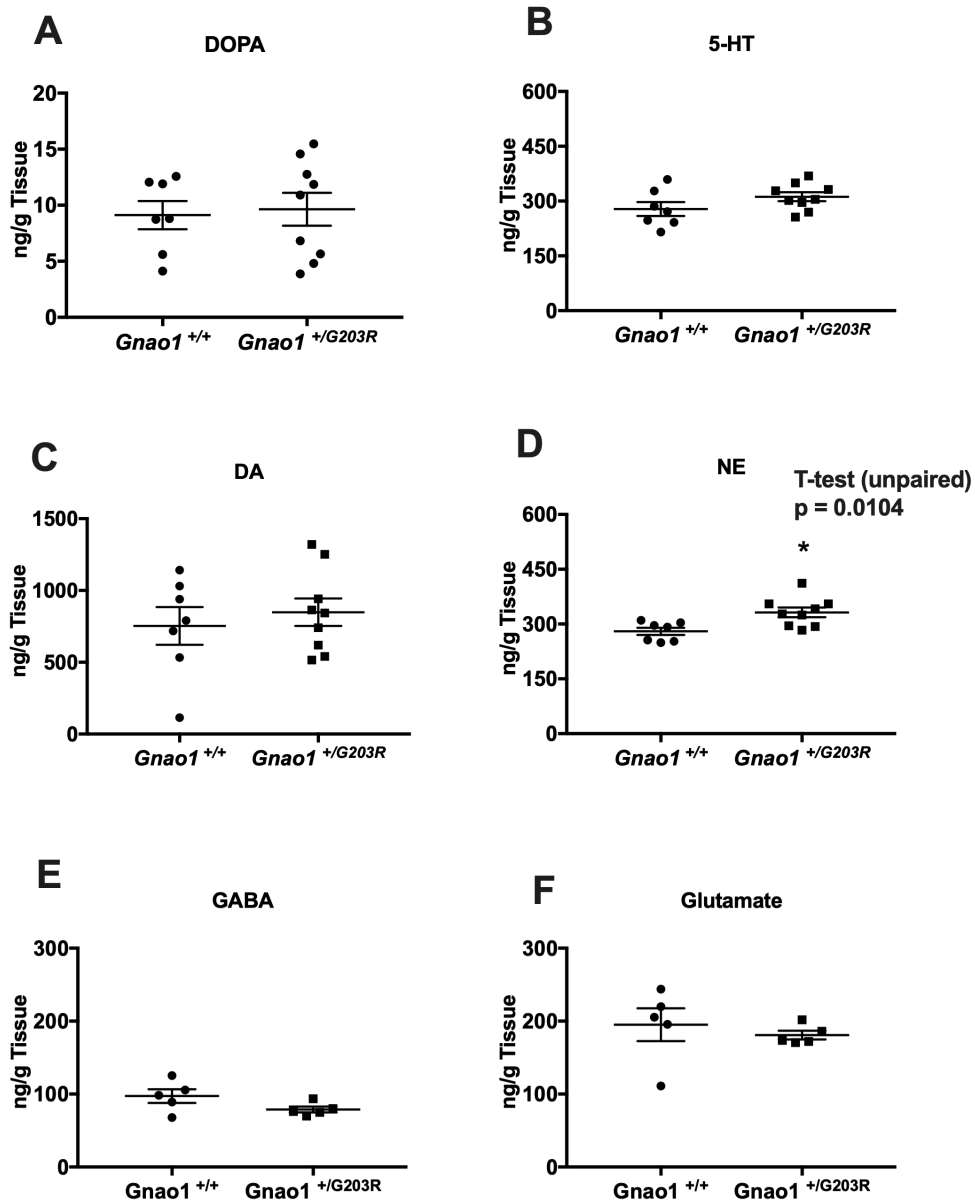


**Figure 2-9. Brain neurotransmitter analysis of *Gnao1*<sup>+/*G203R*</sup> mice (A-C,E&F)** HPLC analysis of brain DOPA, dopamine, 5-HT and amino acid neurotransmitters GABA and glutamate within the left hemisphere of *Gnao1*<sup>+/*G203R*</sup> showed no significant differences compared to WT littermates. Students unpaired t-test showed brain levels of norepinephrine had significantly higher levels within *Gnao1*<sup>+/*G203R*</sup> mice compared to WT littermates.

## Discussion

In this report, we describe the first mouse model carrying a human *GNAO1* mutation associated with disease and we provide evidence to support the concept that GOF mutations are associated with movement disorder [19]. Heterozygous mice carrying the G203R mutation in *Gnao1* exhibit both a mild increase in seizure propensity and evidence of abnormal movements. This fits precisely with the variable seizure pattern of the children who carry this mutation as well as their severe choreoathetotic movements [10, 17, 33, 34, 42]. Also, we examined a possible movement phenotype in mice carrying the RGS-insensitive GOF mutant (*Gnao1*<sup>+/<sup>G184S</sup>) that we reported previously to have a mild seizure phenotype [11]. This mutation has not been reported in humans to our knowledge. As predicted from our mechanistic model [19, 34], the *Gnao1* G184S mutant mice also show movement abnormalities.</sup>

In mouse models of movement disorders, the mouse phenotype is usually not as striking or as easily observed as the clinical abnormalities in the patients [75, 76], however they are often informative about mechanism and therapeutics. For the patient-derived *Gnao1*<sup>+/<sup>G203R</sup> mutant mouse, neither the seizure propensity nor the movement abnormality was obvious without a stress being applied. Male *Gnao1*<sup>+/<sup>G203R</sup> mice showed decreased motor ability on RotaRod, decreased fore paw strength, and gait abnormalities at higher speeds of walking/running. No spontaneous seizures were observed but there was a substantial increase in sensitivity to PTZ-induced seizures in the kindling model in males. This very closely replicates the mild seizure phenotype of female *Gnao1*<sup>+/<sup>G184S</sup> mice [11]. We now show that the female *Gnao1*<sup>+/<sup>G184S</sup> mice also exhibit gait and motor abnormalities.</sup></sup></sup></sup>

Both the *GNAO1* G203R and the G184S mutations show a definite but modest GOF phenotype in biochemical measurements of cAMP regulation [19]. In each case, the maximum percent inhibition of cAMP is not greatly increased but the potency of the  $\alpha_{2A}$  adrenergic agonist, used in those studies to reduce cAMP levels, was increased about 2-fold. This effectively doubles signaling through these two mutant G proteins at low neurotransmitter concentrations (i.e. those generally produced during physiological signaling). This, however, does not prove that cAMP is the primary signal mechanism involved in pathogenesis of the disease. The heterotrimeric G protein,  $G_o$ , of which the *GNAO1* gene product,  $G\alpha_o$ , is the defining subunit, can signal to many different effector mechanisms [34, 38, 77] We recently reviewed the mutations associated with genetic movement disorders and identified both cAMP regulation and control of neurotransmitter release as two *GNAO1* mechanisms that seem highly likely to account for the pathophysiology of *GNAO1* mutants [34]. Since many  $G_o$  signaling effectors (including cAMP and neurotransmitter release) can be mediated by the  $G\beta\gamma$  subunit released from the  $G_o$  heterotrimer, other effectors could also be involved in the disease mechanisms. A recent hypothesis has also been raised that intracellular signaling by  $G\alpha_o$  may be involved [78]. The observation that one of the most common movement disorder-associated alleles (R209H and other mutations in Arg<sup>209</sup>) does not markedly alter cAMP signaling in *in vitro* models, does suggest that the mechanism is more complex than a simple GOF vs LOF distinction at cAMP regulation.

We observed a striking sex difference in the phenotypes of our two mouse models. Female *Gnao1*<sup>+/G184S</sup> mice and male *Gnao1*<sup>+/G203R</sup> mice showed much more prominent movement abnormalities than male G184S and female G203R mutants. However, the patterns of changes in the behavioral tests did not exactly overlap. Only G184S mutants showed significant changes in

open field tests while only the G203R mutants showed the striking reduction in ability to walk/run at higher treadmill speeds. For both mutant alleles, the seizure phenotype was also worse in the sex with the more prominent movement disorder. *GNAO1* encephalopathy is slightly more prevalent (60:40) in female than male patients [34]. It is not uncommon to have sex differences in epilepsy or movement disease progression. One possible explanation is that estrogen prevents dopaminergic neuron depletion by decreasing the uptake of toxins into dopaminergic neurons in Parkinson's disease (PD) animal model induced by neurotoxin [79]. The  $G_{i/o}$  coupled estrogen receptor, GPR30, also contributes to estrogen physiology and pathophysiology [80]. PD is more common in male than female human patients [81], therefore, the pro-dopaminergic properties of estrogen may exacerbate conditions mediated by hyper-dopaminergic symptoms like chorea in Huntington's disease [HD; 79]. Chorea/athetosis is the most prevalent movement pattern seen in *GNAO1*-associated movement disorders [34] so the female predominance correlates with that in HD. Clearly mechanisms of sex differences are complex including differences in synaptic patterns, neuronal densities and hormone secretion [82], but it is beyond the scope of this report to explain how the molecular differences contribute to the distinct behavioral patterns.

Here we show that *Gnao1* GOF mutation G203R impairs motor coordination however the model does not display any obvious movement abnormalities at baseline. We were able to show that *Gnao1*<sup>+/G203R</sup> mice displayed overt postural and motor abnormalities consistent with patient movement disorders after a dose of oxotremorine, a cholinergic agonist. We also showed the *Gnao1*<sup>+/G203R</sup> had an increase susceptibility to oxotremorine at 30 minutes, compared to WT mice. However, our model showed no reprieve or motor abnormalities on the rotarod following injection of OXO that has proved efficacious in one of the patients with G203R variant. A possible

explanation is the receptor selectivity between the drugs. Oxotremorine is a nonselective muscarinic receptor agonist, trihexyphenidyl however is selective to M<sub>1</sub> receptors antagonism. Therefore, it is likely that M1 is not the receptor of interest in the *GNAO1* mechanism. G $\alpha$ <sub>o</sub> proteins have been known to couple to M<sub>2</sub> receptors. It would be interesting to test an M<sub>2</sub> selective cholinergic antagonist in our model.

Since *GNAO1* encephalopathy is often associated with developmental delay and cognitive impairment [34], it would be interesting to see whether the movement phenotype we have seen in female *Gnao1*<sup>+/<sup>G184S</sup></sup> and male *Gnao1*<sup>+/<sup>G203R</sup></sup> mice is due to a neurodevelopmental malfunction or to ongoing active signaling alterations. G<sub>o</sub> coupled GPCRs play an important role in hippocampal memory formation [83, 84]. Additional behavioral tests will be valuable to assess the learning and memory ability of the *Gnao1* mutant mice.

With the increasing recognition of *GNAO1*-associated neurological disorders, it is important to learn about the role of G<sub>o</sub> in the regulation of central nervous system. The novel *Gnao1* G203R mutant mouse model reported here, and further models under development, should facilitate our understanding of *GNAO1* mechanisms in the *in vivo* physiological background rather simply in *in vitro* cell studies. In this study we began initial tests looking at neurotransmitter levels with whole brain of *Gnao1*<sup>+/<sup>G203R</sup></sup> mice. We only showed significant differences in the amount of norepinephrine. Elevated norepinephrine has been heavily linked to being anticonvulsant, however there is also evidence for norepinephrine being proconvulsant as well [85]. To test if the high elevation of NE might be a mechanism behind the kindling phenotype observed in our model it would be interesting to test our PTZ model following administration of propranolol, an adrenoceptor antagonist blocking the effects of

norepinephrine. While these results might explain the seizure phenotype they do not explain the movement disorder. In regards to this we hypothesized that neurotransmitters associated with movement control, such as dopamine or GABA and glutamate, would be decreased in the brain tissue of the *Gnao1*<sup>+/G203R</sup> mice. While we did not see these in our analysis, we still can not rule this out.  $G\alpha_o$  is ubiquitously expressed within the brain but evidence shows it is very abundant within the striatum and cerebellum[1]. Both of these regions are widely known to be involved in motor control. It is possible in our analysis using the whole brain was too generalized. Further studies should be done to look at the more specific regions relevant to our model.

Taken together this animal models can be used to further study mechanisms of GNAO1 associated epilepsy and movement disorders. While we did not show THP as an effective treatment this model can still be used for preclinical drug testing and may permit a true allele-specific personalized medicine approach in drug repurposing for the associated movement disorders.

**CHAPTER 3: BEHAVIORAL ASSESSMENT OF MICE WITH A COMMON *GNAO1* MOVEMENT  
DISORDER VARIANT R209H**

## Statement of Contribution

In the following chapter my role was the following. I planned, performed and analyzed the open field, rotarod, grip strength and risperidone studies for the *Gnao1<sup>+ / R209H</sup>* mouse model. The experiments on developmental milestones were performed by Alex Roy. For all of the studies mentioned above I performed the formal data analysis as well. The data curation and formal analysis for the digigait, kindling studies and western blot experiment was performed by Huijie Feng. Genotyping and breeding of mice was done by Jefferey Leipprandt. Elena Demireva and Huirong Xie at the MSU transgenic core generated the mutant mouse model with CRISPR/cas9 technology. The following chapter was put together and written by myself with edits from Elena Demireva, Huijie Feng and Richard Neubig.

## Abstract

Neurodevelopmental delay with involuntary movements (NEDIM) is characterized by a delay in psychomotor development, hypotonia and early onset of hyperkinetic involuntary movements. Heterozygous *de novo* mutations in the *GNAO1* gene are the cause of NEDIM in patients.  $G\alpha_o$ , the gene product of *GNAO1* is the alpha subunit of the heterotrimeric  $G_{i/o}$  family of G-proteins. It is abundantly found throughout the brain. However, the pathophysiological mechanisms linking  $G\alpha_o$  functions to *GNAO1* clinical manifestations are still poorly understood. In order to begin to understand why mutations in *GNAO1* can cause NEDIM, models need to be validated as predictive. Heterozygous *GNAO1* R209H mutant mice were created using CRISPR/Cas9 to assess whether the mice could replicate aspects of NEDIM clinical patterns. The R209H mutation altered development, increased locomotor activity, and displayed gait differences. This allowed us to explore possible treatments. One drug that has proven effective in a patient with the R209H mutation is risperidone, an atypical neuroleptic. Here we showed that administration of risperidone alleviated the hyperlocomotion observed in our animal model. The present results show that *Gnao1*<sup>+/R209H</sup> mice mirror some aspects of the patient phenotype but also mirror a response to a pharmacological agent.

## Introduction

$G\alpha_o$  is the alpha subunit of the heterotrimeric G-protein and is the most abundant heterotrimeric G protein in brain, comprising 1% of the mammalian brain membrane protein. Therefore, it is no surprise that mutations in its gene, *GNAO1*, have been linked to neurological conditions. Since an initial report in 2013 [87] when four children with epileptic-encephalopathy were identified with mutations in *GNAO1*, a growing number of clinical cases of patients presenting with epilepsy and movement disorders have been found to exhibit *de novo* mutations in the gene encoding the protein  $G\alpha_o$  (*GNAO1*). To date there are over 70 clinical cases of children with mutations in *GNAO1* presenting with early infantile epileptic encephalopathy (EIEE17; OMIM 615473) and/or neurodevelopmental disorder with involuntary movements (NEDIM; OMIM 617493)[13-18, 23, 24, 33, 42, 43, 61-66, 87-101]

There have been forty-three pathological variants of *GNAO1* reported. Our lab has previously classified these variants by the ability of the mutated  $G\alpha_o$  proteins to support inhibition of cAMP production [19].  $G\alpha_o$  proteins with functioning mutations, which inhibit cAMP normally or even more efficiently, are associated with movement disorder patients. Non-functioning mutants, those that showed less cAMP inhibition, are associated with epilepsy patients [19]. Recently our lab created a mouse model with a *GNAO1* GOF mutation, G203R, that was identified in patients who showed both epilepsy and movement disorders. As predicted, the mice exhibited with motor coordination and gait abnormalities as well as enhanced seizure susceptibility in pentylentetrazol (PTZ) kindling studies. While this model's predictivity is a useful

tool in understanding the phenotypic spectrum of GNAO1 disorders, there are other more commonly seen variants being identified.

The R209H mutation is one of the most commonly seen mutations in the clinical cases [24]. Patients with *de novo* R209H mutations display severe choreoathetosis and dystonia but not a seizure phenotype [13, 18, 23, 62, 91, 93]. Interestingly, the R209H mutation was classified as having normal function in cAMP inhibition, however, it still causes a severe form of movement disorder in patients, often requiring intensive care unit admission [23, 91]. The fact that our initial analysis classified R209H as a normal functioning mutation while it is pathological clinically implies our initial *in vitro* functional readout was not sufficient to fully predict the clinical outcome. Therefore, this specific mutation *R209H* is a good choice for us to expand our initial study.

Heterozygous mutant mice (*Gnao1*<sup>+/*R209H*</sup>) were created on C57BL/6J background with CRISPR/Cas9. Using a battery of behavioral tests, we analyzed the mice to determine the phenotypic correlation between our mouse model and the human patients. There is a wide heterogeneity of movement disorders patterns of patients [5] therefore we use a battery of tests to measure motor skills. Our previous model, *Gnao1*<sup>+/*G203R*</sup> displayed motor abnormalities on a few behavioral tests but they did not show significant differences on the open field test. Here we show that *Gnao1*<sup>+/*R209H*</sup> mice of either sex displayed significant hyperactivity during the open field assessment. This difference in model phenotype may account for differences in specific motor disorders of patients. *Gnao1*<sup>+/*R209H*</sup> mice also did not show enhanced seizure susceptibility to PTZ kindling studies. While expected, these findings are promising as patients with that same mutation display hyperactive movement disorders but do not express a seizure phenotype.

Having a model that displays hyperactivity while lacking seizure susceptibility expands on our previous model and shows similarities to patients with the same mutation who also lack seizure disorders while exhibiting hyperactive movement disorders.

Having this new model allowed us to begin allele-specific preclinical drug testing. The neuroleptic risperidone was reportedly beneficial in a patient with R209H [23]. Here we show that risperidone also attenuates the hyperactivity of our animal model. This implies that risperidone treatment may be beneficial for other *GNAO1* patients with the R209H mutation with hyperkinetic movement disorders.

## Materials and Methods

### **Animals**

*Gnao1*<sup>+/R209H</sup> mice on a C57BL/6J background were generated in the MSU transgenic core. Mice (8-12 weeks old) were housed on a 12-hour light/dark cycle, with *ad libitum* access to food and water. All experiments were performed in accordance with NIH guidelines and protocols were approved by the Michigan State University Institutional Animal Care and Use Committee.

### **Generation of *Gnao1* R209H edited mice**

Mutant *Gnao1*<sup>+/R209H</sup> mice were generated using CRISPR/Cas9 genome editing on a C57BL/6J genomic background. CRISPR gRNA selection and locus analysis was performed using the Benchling platform (Benchling, Inc. San Francisco, CA.). A gRNA targeting exon 6 of the *Gnao1* locus (ENSMUSG00000031748) was chosen to cause a double strand break (DSB) 3bp downstream of codon R209. Single stranded oligodeoxynucleotide (ssODN) carrying the R209H mutation CGC > CAC with short homology arms was used as a repair template (Figure 3-1 and Table 3-1). Ribonucleoprotein (RNP) complexes consisting of crRNA/tracrRNA and Alt-R® S.p. Cas9 Nuclease V3 (Integrated DNA Technologies, Inc. Coralville, IA), were used to deliver CRISPR components along with the ssODN to mouse zygotes via electroporation as previously described [Feng 2017, 2019]. Edited embryos were implanted into pseudo-pregnant dams using standard techniques. Resulting litters were screened by PCR (Phire Green HSII PCR Mastermix, F126L, Thermo Fisher, Waltham, MA.), T7 Endonuclease I assay (M0302, New England Biolabs Inc.) and Sanger sequencing (GENEWIZ, Inc. Plainfield, NJ) for edits of the target site.

**Table 3-1. Location and sequence of gRNA and ssODN template for CRISPR-Cas targeting *Gnao1* locus; primers and genotyping method for *Gnao1*<sup>+/R209H</sup> mice**

	<i>Gnao1</i> R209H
Location	Chr 8: 93,950,334
gRNA target 5' N20-PAM -3'	5' AGCGATCTGAACGCAAGAAG TGG 3'
ssODN template (reverse complement)	GTTTCGTCCTCGTGGAGCACCTGGTCATAGCCGCTGAGTGCGAC ACAGAAGATGATGGCCGTGACATCCTCAAAGCAGTGGATCCACTTCTTG tGTTTCAGATCGCTGGCCCCGACGTCAAACAGCCTGCAGGGAGTCAGGG AAAGCTGTGAGGGCGGGGACGCCTA
PCR primers	O586 FWD: 5' GGACAGGTGTCACAGGGGAT 3' O587 REV: 5' ACTGGCCTCCCTTGGCAATA 3'
Genotyping	By Sanger Sequencing

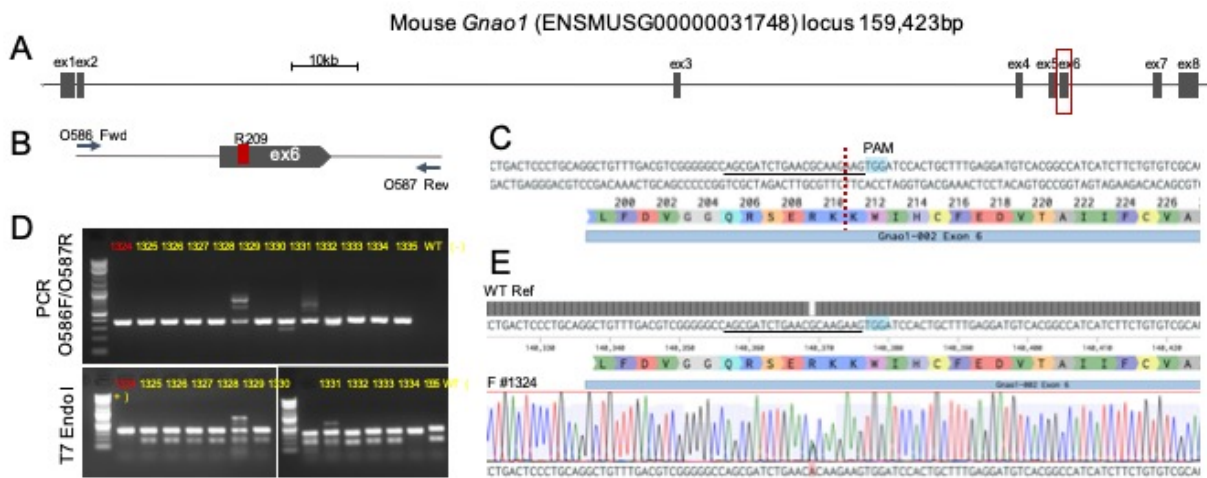


**Figure 3-1. Targeting of the mouse *Gnao1* locus** (A) Mouse *Gnao1* genomic locus (exon size not to scale), red outline is magnified in (B) showing exon 6 and relative location of codon 209, and PCR primers O586 and O587. (C) Location and exact sequence of gRNA target within exon 6, dotted red line denotes DSB, PAM is highlighted and sequence corresponding to gRNA protospacer is underlined (also in E). (D) Raw gel electrophoresis images showing PCR of the target region and T7 Endonuclease I (T7 Endo I) digestion analysis of founders 1324 – 1335 (n=12), with WT, H<sub>2</sub>O (-) and T7Endo I (+) controls. Founder 1324 was positive for the mutation on one allele and WT on the other, note that the single bp mismatch was not reliably detected by T7 Endo I assay. (E) Exact sequence of edited founder 1324 as aligned to WT reference genome, two peaks (G and A) are detected on the sequence chromatogram, indicating the presence of both WT and edited R209H allele.

### ***Genotyping and Breeding***

Studies were done on N1 R209H heterozygotes with comparisons to littermate controls. To generate *Gnao1*<sup>+/R209H</sup> heterozygotes N1 backcrosses, 2 founder *Gnao1*<sup>+/R209H</sup> mice, 1 male and 1 female, were crossed with C57BL/6J mice.

DNA was extracted by an alkaline method (26) ear clips done before weaning. PCR products were generated with primers flanking the mutation site (Fwd 5' GGACAGGTGTCACAGGGGAT 3'; 5' ACTGGCCTCCCTTGGAATA 3'). To produce a X base pair (bp) product reaction conditions were: 0.8 μl template, 4 μl 5x Promega PCR buffer, 0.4 μl 10mM dNTPs, 1 μl 10 μM Forward Primer, 1 μl 10 μM Reverse Primer, 0.2 μl Promega GoTaq and 12.6 μl DNase free water (Promega catalog # M3005, Madison WI). Samples were denatured for 4 minutes at 95°C then underwent 32 cycles of PCR (95° C for 30 seconds, 63° C for 30 seconds, and 72° C for 30 seconds) followed by a 7 minute final extension at 72° C. Ethanol precipitation was done on the PCR products and then samples were sent for Sanger sequencing (GENEWIZ, Inc. Plainfield, NJ).

### ***Developmental Milestone Assessment:***

All tests described below were performed on *Gnao1*<sup>+/R209H</sup> and *Gnao1*<sup>+/+</sup> littermates of either sex on 5-12 days of age (P5,7,10,12). Tests were done in groups so all mice finished one test before the next was performed. Protocols were established based on Feather-Schussler et al [102]. These studies were performed by a male and female researcher.

**Ambulation:** Mice are placed in a clear enclosure where mice are visible from the top as well as the side. For one minute the mice were evaluated and given a score of 0-3. Score of 0

was given if no movement was observed, a score of 1 or 2 was given if slow walking was observed with asymmetric or symmetrical movements respectively. A score of 3 represented fast crawling or walking. Gentle prodding by touching the pup's tail was used to motivate the pup to walk.

**Righting:** Mice were placed on their backs and held in position for 5 seconds. After releasing pups, the time taken to return to prone position was recorded, with a maximum time of 1 minute. Three trials were done, and the average was taken for analysis.

**Negative Geotaxis:** Mice are placed pointed downward on a 45° incline and held for 5 seconds. The time taken for the mice to face upwards was recorded. The maximum testing time was 2 minutes. Three trials were done, and the average was taken for analysis. Mice that fell down the incline or failed to turn were re-tested two additional times. Failure to turn resulted in a score of 2 minutes.

**Grip strength/Hang time:** Mice are placed on a piece of mesh on top of a flat adjustable surface. The Mesh screen is slowly inverted and the approximate angle of the screen when the pup falls off is recorded. If the mouse holds on to the mesh screen until fully inverted, latency to fall is recorded. Three trials were done, and the average was taken for analysis.

**Cliff Aversion:** Mice are placed on the top edge of a box so that their forepaws, digits and snout are over the edge. The time that it takes mice to move from the edge is recorded. This test is repeated 3 times for a maximum of 30 seconds a trial. If the pup does not move away from the edge within 30 sec, a score of 30 seconds is recorded. If the pup falls off the edge, a single additional trial can be performed.

### **Adult Behavioral Assessment**

Between 8-12 weeks of age male and female *Gnao1*<sup>+/R209H</sup> mice and their *Gnao1*<sup>+/+</sup> littermates underwent a battery of behavioral testing to assess motor phenotype as described previously [103]. Before each experiment, mice were acclimated for 10 minutes to the testing room. Experiments were performed by two female researchers.

### **Open Field**

The open field test is frequently used to assess locomotion, exploration and anxiety [68, 104]. The test was conducted in the Fusion VersaMax clear 42 cm x 42cm x 30cm arenas (Omnitech Electronics, Inc. Columbus, Ohio). *Gnao1*<sup>+/R209H</sup> mice of either sex and littermates were placed in the arena for 30 minutes. Using the Fusion Software, we evaluated distance traveled (cm) in terms of novelty, sustained, and total movement corresponding to the first 10 minutes, 10-20 minutes and total of 30 minutes, respectively. As a potential measure of anxiety, the fraction of time spent in the center was assessed. The center area was defined as the 20.32cm x20.32cm area within the middle of the arena.

### **Rotarod**

To assess motor skills in *Gnao1*<sup>+/R209H</sup> mice we used the Economex accelerating rotaRod (Columbus Instruments OH). The entire protocol occurred over a two-day period. Day 1 mice were trained on across three-2 min training sessions, with 10 minutes between each training trial. The first two sessions the rotarod maintained a constant rotational speed of 5 rpm, while the third training trial started at 5 rpm and accelerated 0.1rpm/sec throughout the 2 minutes.

The following day mice ran three more trials, two 2 min trials and a final 5 min trial, with a 10 min break in between. Each of these tests started at 5rpm with constant acceleration of 0.1 rpm/sec. For all training and test trials latency to fall off the spindle was recorded.

### ***Grip Strength***

To assess mouse grip strength, we used seven home-made weights (10, 18, 26, 34, 42, 49, 57 grams). The mouse was held by the middle/base of the tail and lowered to the weight once the mouse grasped the weighted ring with its forepaws the mouse was lifted until weights cleared the bench. For each weight a mouse was given up to three trials to suspend the weight for 3 seconds. If cleared the next heaviest weight was tried, otherwise total time and maximum weight lifted was recorded. Protocol and calculated score was adapted from [51], and normalized to mouse body weight which was measured the day of the test.

### ***DigiGait***

Mouse gait analysis was performed on the DigiGait apparatus (Mouse Specifics, Inc, Framingham, MA). After acclimation, each mouse was subject to run at speed 18, 20, 22, 25, 28, 32, 36 cm/s on DigiGait for 10 sec with a video camera located at the bottom of the belt. There was a 5 min rest between each speed. Then all the recordings were analyzed with DigiGait analysis program.

### ***PTZ Kindling Study***

A PTZ kindling protocol was performed as described [11, 103] to assess mouse susceptibility to epilepsy. Mice were injected with 40mg/kg PTZ (i.p.) every other day and observed for 30 minutes and scored for 24 days. Kindling, which was defined as tonic-clonic seizures on two consecutive injection days or death, marked the end of the study for each animal.

### ***Tests of Risperidone on motor behavior***

Naïve 8-12 week old *Gnao1*<sup>+/R209H</sup> and *Gnao1*<sup>+/+</sup> littermates of either sex were tested for effects of risperidone on their hyperactivity. The entire test occurred over 5 days; 3 days of testing with a break in between each testing day. On Monday mice underwent the open field protocol as described above to establish baseline. Wednesday mice were habituated in the experimental room for 10 min then given a singly i.p. dose of either 2mg/kg, 0.5mg/kg risperidone (Cayman Chemical) or vehicle control. Risperidone was prepared by dissolving in DMSO at a concentration of 5mg/ml, Further dilutions were done in DI water. 30 minutes following injection mice were placed in the open field arena for a 30-minute testing time. On Friday mice underwent the same open field protocol as Monday, this was done to assess locomotor activity following risperidone depletion.

### ***SDS-PAGE and Western Blots***

Mice between 6 to 8 weeks old were sacrifice and their brains were dissected into different regions and flash-frozen in liquid nitrogen. For western blots analysis, tissues were thawed on ice and homogenized with 0.5mm zirconium beads in the Bullet Blender (Next

Advance; Troy, NY) in radioimmunoprecipitation assay buffer (RIPA buffer) with protease inhibitor. Sample homogenates were centrifuged for 5 min at 4°C at 13,000 G. Tissue lysates were then moved to a new tube and protein concentrations were determined using the bicinchoninic acid method (BCA method; Pierce; Rockford, IL). Protein concentration was normalized for all tissues with RIPA buffer and 2x SDS sample buffer containing  $\beta$ -mercaptoethanol (Sigma-Aldrich) as a reducing agent. For all samples and tissue types, 30  $\mu$ g of protein was loaded onto a 12% Bis-Tris gradient gel, and samples were separated by running the gel for 1.5 hrs at 160V. Samples were then transferred to an Immobilon-FL PVDF membrane (Millipore, Billerica, MA) for 2 h at 100 V, 400 mA or overnight at 30V, 50mA on ice and subjected to Quantitative Infrared Western immunoblot analysis. Immediately after transfer, PDVF membranes were washed and blocked in Odyssey PBS blocking buffer (Li-Cor) for 40 min at RT. The membranes were then incubated with anti-G $\alpha$ o (rabbit; 1:1,000; sc-387; Santa Cruz biotechnologies, Santa Cruz, CA) and anti-actin (goat; 1:1,000; sc-1615; Santa Cruz) antibodies diluted in Odyssey blocking buffer with 0.1% Tween-20 overnight at 4°C. Following four 5 min washes in phosphate-buffered saline, 0.1 % Tween-20 (PBS-T), the membrane was incubated for 1h at room temperature with secondary antibodies (both 1:10,000; IRDye<sup>®</sup> 800CW Donkey anti-rabbit; IRDye<sup>®</sup> 680RD Donkey anti-goat; LI-COR Biosciences) diluted in Odyssey blocking buffer with 0.1 % Tween-20. The membrane was subjected to four 5 min washes in PBS-T and a final rinse in PBS for 5 min. The membrane was kept in the dark and the infrared signals at 680 and 800nm were detected with an Odyssey Fc image system (LI-COR Biosciences). The G $\alpha$ o polyclonal antibody recognizes an epitope located between positions 90-140 G $\alpha$ o (Santa Cruz, personal communication).

### ***Statistical Analysis***

This data was analyzed with the unpaired Students *t*-test, Mantel-Cox, *two-way* ANOVA with Bonferroni corrections. All analysis was done using Graphpad Prism 7.0 (GraphPad; La Jolla, CA). Multiple comparison correction of the dataset from DigiGait was performed as described before [103]. A  $p < 0.05$  was considered critical value for significant throughout the entire study. Detailed discussion can be found within figure legends.

## Results

### ***Gnao1<sup>+ /R209H</sup> mice have expected frequency and normal viability***

Out of 98 offspring, 51 heterozygotes and 47 WT were observed between a cross of *Gnao1<sup>+ /R209H</sup>* with WT mice. *Gnao1<sup>+ /R209H</sup>* mice exhibit no overt postural abnormalities at basal conditions. Weights between adult mice showed no statistically significant differences between WT and Het of either sex.

### ***Gnao1<sup>+ /R209H</sup> Mice display delayed development of milestones on assessments of negative geotaxis***

As children with *GNAO1* exhibit motor developmental delay and intellectual delay [18, 23, 62, 93], we assessed mice pups between P4 to P12 for neonatal motor deficits. *Gnao1<sup>+ /R209H</sup>* mice exhibited a reduced time to prone position at P7 during the negative geotaxis test compared to their wildtype littermates (Figure 3-2C). This might suggest a motor coordination delay which is consistent with patient observations. The model showed no significant differences in ambulation, righting reflex, cliff avoidance, and hang time (Figure 3-2A, 3-2B, 3-2D).

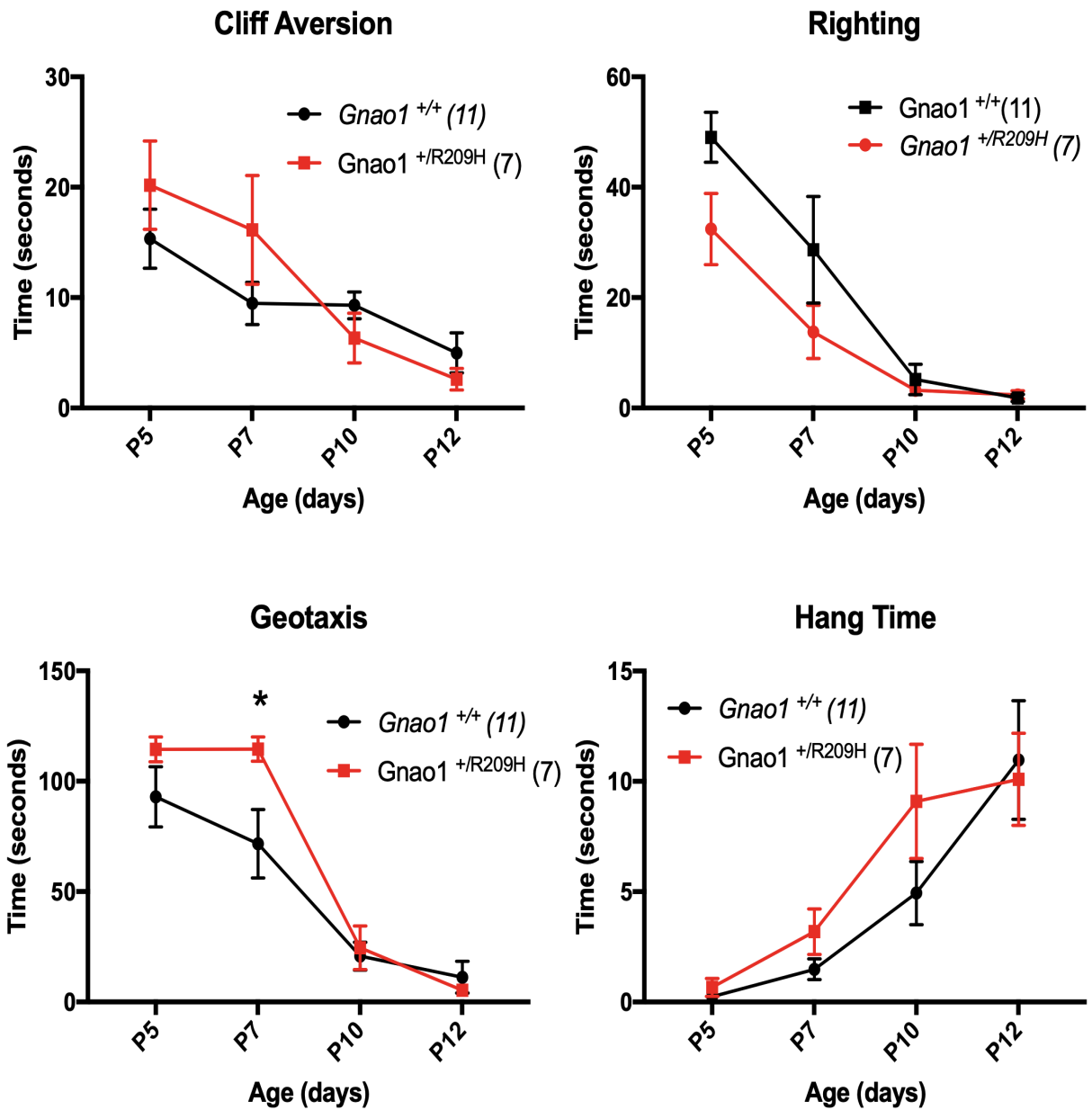


**Figure 3-2.** *Gnao1*<sup>+/R209H</sup> exhibited a developmental delay during the negative geotaxis assessment (A-C) *Gnao1*<sup>+/R209H</sup> mice do not exhibit significant delays in the cliff aversion, righting or hang time tests. (C) *Gnao1*<sup>+/R209H</sup> exhibit a delay on P7 compared to wildtype littermates (2-way ANOVA with Bonferroni multiple comparison post-test).

### ***Gnao1<sup>+R209H</sup> of either sex have hyperactive phenotype in the Open Field arena***

Patients with R209H mutation present with hyperkinetic movement disorders [18, 23, 62, 93]. In order to see if our mouse model phenocopied patients of the same mutation, *Gnao1<sup>+R209H</sup>* mice were subject to a battery of behavioral tests. Open field arena was used to test overall locomotion activity. It was reported that novel environments may overshadow potential behavioral impairments [69]. To account for this, we divided the test into two sections, novelty as the first 10 minutes then minutes 10-30 as sustained time. *Gnao1<sup>+R209H</sup>* mice of both sexes showed significantly increased activity in the novel period compared to their wildtype littermates. However, both male and female *Gnao1<sup>+R209H</sup>* displayed significant hyperactivity in the sustained period of the open field test as well (Figure 3-3B). This suggests the observed hyperkinetic movements are due to strain differences but not environmental salience. Additionally, the open field test may be used to assess anxiety-like behaviors. In a measure for anxiety-like behavior male and female *Gnao1<sup>+R209H</sup>* mice also displayed reduced time in center (Figure 3-3B). An accelerating rotarod was used to assess motor coordination and balance. Neither male nor female *Gnao1<sup>+R209H</sup>* mice display an impaired performance (Figure 3-3C). Grip strength, which is used to assess for differences in neuromuscular tone showed no differences between *Gnao1<sup>+R209H</sup>* and wildtype littermates in either sexes (Figure 3-3D).

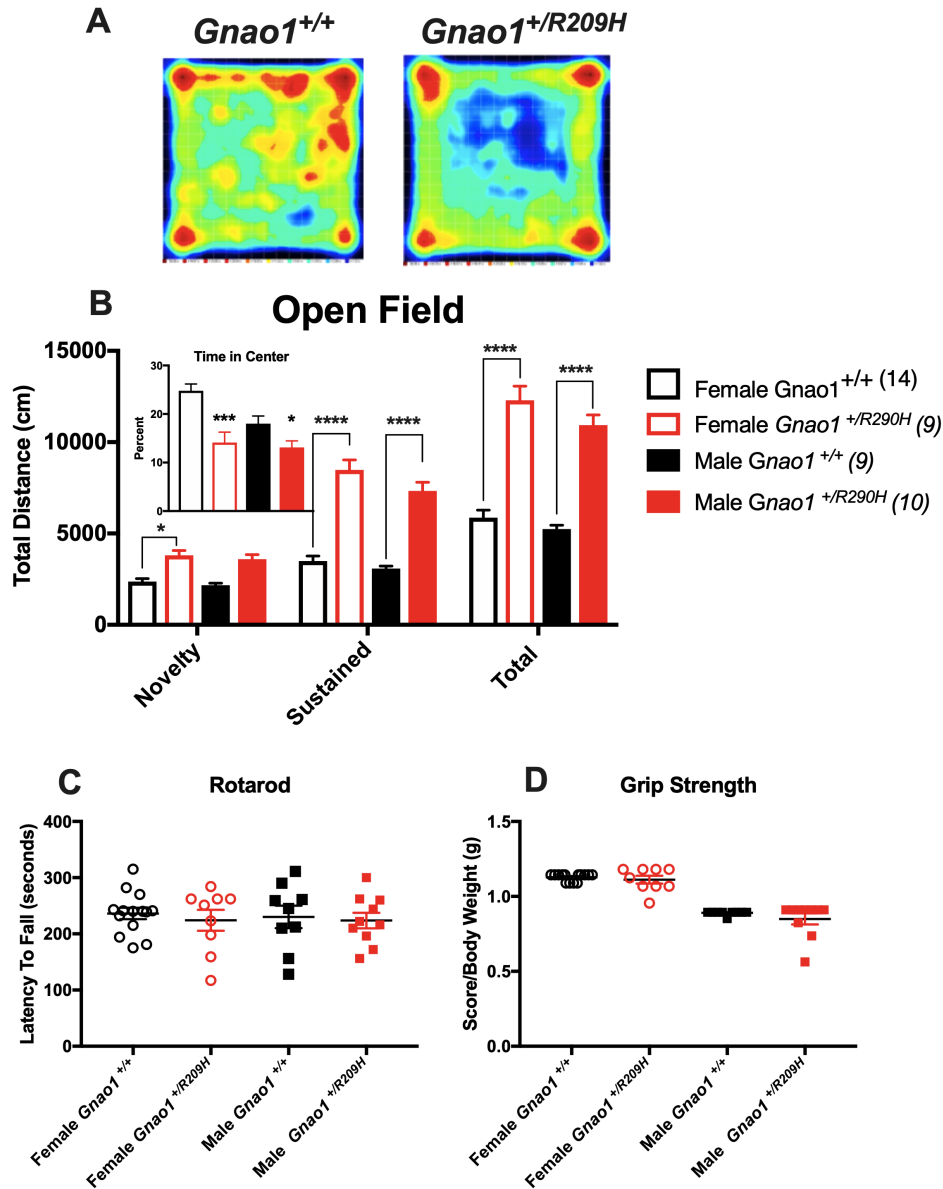


**Figure 3-3. *Gnao1*<sup>+/R209H</sup> shows significant hyperactivity and reduced time in center in the open field arena** (A) Representative heat maps show *Gnao1*<sup>+/R209H</sup> comparing time *Gnao1*<sup>+/+</sup> and *Gnao1*<sup>+/R209H</sup> (B) Time spent in the open field arena was separated by time of 0-10 minutes (novelty) and 10-30 minutes (sustained). *Gnao1*<sup>+/R209H</sup> male and female mice exhibit increased locomotion in the novelty period. Hyperactivity was maintained throughout the sustained period as mice continued to show significant increase in distance traveled (cm) (2- way ANOVA; \*\*\*\*p < 0.0001, \*\*\*p < 0.001, \* p < 0.05). *Gnao1*<sup>+/R209H</sup> Mice of both sex spend less time in center areas of the open field arena compared to wildtype littermates. (C) Male nor female *Gnao1*<sup>+/R209H</sup> mice show significant differences on the rotarod. (D) There is no significant difference between grip strength between wildtype and *Gnao1*<sup>+/R209H</sup> mice. Data are shown as mean ± SEM.

**Male *Gnao1*<sup>+/*R209H*</sup> mice display reduced stride length**

Gait patterns were assessed using DigiGait analysis. Male *Gnao1*<sup>+/*R209H*</sup> mice showed reduced stride length compared to wildtype littermates (P<0.001, 2-way ANOVA). Female *Gnao1*<sup>+/*R209H*</sup> mice do not show significant differences from WT (Figure 3-4C & 3-4D). However, the female *Gnao1*<sup>+/*R209H*</sup> showed a significantly reduced maximum speed to run on the treadmill (Figure 3-4E).

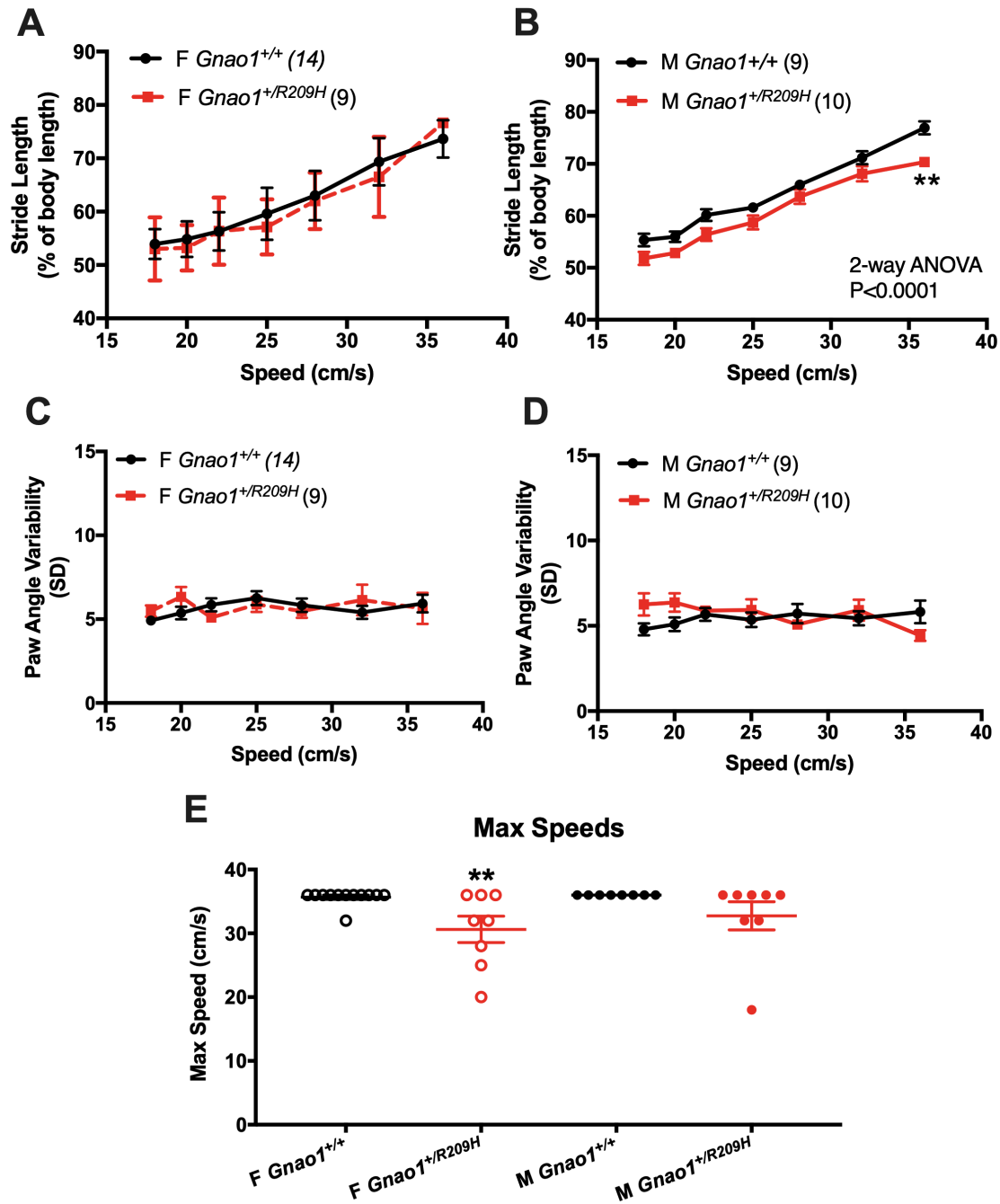


**Figure 3-4. Male and Female *Gnao1*<sup>+/R209H</sup> mice shows gait abnormalities in different tests on the DigiGait imaging system (A & B) Male *Gnao1*<sup>+/R209H</sup> mice showed reduced stride length compared to wildtype littermates(2-way ANOVA with Bonferroni multiple comparison post-test) , while female *Gnao1*<sup>+/R209H</sup> mice remain normal. (C & D) Neither male or female *Gnao1*<sup>+/R209H</sup> exhibited significant differences in stride length compared to wildtype littermates. (E) at speeds greater than 25 cm/s Female *Gnao1*<sup>+/R209H</sup> shows reduced ability to run on a treadmill**

***Gnao1*<sup>+/R209H</sup> mice are not sensitive to PTZ kindling**

Repeated application of a sub-threshold convulsive stimulus, leads to the generation of full-blown convulsions [72]. GNAO1 variants differ in their ability to cause epileptic seizure, *GNAO1*<sup>+/R209H</sup> patients do not exhibit seizure disorders [18, 23, 62, 93]. In accordance with the patients' symptoms, *Gnao1*<sup>+/R209H</sup> mice of neither sex showed increased susceptibility to epileptic seizures (Figure 3-5 A&B).

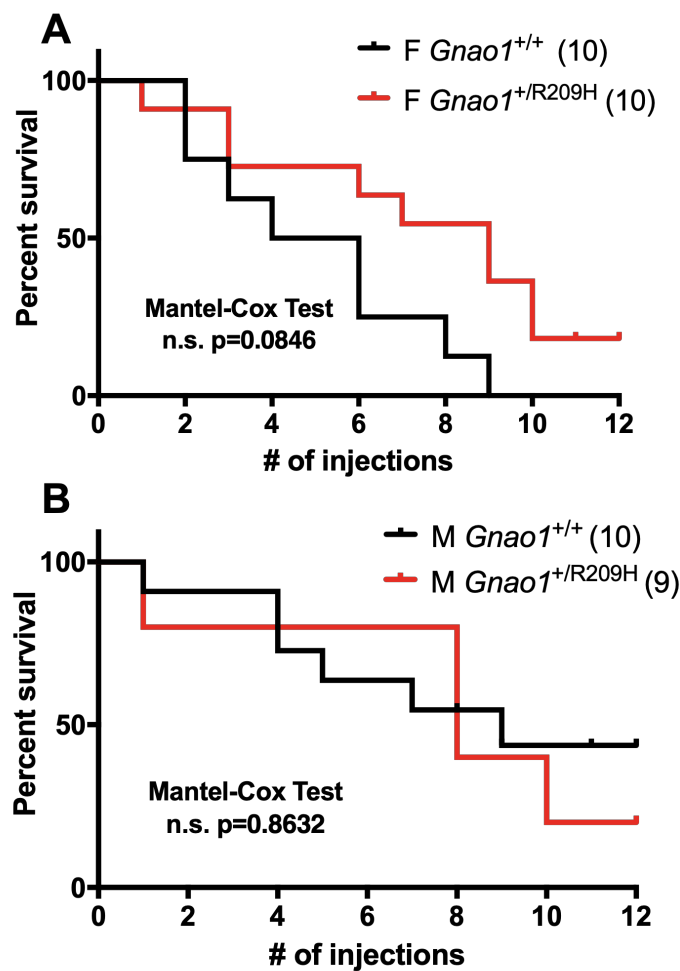


**Figure 3-5. *Gnao1*<sup>+/R209H</sup> mice do not have an enhanced Pentylentetrazol (PTZ) kindling response (A&B)** Neither Male or female *Gnao1*<sup>+/R209H</sup> mice showed significant differences in sensitivity to PTZ injection compared to wildtype littermates. Mantel-cox test ns

### ***Risperidone treatment attenuated the hyperactivity of $Gnao1^{+/R209H}$ mice***

Patients with *GNAO1* mutations were tested with multiple treatments to alleviate motor symptoms, (Table 3-2). Risperidone, an atypical antipsychotic drug showed effects in one of the patients. In the literature, risperidone has also been shown to control drug-induced dyskinesia [105]. We show that  $Gnao1^{+/R209H}$  mice exhibit complete abrogation of movement at 2mg/kg risperidone, which recovers after 2 days (Figure 3-6A&C). WT mice also show a significant decrease in locomotion after 2mg/kg risperidone treatment (Figure 3-6A). After a single 0.5mg/kg dose of risperidone both WT and  $Gnao1^{+/R209H}$  mice exhibit a decrease in locomotion (Figure 3-6B). As expected, hyperactivity of mutant mice was observed during baseline testing on day 1. The hyperactivity returned following a 2-day washout period (Figure 3-6C). Neither 2.0 mg/kg nor 0.5 mg/kg selectively affected  $Gnao1^{+/R209H}$  as assessed by percent suppression (Supplement Figure 3-1).

**Table 3-2. GNAO1 R209H patient classification**

Patient No.	Sex	Amino Acid Change	Age of Onset	Presence of Epilepsy	Movement Disorder	Treatment	Motor Developmental Delay(MDD)/Intellectual Delay(ID)	Reference
1	M	R209H	17 mo	-	Chorea	DBS	MDD	Kulkarni et. al (2016)
2	M	R209H	2 y	-	Chorea	DBS	MDD	Kulkarni et. al (2016)
3	M	R209H	3 y	-	Chorea	Risperidone, BZD	MDD/ID	Anath et. al (2016)
4	M	R209H	1 y	-	Chorea	NA	MDD/ID	Menke et al (2016)
5	M	R209H	10 mo	-	Chorea Dystonia	TBZ, THP	MDD/NA	Dhamija et al (2016)
6	M	R209H	15 mo	-	Chorea, Dystonia	DBS	MDD/ID	Marecos et al (2018)
7	F	R209H	6 mo	-	Dystonia	NA	MDD/MID	Kelly et al (2018)
-	F	R209C	NA	NA	Chorea	NA	MDD/ID	Saitsu et al (2016)
-	F	R209G	3 y	-	Chorea	None	MDD/ID	Anath et al (2016)
-	M	R209L	2 y	-	Chorea	NA	MDD/ID	Menke et al (2016)

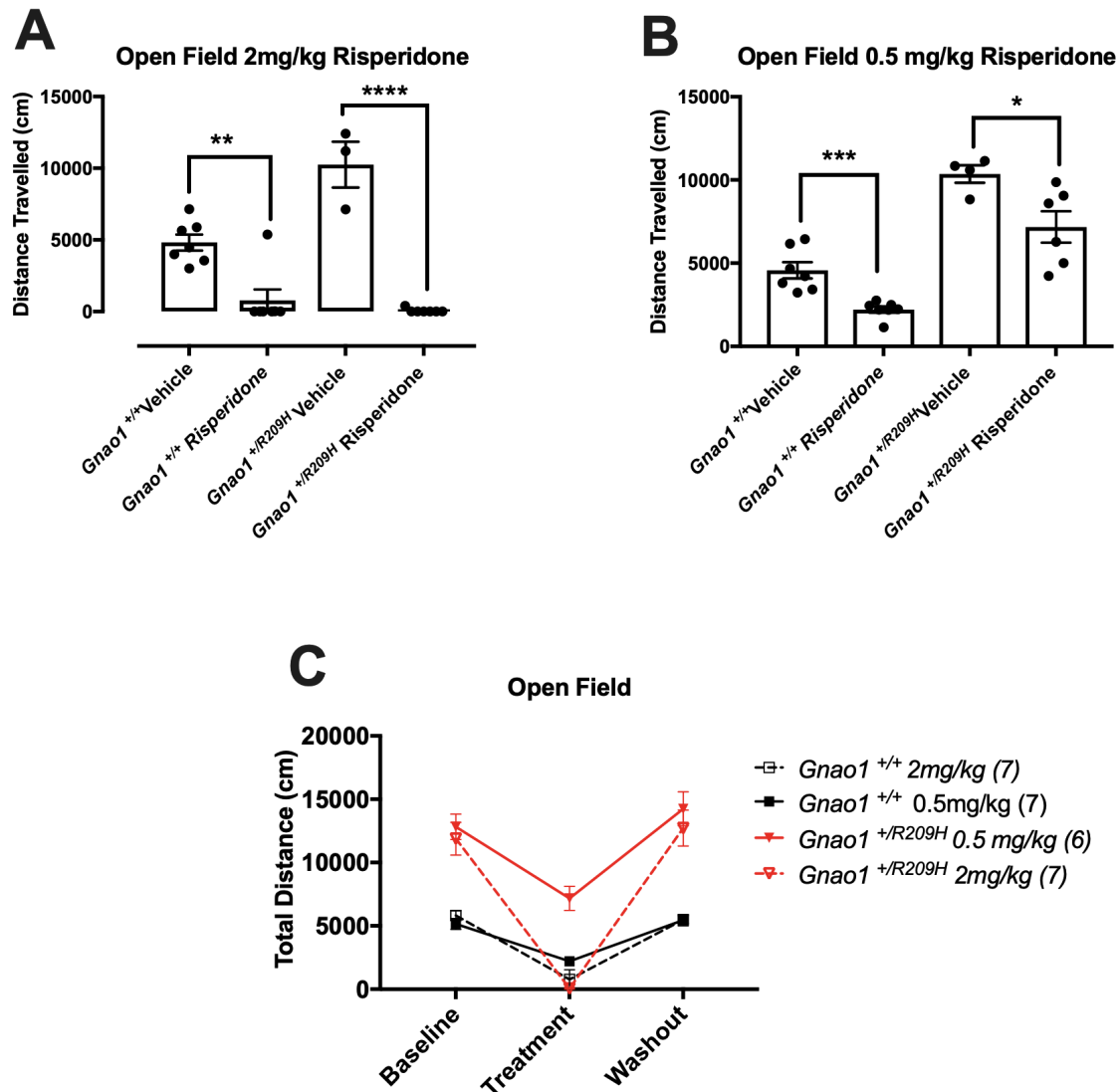


**Figure 3-6. Risperidone treatments decreases hyperkinetic movements in *Gnao1*<sup>+/R209H</sup>**

(A) *Gnao1*<sup>+/R209H</sup> mice show complete abrogation of movement compared to vehicle treated *Gnao1*<sup>+/R209H</sup> following a 2.0 mg/kg dose of risperidone. Students unpaired T-test (B) At 0.5 mg/kg both WT and *Gnao1*<sup>+/R209H</sup> exhibit a significant decrease in locomotion. Students unpaired T-test. Wildtype mice also show a decrease in locomotion after 0.5 mg/kg risperidone treatment, (C) Comparison of 2.0 mg/kg and 0.5 mg/kg treatment in WT and *Gnao1*<sup>+/R209H</sup> mice. Hyperactivity of *Gnao1*<sup>+/R209H</sup> mice was observed during baseline testing and recovered following the 2-day risperidone washout.

***Gnao1*<sup>+/<sup>R209H</sup></sup> mice did not show any abnormality in  $G\alpha_o$  protein expression**

Cortex, hippocampus, striatum, cerebellum, brain stem and olfactory bulb were harvested and homogenized to measure mutation R209H's effect on  $G\alpha_o$  protein expression level. Western blots showed no difference in the above brain regions of  $G\alpha_o$  protein expression between WT and *Gnao1*<sup>+/<sup>R209H</sup></sup> (Figure 3-7), which is consistent with our tested protein expression level in HEK293T cells with transiently transfected R209H plasmid [19]

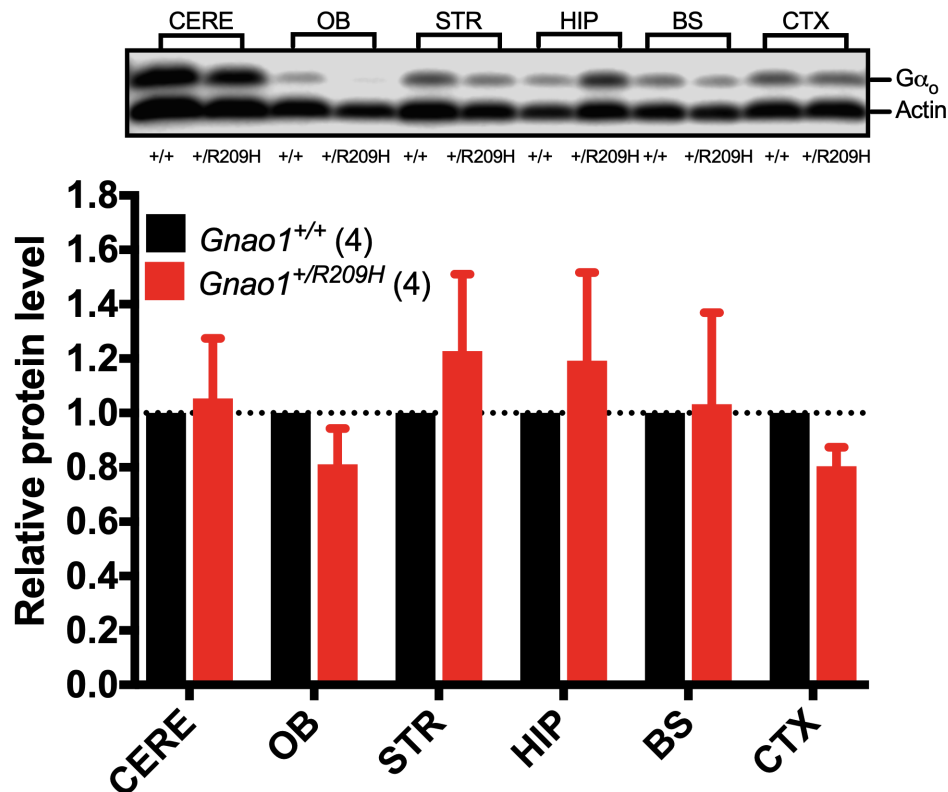


**Figure 3-7. Western blot shows no statistical difference in  $G\alpha_o$  protein between *Gnao1*<sup>+/<sup>R209H</sup></sup> and WT mice** Brain regions (cortex, hippocampus, striatum, cerebellum, brain stem and olfactory bulb homogenates) from WT and *Gnao1*<sup>+/<sup>R209H</sup></sup> mice were quantified for levels of  $G\alpha_o$  protein. There was no significant difference in any of the regions between WT and mutant mice.

## Discussion

Here we show that the *Gnao1 R209H* mutant mice display both motor and developmental abnormalities which is consistent with R209H patients, who present with psychomotor delay with the presence of involuntary movements (NEDIM). The mouse developmental milestones showed a significant delay in onset of negative geotaxis. Differences in this test likely correlate with a delay in motor coordination [102]. The *Gnao1*<sup>+/R209H</sup> mice displayed a significant hyperkinetic phenotype in the open field arena and shorter stride length on digigait analysis. Moreover, we also showed that R209H mice are also not sensitive to PTZ-kindling. All the above results are consistent with human patients with the R209H mutation. Interestingly, *Gnao1*<sup>+/R209H</sup> mice did not display any significant differences in the RotaRod test, which is traditionally used to assess motor coordination of rodents [51]. In addition, there were no significant differences observed from the grip strength assessment. This result was unexpected as our previous *GNAO1* Mouse model, *Gnao1*<sup>+/G203R</sup>, showed significant motor impairments in the both tests [103]. Patients with either the G203R or R209H mutations both display movement disorder; however, patients with the G203R variant have been reported with chorea, dystonia and/or dyskinesias [4] while patients with the R209H variant most commonly are diagnosed with chorea[3]. One likely explanation for the motor differences between the mutant mouse models might be behind the heterogeneity of movement disorders between patients. As hyperkinetic movements in patients have been shown to be exacerbated under stress, illness or high temperature [23, 61], it would be interesting to see if we could induce abnormalities through physical or pharmacological induction.

It is important to find an effective treatment as patients with the R209H mutation experience multiple incidents of hospitalizations [23, 24, 91]. Deep brain stimulation in the Globus pallidus has proven effective in *GNAO1* patients in attenuating MD [18, 63, 65, 92]. However, the invasive treatment is reserved for refractory patients. Risperidone is one of the oral treatments that has proven to be beneficial, specifically in a patient with the R209H mutation [23]. Risperidone is an atypical neuroleptic, antagonizing D<sub>2</sub> and 5-HT receptors. G $\alpha_o$  couples to a myriad of G-protein coupled receptors including the dopamine D<sub>2</sub> receptor which is involved in movement control [106]. In our experiment, risperidone was able to significantly decrease the hyperlocomotion seen in our heterozygous mutant. This is a promising finding which might allow physicians to narrow down which drugs they try first in the patients. At both the 0.5 mg/kg and 2.0 mg/kg dose of risperidone, hyperactivity was attenuated in our R209H mouse model. However, this response was not selective to our *Gnao1*<sup>+/*R209H*</sup> model as the WT mice also displayed a significant decrease in locomotion. This outcome suggests that risperidone treatment may be effective in repressing global movement, while not specifically targeting a R209H mechanism.

While G $\alpha_o$  regulates cAMP production through AC, studies have shown that G $\alpha_o$  also negatively regulates N-type calcium channels in the presynaptic nerve terminal, reducing release of neurotransmitters [37]. Mutations in other genes known to regulate neurotransmitter release have also been found in individuals with motor impairments [107, 108]. To look into this, future studies should be done to measure concentration of released dopamine and 5-HT within the brains of the *Gnao1*<sup>+/*R209H*</sup> mice.

In our previous work, we uncovered a mutation pattern where GOF mutations for to cAMP inhibition are associated with movement disorders and LOF mutations correlate to EIEE17[19]. However, in that model the R209H mutation was classified as having normal-function. This possibly implies that the mechanism is more complex than cAMP inhibition. Since the canonical pathways of  $G\alpha_o$  also include  $G\beta\gamma$ -mediated inhibition of N-type calcium channels and activation of GIRK channels, it is possible that the R209H mutation could affect other mechanistic pathways of *GNAO1*.

## CHAPTER 4: CONCLUSIONS AND FUTURE DIRECTIONS

The goals of my thesis work were to: 1) define a phenotype in various *GNAO1* mutant mouse models, 2) assess those models' response to pharmacological treatments and 3) begin to elucidate molecular differences within the models.

In Chapters 1 and 2, we defined 3 animal models with gain-of-function associated mutations; *Gnao1*<sup>+/*G184S*</sup>, *Gnao1*<sup>+/*G203R*</sup>, and *Gnao1*<sup>+/*R209H*</sup>. Aside from the G184S model which has not been found in patients, each of these models displayed behavioral abnormalities consistent with patients presenting with the same variant. We were then able to use these models in studying response to treatment in an allele-specific personalized medicine approach. While both trihexyphenidyl and risperidone alleviated MD symptoms in certain patients, only risperidone treated mice showed suppression of the mutant phenotype. Biologically, risperidone works by inhibiting dopamine and 5-HT. As it was effective in reducing the hyperactive phenotype it is possible that this is a mechanism by which R209H variants, alter movement in the patients; however, as risperidone did not seem to exert a more significant effects on the *Gnao1*<sup>+/*R209H*</sup> mice compared to wildtype mice, this needs to be further studied.

G $\alpha_o$  has been shown to decrease release of neurotransmitters through modulation of potassium and calcium channels [5, 6] as well as by direct effects on the vesicle release machinery [109]. Surprisingly in our *Gnao1*<sup>+/*G203R*</sup> model we showed no statistically significant decrease within any neurotransmitters we measured by HPLC. In fact, we saw an increase in the amount of norepinephrine within the brain hemisphere samples of the *Gnao1*<sup>+/*G203R*</sup> mice. This result may be less surprising as norepinephrine serves as both pro and anti-convulsant in models of epilepsy [85]. Therefore, our result showing increased amounts of epinephrine in a model positive for PTZ sensitivity, may serve as an indicator that in patients with EIEE, norepinephrine may be playing a

proconvulsant role. Follow-up studies looking at the effects depletion of norepinephrine has on our PTZ kindling test might be useful in indicating a treatment option for *GNAO1* patients presenting with epilepsy.

We analyzed neurotransmitters only for our G203R mice; future studies should also be done to look at our other model *Gnao1*<sup>+/*R209H*</sup> as well. Additionally, our first analysis used an entire brain hemisphere to look at neurotransmitters. It is widely known that movement is controlled within specific regions of the brain including the striatum and the cerebellum. It is also known that our protein of interest  $G\alpha_o$  is respectively more abundant within the cerebellum, striatum and hippocampus [1]. By choosing to first look at the whole brain, we may have missed subtle regional differences that other areas compensate for. Additionally, the lack of significant difference between WT and mutant might be due to the differences between total levels of neurotransmitters and specific amount of neurotransmitters released. Future work should be done in analyzing regions specific to both movement and the  $G\alpha_o$  protein targeting amount of released neurotransmitters.

We saw that the nonselective cholinergic agonist, oxotremorine brought about motor and postural abnormalities in the *Gnao1*<sup>+/*G203R*</sup> mice that were not as pronounced in WT mice. Interestingly, pilot studies using trihexyphenidyl, a cholinergic antagonist showed no reprieve of motor abnormalities. As such it may be valuable to test the response of *Gnao1*<sup>+/*G203R*</sup> mice to a nonselective cholinergic antagonist or an M2 selective antagonist such as benztropine.

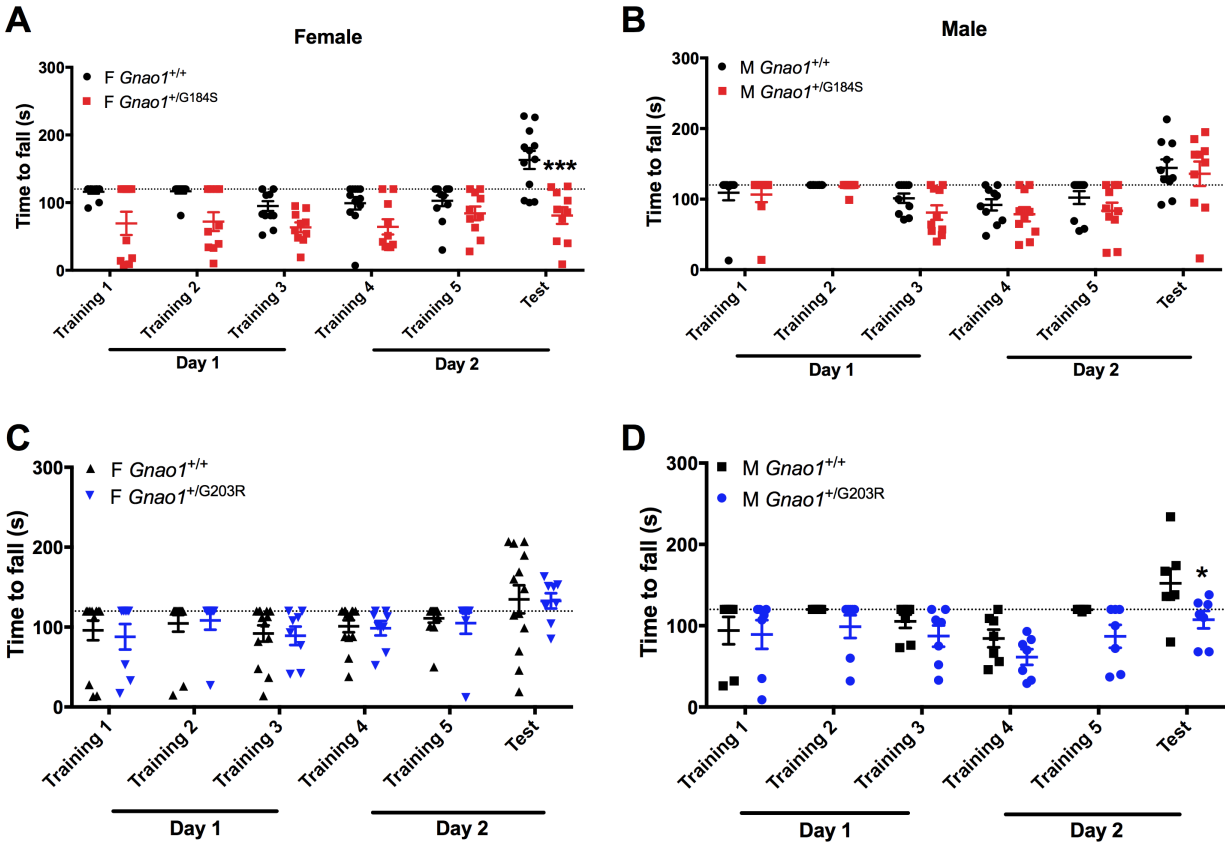
This work assessed on 2 out of the 35 *GNAO1* variants that are currently known. However, with the increasing availability of genomic sequencing, more patients and more variants, of *GNAO1* will likely be identified. It would be beneficial to try and create different variant models.

The ultimate goal of creating predictive animal models of human *GNAO1* mutations is to apply what we learn about the mechanisms of  $G\alpha_o$  mutations from those models to clinical applications. Overall from work described here in my thesis, I have identified 2 comparative models that will continue to be useful in researching the *GNAO1*-associated disorders of NEDIM and EIEE17. The *Gnao1*<sup>+/*R209H*</sup> and *Gnao1*<sup>+/*G203R*</sup> mouse models should be able to guide drug repurposing efforts.

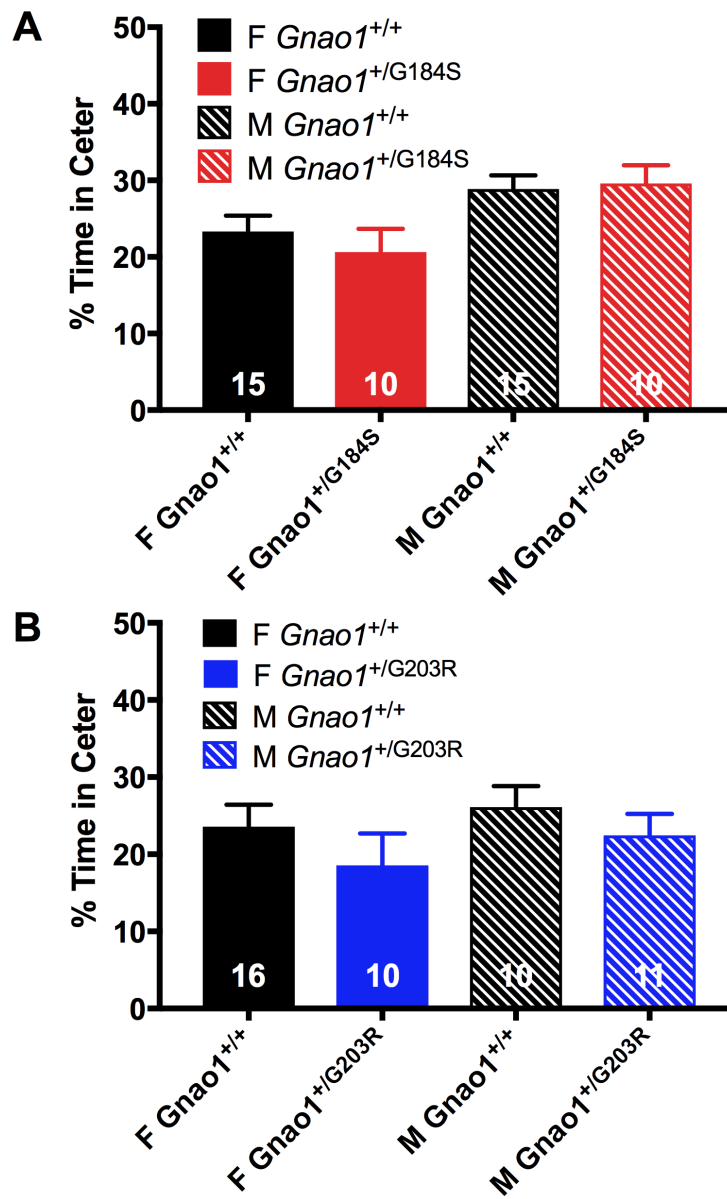
## **APPENDICES**

## **APPENDIX A**

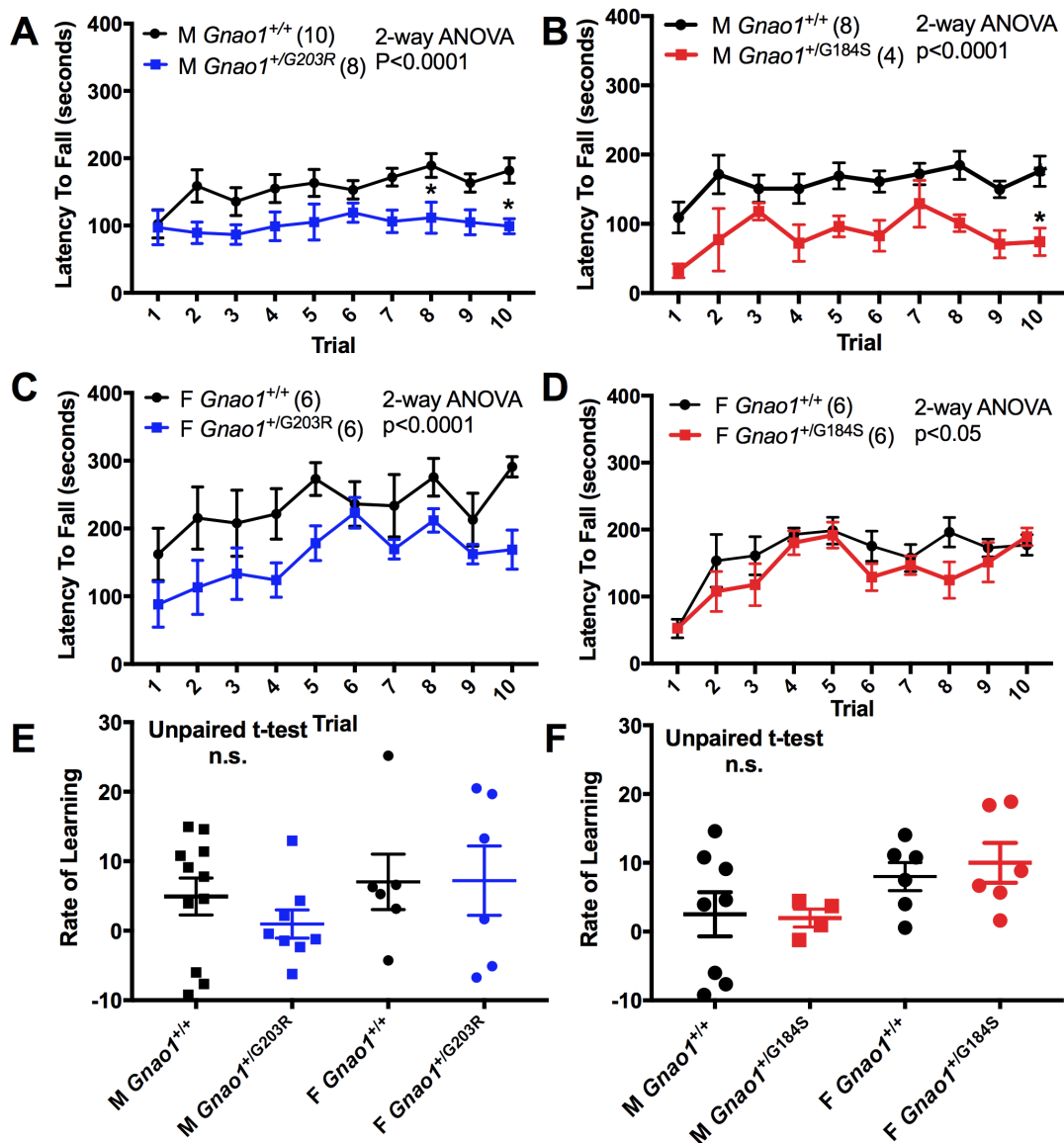
### **Chapter 2**



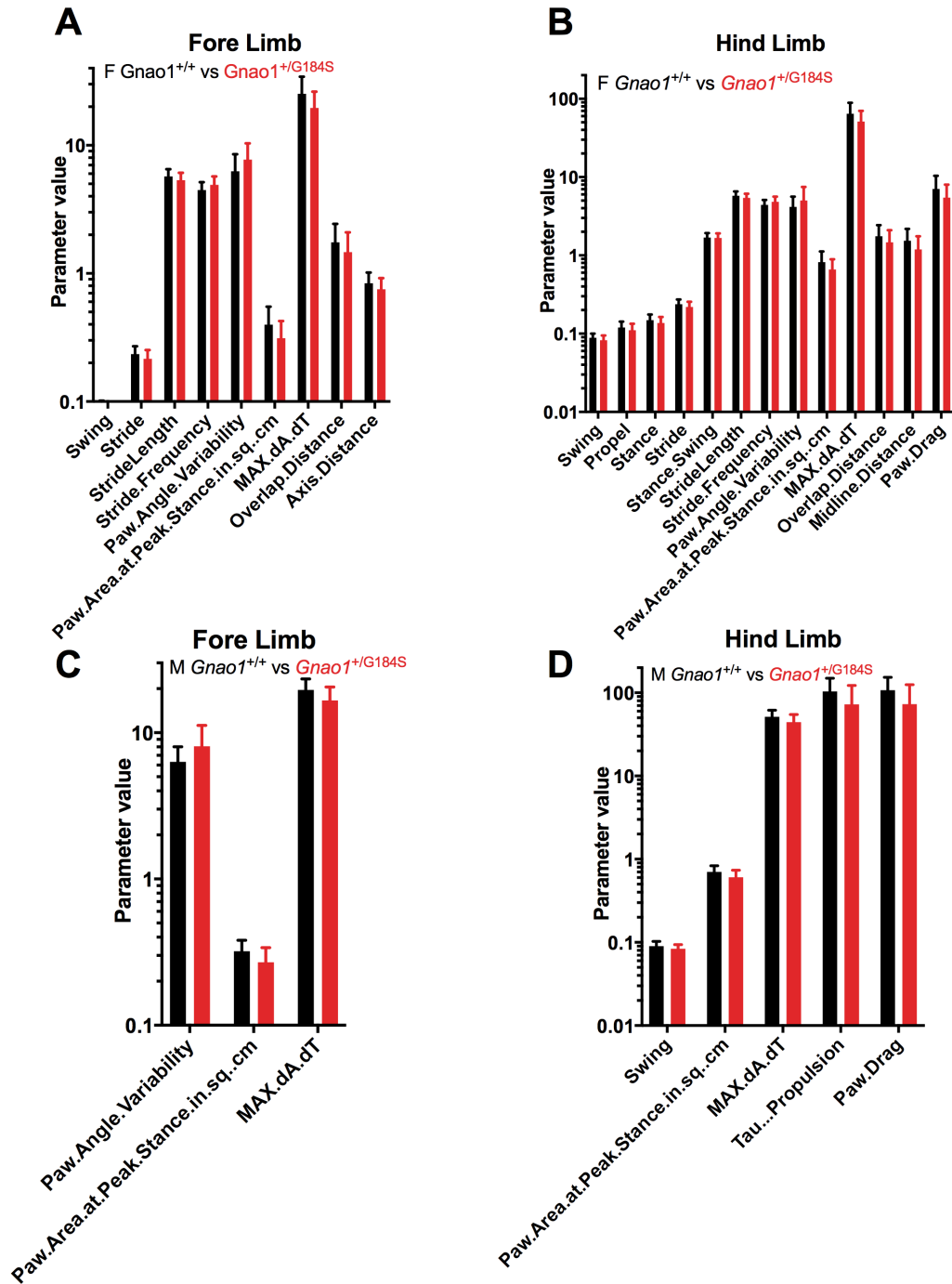
**Supplemental Figure 2-1. RotaRod test was conducted with 5 training sessions and 1 test session over two consecutive days (A) Female *Gnao1*<sup>+/G184S</sup> mice showed significantly motor abnormalities in test trial at day 2 (unpaired t-test; \*\*\*p<0.001). (B) Male *Gnao1*<sup>+/G184S</sup> mice did not show any significance in any training or test session. (C) Female *Gnao1*<sup>+/G203R</sup> mice did not exhibit any motor abnormalities in any RotaRod trial or test session. (D) Male *Gnao1*<sup>+/G203R</sup> mice showed significantly decreased capability in motor balance (unpaired t-test; \*p<0.05).**



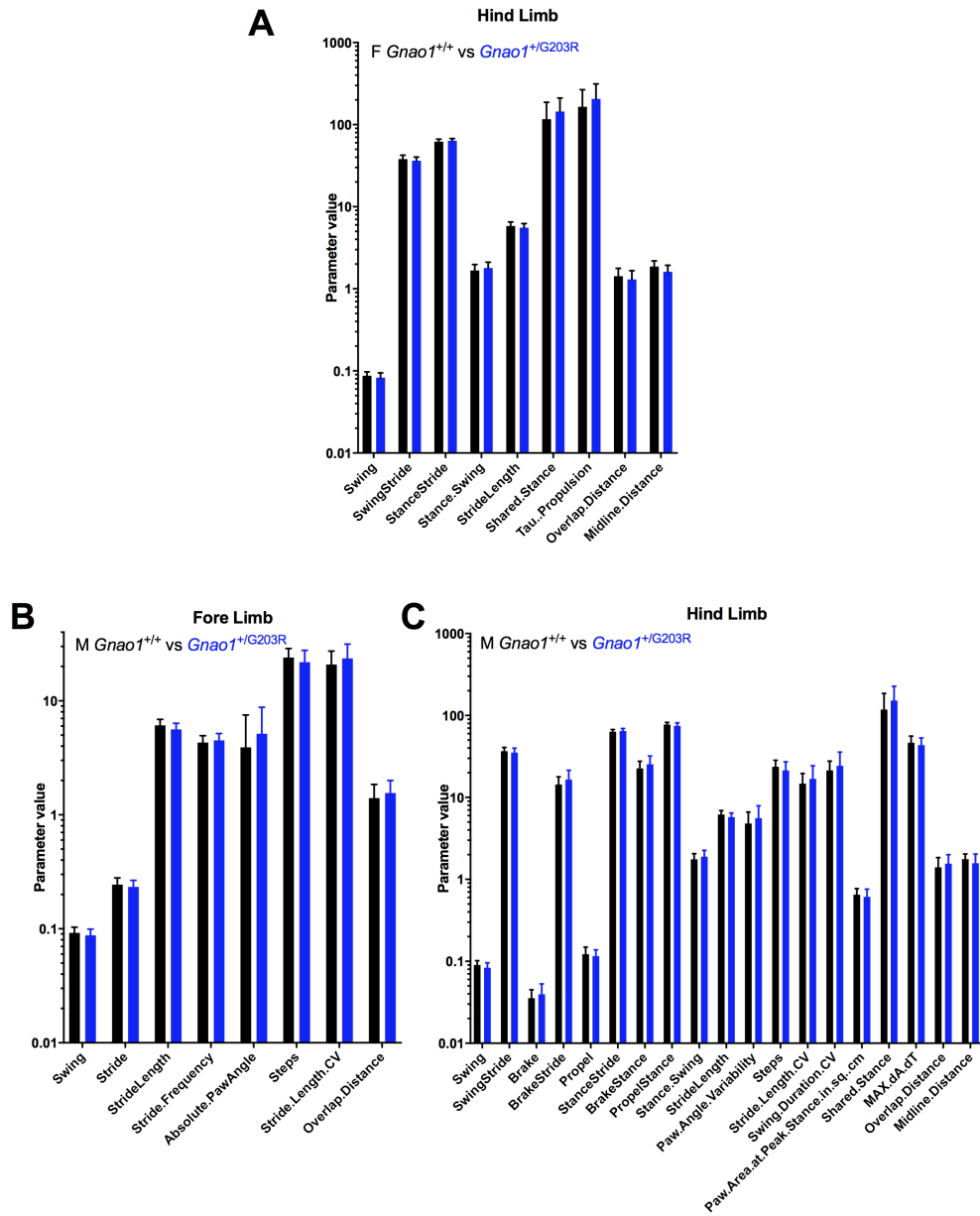
**Supplemental Figure 2-2. Time spent at the center in the Open Field Test** A) No significant differences were observed between *Gnao1*<sup>+/G184S</sup> mice and their littermate controls. B) No significant differences were observed between *Gnao1*<sup>+/G203R</sup> mice and their littermate controls.



**Supplemental Figure 2-3.** RotaRod learning curve was collected in 10 consecutive tests with a 5-min break between each test (A, C & E) Short-term learning curve comparison between  $Gnao1^{+/+}$  and  $Gnao1^{+/G203R}$  in both sexes. (A & C) Both male and female  $Gnao1^{+/G203R}$  mice showed reduced capability of keeping balance on RotaRod. (E) No significant difference in either sexes between  $Gnao1^{+/+}$  and  $Gnao1^{+/G203R}$  mice was observed comparing the rate of learning. (B, D & F) Short-term learning curve comparison between  $Gnao1^{+/+}$  and  $Gnao1^{+/G184S}$  in both sexes. (B & D) Both male and female  $Gnao1^{+/G184S}$  mice showed reduced capability of keeping balance on RotaRod. (F) No significant difference in either sexes between  $Gnao1^{+/+}$  and  $Gnao1^{+/G184S}$  mice was observed comparing the rate of learning.



**Supplemental Figure 2-4. False discovery rate (FDR) calculation probed through all the parameters given by DigiGait in *Gnao1*<sup>+/G184S</sup> mice** All parameters showed significance at belt speed 25 cm/s are plotted. A&B) Female *Gnao1*<sup>+/G184S</sup> and their littermate controls showed parameters with significance detected by the FDR analysis. C&D) Male *Gnao1*<sup>+/G184S</sup> and their littermates controls showed parameters with significance detected by the FDR analysis. FDR is calculated by a two-stage step-up method of Benjamini, Krieger and Yekutieli. Significant values are defined as  $q < 0.01$ .



**Supplemental Figure 2-5. False discovery rate (FDR) calculation probed through all the parameters given by DigiGait in *Gnao1*<sup>+/G203R</sup> mice** All parameters that showed significance are plotted here. A&B) Female *Gnao1*<sup>+/G203R</sup> and their littermate controls showed 9 parameters with significance detected by the FDR analysis. C&D) Male *Gnao1*<sup>+/G203R</sup> and their littermates controls exhibited 27 parameters with significance detected by the FDR analysis in fore and hind limb data combined. FDR is calculated by a two-stage step-up method of Benjamini, Krieger and Yekutieli. Significant values are defined as  $q < 0.01$ .

## Supplemental Table 2-1. Gait analysis parameters Male Gnao1 G203R mutants

Feng et al Table S1 Gait analysis parameters Male Gnao1 G203R mutants

Measured Parameter	Fore Limb		Hind Limb		Fore Limb						Hind Limb					
	p	FDR	p	FDR	M Gnao1+/+	SD	n	M Gnao1+/G203R	SD	n	M Gnao1+/+	SD	n	M Gnao1+/G203R	SD	n
Swing	0.000086	Yes	<0.000001	Yes	0.09211667	0.0111967	180	0.08760833	0.01176783	240	0.09002222	0.01187409	180	0.08343333	0.01239566	240
X.SwingStride	0.560859	No	0.000966	Yes	38.07777778	3.54836583	180	37.85083333	4.2332119	240	36.68666667	3.98361729	180	35.24083333	4.70652526	240
Brake	0.653649	No	0.000399	Yes	0.06939444	0.016458	180	0.06865	0.01707632	240	0.03542222	0.0096027	180	0.0396125	0.01337189	240
X.BrakeStride	0.060086	No	<0.000001	Yes	28.40222222	4.89821488	180	29.43125	5.96865439	240	14.345	3.47436381	180	16.53625	4.86819351	240
Propel	0.003957	No	0.006698	Yes	0.08235556	0.01995907	180	0.076825	0.01889352	240	0.12215	0.0268225	180	0.115625	0.0221926	240
X.PropelStride	0.105634	No	0.088909	No	33.52	4.68472378	180	32.71791667	5.25089869	240	48.96611111	4.21758972	180	48.225	4.54530426	240
Stance	0.020015	No	0.413195	No	0.15173889	0.02844761	180	0.1454875	0.02613979	240	0.15759444	0.03072707	180	0.15522917	0.02815843	240
X.StanceStride	0.560859	No	0.000966	Yes	61.92222222	3.54836583	180	62.14916667	4.2332119	240	63.31333333	3.98361729	180	64.75916667	4.70652526	240
Stride	0.001621	Yes	0.010476	No	0.24383333	0.03618381	180	0.23310833	0.03278618	240	0.24762222	0.03807229	180	0.23864167	0.03329752	240
X.BrakeStance	0.073312	No	0.000004	Yes	45.82444444	7.20043157	180	47.23583333	8.50521667	240	22.61888889	5.02721964	180	25.36166667	6.5864662	240
X.PropelStance	0.073312	No	0.000004	Yes	54.17555556	7.20043157	180	52.76416667	8.50521667	240	77.38111111	5.02721964	180	74.63875	6.58555209	240
Stance.Swing	0.496204	No	0.000155	Yes	1.65222222	0.25378818	180	1.67083333	0.29341328	240	1.75555556	0.3053018	180	1.88625	0.375531	240
Stride.Length	<0.000001	Yes	<0.000001	Yes	6.09777778	0.77988392	180	5.60791667	0.74607749	240	6.17777778	0.72670955	180	5.73458333	0.71873598	240
Stride.Frequency	0.002659	Yes	0.024506	No	4.30055556	0.63908954	180	4.49708333	0.67417378	240	4.25111111	0.64785757	180	4.39541667	0.64873536	240
PawAngle	0.255886	No	0.576762	No	-2.13944444	4.87883924	180	-1.50833333	6.12588422	240	0.39222222	17.03757417	180	1.335	17.17832949	240
Absolute.PawAngle	0.000619	Yes	0.7785	No	3.90722222	3.61305873	180	5.14166667	3.64193574	240	16.34777778	4.65733584	180	16.2	5.77465245	240
Paw.Angle.Variability	0.477312	No	0.000239	Yes	8.12333333	2.56029197	180	8.31791667	2.92469857	240	4.79555556	1.82575682	180	5.57333333	2.32933748	240
Stance.Width	0.50287	No	0.718181	No	4.77777778	4.11368551	180	4.51666667	3.82128663	240	9.53888889	8.65887596	180	9.85416667	8.99741847	240
StepAngle	0.530415	No	0.990996	No	92	97.32018227	180	86.1125	93.39500767	240	46.90555556	62.27966276	180	46.975	62.43865106	240
SLVar	0.19286	No	0.158581	No	1.24272222	0.32258874	180	1.28591667	0.34549218	240	0.89744444	0.27275979	180	0.95095833	0.45003245	240
SWVar	0.753361	No	0.324024	No	18.37222222	19.78855562	180	17.77083333	19.10096449	240	8.52777778	12.16526356	180	9.69583333	11.87042946	240
StepAngleVar	0.566174	No	0.422419	No	85.73888889	114.0590048	180	92.2875	116.870725	240	83.06111111	110.7694855	180	92.04583333	115.4575489	240
X.Steps	0.000053	Yes	0.000013	Yes	24.00833333	4.7819712	180	21.81875	5.87860657	240	23.67777778	4.70635557	180	21.32291667	5.88666941	240
Stride.Length.CV	0.000167	Yes	0.001176	Yes	20.82244444	6.52396481	180	23.578375	7.92635878	240	14.70616667	4.90287218	180	16.811125	7.52811028	240
Stance.Width.CV	0.957513	No	0.256205	No	82.95	94.95293012	180	83.45	95.25775208	240	128.21111111	154.5150275	180	111.1208333	150.8803385	240
Step.Angle.CV	0.205403	No	0.276243	No	81.05555556	111.6869989	180	96.21666667	127.9222556	240	99.85555556	121.4064747	180	113.7708333	135.1570046	240
Swing.Duration.CV	0.004977	No	0.001453	Yes	27.594	7.89706951	180	29.98779167	9.08822921	240	21.31672222	6.46662759	180	24.35395833	11.41084435	240
Paw.Area.at.Peak.Stance.in.sq.cm	0.111782	No	0.004248	Yes	0.30805556	0.04937709	180	0.2975	0.07788791	240	0.64966667	0.12237364	180	0.61033333	0.14986149	240
Paw.Area.Variability.at.Peak.Stance	0.534568	No	0.074908	No	0.02894444	0.01608279	180	0.02995833	0.01688003	240	0.05305556	0.033092	180	0.05908333	0.03507305	240
Hind.Limb.Shared.Stance.Time			0.286417	No	1	0	180	1	0	240	22	26.92406039	180	24.97916667	29.29998471	240
X.Shared.Stance			0.000002	Yes	1	0	180	1	0	240	118.0833333	67.80483618	180	152.3458333	74.75690858	240
StanceFactor	0.656453	No	0.927493	No	11.30555556	11.54350393	180	11.8375	12.53391424	240	13.59444444	13.27605364	180	13.475	13.32500873	240
Gait.Symmetry	0.034845	No	0.034845	No	1.01388889	0.04501259	180	1.02416667	0.05217581	240	1.01388889	0.04501259	180	1.02416667	0.05217581	240
MAX.dA.dT	0.926219	No	0.001727	Yes	16.896	3.37636885	180	16.8605	4.22700441	240	46.49827778	9.49935633	180	43.518625	9.64248797	240
MIN.dA.dT	0.31531	No	0.646552	No	-5.16177778	1.45335565	180	-5.31579167	1.6247547	240	-8.88127778	1.91057189	180	-8.980875	2.39585688	240
Tau.Propulsion			0.455592	No	1	0	180	1	0	240	178.9333333	101.5146521	180	186.7458333	109.3986127	240
Overlap.Distance	0.000567	Yes	0.000567	Yes	1.4025	0.4440782	180	1.55470833	0.44461341	240	1.4025	0.4440782	180	1.55470833	0.44461341	240
Paw.Placement.Positioning.PPP	0.009576	No	0.009576	No	0.47255556	0.209826	180	0.53175	0.24509639	240	0.47255556	0.209826	180	0.53175	0.24509639	240
Ataxia.Coefficient	0.065892	No	0.031149	No	0.899	0.30885281	180	0.95725	0.328734	240	0.63983333	0.24794907	180	0.7065	0.35345432	240
Midline.Distance	0.000511	Yes	0.000002	Yes	-2.22233333	0.34125483	180	-2.37679167	0.51249994	240	1.76005556	0.28026224	180	1.57204167	0.46433242	240
Axis.Distance	0.813623	No	0.774806	No	0.01011111	0.83342464	180	-0.00895833	0.80948622	240	0.02372222	1.34792041	180	-0.01433333	1.34621132	240
Paw.Drag			0.013423	No	1	0	180	1	0	240	218.8277778	112.0513066	180	190.6458333	117.356213	240

## Supplemental Table 2-2. Gait analysis parameters Female Gnao1 G203R mutants

Feng et al Table S2 Gait analysis parameters Female Gnao1 G203R mutants

Measured Parameter	Fore Limb		Hind Limb		Fore Limb						Hind Limb					
	p	FDR	p	FDR	F Gnao1+/-	SD	n	F Gnao1+/G203R	SD	n	F Gnao1+/-	SD	n	F Gnao1+/G203R	SD	n
Swing	0.143574	No	0.000042	Yes	0.0862619	0.0112876	210	0.08485044	0.011845	226	0.08701905	0.0103341	210	0.08259735	0.011866	226
X.SwingStride	0.040102	No	0.000039	Yes	38.2376191	3.4885409	210	37.58362832	3.1433241	226	37.98428571	4.4849659	210	36.3	3.9776487	226
Brake	0.610655	No	0.239211	No	0.06979524	0.019761	210	0.07067699	0.0163127	226	0.03703333	0.0117622	210	0.03834513	0.0114719	226
X.BrakeStride	0.151434	No	0.045932	No	30.4114286	5.6522649	210	31.14867257	5.0584954	226	15.94428571	4.3353439	210	16.8199115	4.766196	226
Propel	0.962205	No	0.766869	No	0.07122857	0.0153668	210	0.07115487	0.0169689	226	0.10746667	0.0239663	210	0.10812832	0.0226036	226
X.PropelStride	0.858596	No	0.055104	No	31.35	4.8383758	210	31.26681416	4.8963937	226	46.06619048	4.7852095	210	46.88185841	4.0616338	226
Stance	0.747729	No	0.463647	No	0.14104286	0.0265394	210	0.14184071	0.0252212	226	0.14451429	0.029293	210	0.14648673	0.0268555	226
X.StanceStride	0.040102	No	0.000039	Yes	61.762381	3.4885409	210	62.41637168	3.1433241	226	62.01571429	4.4849659	210	63.70044248	3.9787156	226
Stride	0.780626	No	0.445327	No	0.22737619	0.0347068	210	0.22645575	0.0342293	226	0.23155238	0.0346545	210	0.22903982	0.0339969	226
X.BrakeStance	0.30554	No	0.327424	No	49.1166667	8.051334	210	49.8840708	7.5687729	226	25.63047619	6.3902157	210	26.23938053	6.5617814	226
X.PropelStance	0.30554	No	0.327424	No	50.8833333	8.051334	210	50.1159292	7.5687729	226	74.36952381	6.3902157	210	73.76061947	6.5617814	226
Stance.Swing	0.050429	No	0.000053	Yes	1.63809524	0.2335009	210	1.68141593	0.2274687	226	1.66857143	0.3092867	210	1.79070796	0.3146108	226
Stride.Length	0.003872	No	0.000285	Yes	5.70190476	0.7409397	210	5.50530973	0.6725528	226	5.80761905	0.7083501	210	5.5659292	0.6710776	226
Stride.Frequency	0.83429	No	0.456267	No	4.63333333	0.7236493	210	4.64778761	0.7174148	226	4.54809524	0.6820467	210	4.59734513	0.6955682	226
PawAngle	0.275233	No	0.711622	No	-2.0414286	5.1145489	210	-1.51504425	4.944406	226	0.40666667	18.071952	210	1.02699115	16.942806	226
Absolute.PawAngle	0.653751	No	0.017128	No	4.27380952	3.4631111	210	4.13274336	3.0979403	226	17.21047619	5.3985099	210	15.92699115	5.7724885	226
Paw.Angle.Variability	0.083677	No	0.459013	No	7.08	2.9170313	210	7.53495575	2.560203	226	5.24428571	2.5795276	210	5.44778761	3.1063833	226
Stance.Width	0.304131	No	0.992695	No	4.65238095	3.9041285	210	4.28318584	3.588795	226	8.97619048	8.1636612	210	8.96902655	8.1553754	226
Step.Angle	0.676222	No	0.265709	No	87.4904762	95.888554	210	83.71238938	92.843532	226	46.68095238	62.270502	210	53.61946903	67.358321	226
SLVar	0.46197	No	0.160859	No	1.11104762	0.3637969	210	1.13581947	0.3330556	226	0.82042857	0.3400398	210	0.86349558	0.299672	226
SWVar	0.597496	No	0.235126	No	14.8666667	16.15035	210	15.69026549	16.365318	226	7.22380952	9.302076	210	8.37610619	10.810084	226
Step.Angle.Var	0.590118	No	0.742411	No	94.5571429	123.21106	210	88.42920354	114.15516	226	93.55714286	122.72527	210	89.84955752	112.67252	226
X.Steps	0.287034	No	0.176573	No	23.7642857	5.9102466	210	24.34070796	5.3805268	226	23.34761905	5.9556269	210	24.08628319	5.4387774	226
Stride.Length.CV	0.134218	No	0.029457	No	20.0334286	7.9432229	210	21.13402655	7.3727667	226	14.45657143	6.7501268	210	15.80809735	6.1679082	226
Stance.Width.CV	0.183108	No	0.787718	No	71.4761905	83.50877	210	82.69469027	91.571949	226	127.6666667	155.40339	210	123.6283186	157.26751	226
Step.Angle.CV	0.500567	No	0.496458	No	92.3857143	125.23065	210	100.6283186	129.68952	226	96.90952381	123.48735	210	105.039823	125.67239	226
Swing.Duration.CV	0.009699	No	0.012817	No	25.4634286	9.9336491	210	27.70469027	8.038455	226	20.35714286	10.045441	210	22.57513274	8.4641854	226
Paw.Area.at.Peak.Stance.In.sq.cm	0.046636	No	0.120876	No	0.31547619	0.0784235	210	0.30084071	0.0747244	226	0.624	0.138264	210	0.60482301	0.1192093	226
Paw.Area.Variability.at.Peak.Stance	0.25505	No	0.123726	No	0.03247619	0.0177047	210	0.03048673	0.0186722	226	0.06057143	0.0355498	210	0.05575221	0.029599	226
Hind.Limb.Shared.Stance.Time			0.219455	No	1	0	210	1	0	226	19.06190476	23.988055	210	21.98230088	25.48742	226
X.Shared.Stance			0.000033	Yes	1	0	210	1	0	226	116.7095238	70.404616	210	144.300885	86.869808	226
StanceFactor	0.618239	No	0.752284	No	11.6952381	12.247545	210	12.27876106	12.170536	226	13.52380952	13.510298	210	13.12389381	12.926894	226
Gait.Symmetry	0.044325	No	0.044325	No	1.0192381	0.0513119	210	1.01123894	0.0292767	226	1.0192381	0.0513119	210	1.01123894	0.0292767	226
MAX.dA.dT	0.093152	No	0.528498	No	16.9396667	4.1600988	210	16.29477876	3.8423131	226	43.48771429	9.941629	210	42.92628319	8.6321179	226
MIN.dA.dT	0.001558	No	0.000411	Yes	-5.1652381	1.8030427	210	-4.63566372	1.6700964	226	-9.69890952	2.6687581	210	-8.8219469	2.4798691	226
Tau.Propulsion			0.000043	Yes	1	0	210	1	0	226	164.8380952	101.35854	210	206.1415929	106.91923	226
Overlap.Distance	0.000346	No	0.000346	Yes	1.42585714	0.3488621	210	1.30376106	0.3572146	226	1.42585714	0.3488621	210	1.30376106	0.3572146	226
Paw.Placement.Positioning.PPP	0.122248	No	0.122248	No	0.44066667	0.1970416	210	0.47349558	0.2414856	226	0.44066667	0.1970416	210	0.47349558	0.2414856	226
Ataxia.Coefficient	0.125326	No	0.01669	No	0.85080952	0.36314	210	0.90159292	0.3272514	226	0.62028571	0.3216493	210	0.69393805	0.3180957	226
Midline.Distance	0.844898	No	<0.000001	Yes	-1.9551905	0.4090709	210	-1.96256637	0.3777178	226	1.8667619	0.3241286	210	1.61292035	0.3222468	226
Axis.Distance	0.882318	No	0.987517	No	-0.0137143	0.794259	210	-0.00261062	0.7706896	226	-0.004	1.2942361	210	-0.00207965	1.2662788	226
Paw.Drag			0.744503	No	1	0	210	1	0	226	212.1142857	132.61357	210	215.9734513	114.3211	226

## Supplemental Table 2-3. Gait analysis parameters Male Gnao1 G184S mutants

Feng et al Table S3 Gait analysis parameters Male Gnao1 G184S mutants

Measured Parameter	Fore Limb		Hind Limb		Fore Limb						Hind Limb					
	p	FDR	p	FDR	M Gnao1+/-	SD	n	M Gnao1+G184S	SD	n	M Gnao1+/-	SD	n	M Gnao1+G184S	SD	n
Swing	0.043466	No	<b>0.000278</b>	<b>Yes</b>	0.09253061	0.0141627	98	0.08857143	0.011722	84	0.09	0.0127724	98	0.08357143	0.0102043	84
X.SwingStride	0.726843	No	0.117241	No	37.83979592	3.1936386	98	37.6702381	3.3344055	84	36.51428571	5.1117008	98	35.3	5.2765451	84
Brake	0.826349	No	0.812719	No	0.05344898	0.0115937	98	0.05385714	0.0134703	84	0.02879592	0.0075135	98	0.02907143	0.0081415	84
X.BrakeStride	0.180502	No	0.197797	No	21.91020408	4.0355505	98	22.75119048	4.3988359	84	11.57857143	2.4412372	98	12.08333333	2.8270992	84
Propel	0.148248	No	0.66152	No	0.09986735	0.0236179	98	0.09477381	0.023563	84	0.13060204	0.029081	98	0.12857143	0.0333879	84
X.PropelStride	0.318489	No	0.336379	No	40.25714286	4.5416969	98	39.57857143	4.5858365	84	51.91632653	4.6134205	98	52.62738095	5.3388179	84
Stance	0.27969	No	0.731504	No	0.15326531	0.028498	98	0.14857143	0.0298184	84	0.15944898	0.0336318	98	0.15763095	0.0377269	84
X.StanceStride	0.726843	No	0.117241	No	62.16020408	3.1936386	98	62.3297619	3.3344055	84	63.48571429	5.1117008	98	64.7	5.2765451	84
Stride	0.140428	No	0.173925	No	0.24587755	0.0396769	98	0.23721429	0.0389603	84	0.24947959	0.0391545	98	0.24122619	0.0423552	84
X.BrakeStance	0.197014	No	0.382853	No	35.25306122	6.2745798	98	36.49047619	6.6003216	84	18.21020408	3.3839064	98	18.70238095	4.2032969	84
X.PropelStance	0.197014	No	0.384084	No	64.74693878	6.2745798	98	63.50952381	6.6003216	84	81.78979592	3.3839064	98	81.29880952	4.2045728	84
Stance.Swing	0.810208	No	0.075995	No	1.66326531	0.2230934	98	1.67142857	0.2341719	84	1.79183673	0.3701974	98	1.89642857	0.4203975	84
Stride.Length	0.047635	No	0.036347	No	6.17959184	0.9320147	98	5.93333333	0.693226	84	6.26122449	0.9164738	98	6.01071429	0.634551	84
Stride.Frequency	0.153098	No	0.096182	No	4.29387755	0.6895115	98	4.44761905	0.7554582	84	4.22346939	0.6697901	98	4.40238095	0.7735034	84
Paw.Angle	0.223604	No	0.783411	No	-0.00102041	4.7029821	98	0.91547619	5.4220321	84	-0.05204082	17.660751	98	0.675	17.87932	84
Absolute.PawAngle	0.062068	No	0.583264	No	3.73163265	2.8371467	98	4.55119048	3.046922	84	17.08877551	4.1070692	98	16.66309524	6.2551719	84
Paw.Angle.Variability	<b>0.000004</b>	<b>Yes</b>	0.007857	No	6.31938776	1.7027969	98	8.06666667	3.1549286	84	4.2877551	1.9761081	98	5.24047619	2.7850772	84
Stance.Width	0.931208	No	0.50059	No	3.83673469	3.0348283	98	3.79761905	3.0528666	84	7.12244898	6.2363506	98	7.78571429	7.0198882	84
Step.Angle	0.781449	No	0.542101	No	48.89795918	51.835284	98	46.78571429	50.288342	84	25.30612245	32.434997	98	22.44047619	30.489718	84
SLVar	0.018345	No	0.480115	No	1.18122449	0.4015749	98	1.32916667	0.4364264	84	0.91683673	0.309591	98	0.9572619	0.4562322	84
SWVar	0.268206	No	0.49907	No	12.31632653	12.961161	98	14.6547619	15.444206	84	6.80612245	7.6934276	98	7.66666667	9.442704	84
Step.Angle.Var	0.51712	No	0.419338	No	45.3877551	58.864099	98	39.98809524	52.336606	84	42.21428571	51.158184	98	36.42857143	44.194064	84
X.Steps	0.201763	No	0.192532	No	21.35714286	4.3328046	98	22.25595238	5.1316958	84	21.0255102	4.4032395	98	21.95238095	5.1569459	84
Stride.Length.CV	0.009988	No	0.274044	No	19.70622449	7.7856016	98	22.82186667	8.3634236	84	14.93540816	5.4905719	98	16.00988095	7.6712154	84
Stance.Width.CV	0.245913	No	0.866251	No	29.3877551	33.936154	98	35.82142857	40.621426	84	57.7244898	69.576003	98	59.47619048	70.164948	84
Step.Angle.CV	0.386308	No	0.314724	No	33.97959184	48.807634	98	40.55952381	53.357704	84	48.95918367	59.292655	98	58.16666667	63.81578	84
Swing.Duration.CV	0.495053	No	0.13408	No	25.39285714	8.1613281	98	26.30416667	9.8202879	84	21.32826531	7.197867	98	23.49071429	11.914931	84
Paw.Area.at.Peak.Stance.in.sq.cm	<b>&lt;0.000001</b>	<b>Yes</b>	<b>0.000001</b>	<b>Yes</b>	0.32091837	0.0605148	98	0.26928571	0.0702111	84	0.70244898	0.1316122	98	0.60595238	0.1286643	84
Paw.Area.Variability.at.Peak.Stance	0.002006	No	0.082786	No	0.01877551	0.0098719	98	0.02559524	0.0187148	84	0.04530612	0.030127	98	0.05357143	0.0337833	84
Hind.Limb.Shared.Stance.Time			0.669308	No	1	0	98	1	0	84	14.24489796	17.100709	98	15.35714286	17.924637	84
X.Shared.Stance			0.051594	No	1	0	98	1	0	84	74.91836735	45.56058	98	87.82142857	42.745862	84
StanceFactor	0.396136	No	0.831523	No	8.70408163	9.4859736	98	7.57142857	8.2932484	84	9.25510204	9.6744016	98	9.55952381	9.5328869	84
Gait.Symmetry	0.688994	No	0.688994	No	1.01755102	0.0511529	98	1.01452381	0.0503579	84	1.01755102	0.0511529	98	1.01452381	0.0503579	84
MAX.dA.dT	<b>&lt;0.000001</b>	<b>Yes</b>	<b>0.000008</b>	<b>Yes</b>	19.58153061	3.7431478	98	16.61440476	3.9087463	84	51.415	10.373366	98	44.32047619	10.399373	84
MIN.dA.dT	0.891498	No	<b>0.000429</b>	<b>Yes</b>	-4.68867347	0.9273804	98	-4.71535714	1.6546185	84	-8.24183673	2.1764496	98	-9.5402381	2.7031744	84
Tau.Propulsion			<b>0.000017</b>	<b>Yes</b>	1	0	98	1	0	84	103.755102	45.984547	98	72.35714286	49.842316	84
Overlap.Distance	0.001809	No	<b>0.001809</b>	<b>Yes</b>	1.40122449	0.3999259	98	1.61261905	0.5000846	84	1.40122449	0.3999259	98	1.61261905	0.5000846	84
Paw.Placement.Positioning.PPP	0.00764	No	0.00764	No	0.43704082	0.1825829	98	0.51178571	0.1905993	84	0.43704082	0.1825829	98	0.51178571	0.1905993	84
Ataxia.Coefficient	0.055735	No	0.187315	No	0.81897959	0.3422138	98	0.91821429	0.3516473	84	0.61469388	0.248655	98	0.6727381	0.3411474	84
Midline.Distance	0.998012	No	0.035382	No	-2.76357143	0.3019703	98	-2.76369048	0.3417171	84	1.40795918	0.2798857	98	1.51952381	0.4244029	84
Axis.Distance	0.836286	No	0.951005	No	0.03887755	0.8386733	98	0.01333333	0.8200578	84	0.01989796	1.3185305	98	0.00738095	1.4239324	84
Paw.Drag			<b>0.000004</b>	<b>Yes</b>	1	0	98	1	0	84	107.2653061	45.749779	98	72.89285714	52.00487	84

## Supplemental Table 2-4. Gait analysis parameters Female Gnao1 G184S mutants

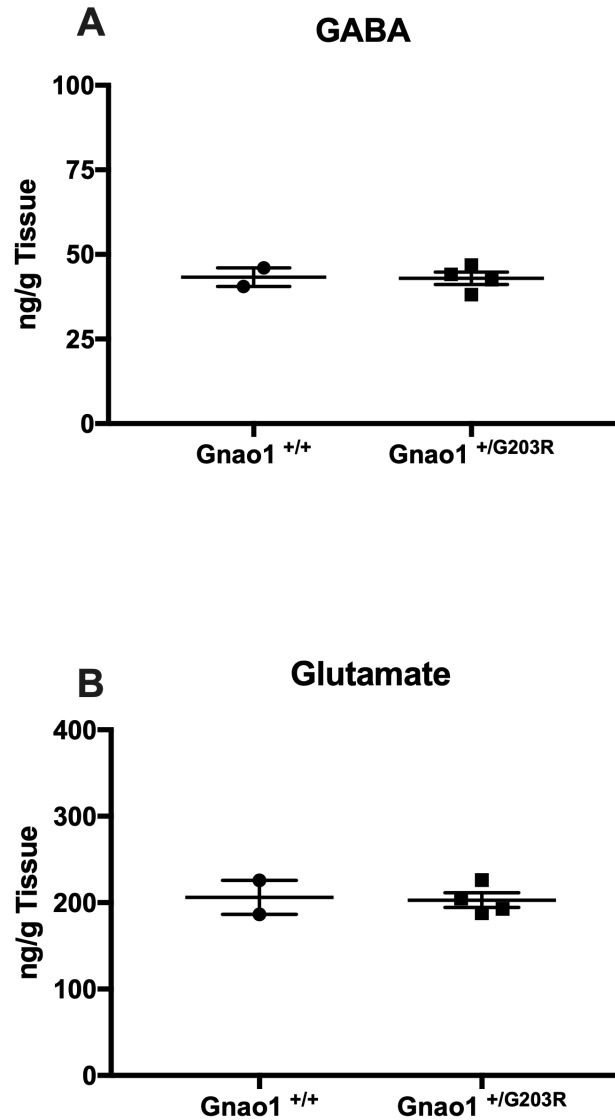
Feng et al Table S4 Gait analysis parameters Female Gnao1 G184S mutants

Measured Parameter	Fore Limb		Hind Limb		Fore Limb						Hind Limb					
	p	FDR	p	FDR	F Gnao1+/-	SD	n	F Gnao1+/G184S	SD	n	F Gnao1+/-	SD	n	F Gnao1+/G184S	SD	n
Swing	<b>0.000002</b>	Yes	<b>0.00019</b>	Yes	0.08906667	0.012567	90	0.080841	0.012049	132	0.088633	0.011621	90	0.082333	0.012478	132
X.SwingStride	0.352054	No	0.571929	No	38.21333	3.504418	90	37.76212	3.562839	132	37.53889	3.24618	90	37.79697	3.394359	132
Brake	0.018172	No	0.041827	No	0.062156	0.017608	90	0.056508	0.017191	132	0.029	0.01003	90	0.026402	0.00874	132
X.BrakeStride	0.605581	No	0.827244	No	26.46	5.698922	90	26.05303	5.79599	132	12.18	3.40298	90	12.075	3.589752	132
Propel	0.073513	No	<b>0.003264</b>	Yes	0.083178	0.019603	90	0.078295	0.02004	132	0.119811	0.022828	90	0.110394	0.023384	132
X.PropelStride	0.303687	No	0.75231	No	35.33444	5.498685	90	36.1803	6.320866	132	50.28222	3.871491	90	50.11818	3.746567	132
Stance	0.004809	No	<b>0.001181</b>	Yes	0.145322	0.026527	90	0.134818	0.027276	132	0.148811	0.026549	90	0.136818	0.026794	132
X.StanceStride	0.352054	No	0.571929	No	61.78667	3.504418	90	62.23788	3.562839	132	62.46111	3.24618	90	62.20303	3.394359	132
Stride	<b>0.000183</b>	Yes	<b>0.000242</b>	Yes	0.234389	0.035201	90	0.215674	0.03649	132	0.237511	0.035089	90	0.219182	0.03649	132
X.BrakeStance	0.490318	No	0.875453	No	42.76444	8.767346	90	41.91894	9.074334	132	19.45556	5.068056	90	19.34394	5.293627	132
X.PropelStance	0.489918	No	0.875453	No	57.23556	8.767346	90	58.08182	9.073969	132	80.54444	5.068056	90	80.65606	5.293627	132
Stance.Swing	0.335195	No	0.536831	No	1.64	0.240692	90	1.672727	0.252647	132	1.687778	0.237888	90	1.667424	0.242599	132
Stride.Length	<b>0.0007</b>	Yes	<b>0.000352</b>	Yes	5.707778	0.807719	90	5.342424	0.755956	132	5.781111	0.775306	90	5.420455	0.691799	132
Stride.Frequency	<b>0.000035</b>	Yes	<b>0.000096</b>	Yes	4.468889	0.682797	90	4.908333	0.810338	132	4.415556	0.680369	90	4.823485	0.795393	132
PawAngle	0.167612	No	0.464223	No	4.784444	2.854089	90	4.209848	3.153645	132	16.32778	4.441025	90	16.82121	5.22535	132
Absolute.PawAngle	0.167612	No	0.464223	No	4.784444	2.854089	90	4.209848	3.153645	132	16.32778	4.441025	90	16.82121	5.22535	132
Paw.Angle.Variability	<b>0.000023</b>	Yes	<b>0.003025</b>	Yes	6.265556	2.252647	90	7.730303	2.613352	132	4.153333	1.479538	90	5.02197	2.460662	132
Stance.Width	0.022922	No	0.068763	No	1.684444	0.330259	90	1.536364	0.333114	132	2.566667	0.475299	90	2.410606	0.412918	132
Step.Angle	0.998777	No	0.466437	No	64.84444	7.514911	90	64.84697	9.138359	132	56.06222	8.526091	90	54.86515	8.435848	132
SLVar	0.164572	No	0.379246	No	1.152444	0.381574	90	1.092273	0.261539	132	0.793778	0.335337	90	0.757652	0.273303	132
SWVar	0.200099	No	0.091884	No	0.349556	0.098164	90	0.375	0.104679	132	0.220667	0.097547	90	0.259242	0.129024	132
StepAngleVar	0.882892	No	0.454172	No	13.42622	4.439098	90	13.54348	3.867871	132	12.55133	3.478382	90	12.06667	3.238623	132
X.Steps	0.00456	No	0.006296	No	18.32778	5.488579	90	20.31818	4.78319	132	18.08889	5.451305	90	19.98864	4.73676	132
Stride.Length.CV	0.568182	No	0.504883	No	20.47044	6.723017	90	20.97265	6.21845	132	13.79056	5.541985	90	14.31485	5.874303	132
Stance.Width.CV	0.007756	No	0.02606	No	21.188	6.590364	90	25.38455	8.830206	132	8.748444	4.294501	90	10.9447	5.480517	132
Step.Angle.CV	0.734363	No	0.682633	No	21.42844	8.660338	90	22.01364	9.055266	132	22.82822	6.986445	90	22.30394	6.351191	132
Swing.Duration.CV	0.412289	No	0.494238	No	25.59067	8.521292	90	24.72242	7.146669	132	18.19433	6.749598	90	18.80689	6.401079	132
Paw.Area.at.Peak.Stance.in.sq.cm	<b>0.000002</b>	Yes	<b>0.000015</b>	Yes	0.398111	0.152248	90	0.311288	0.11312	132	0.818667	0.301436	90	0.660227	0.230086	132
Paw.Area.Variability.at.Peak.Stance	0.291841	No	0.294115	No	0.031556	0.019309	90	0.029091	0.015356	132	0.067	0.056299	90	0.059773	0.045725	132
Hind.Limb.Shared.Stance.Time	0.167306	No	0.112442	No			90			132	0.057378	0.021	90	0.051152	0.019511	132
X.Shared.Stance	0.25904	No	0.28745	No			90			132	37.59111	8.462962	90	36.32273	8.859942	132
StanceFactor	<b>&lt;0.000001</b>	Yes	0.357268	No	1.009333	0.075179	90	0.988788	0.077291	132	1.009556	0.047095	90	1.019545	0.061129	132
Gait.Symmetry	0.014025	No	0.25904	No	1.012889	0.039413	90	1.018333	0.032011	132	1.012889	0.039413	90	1.018333	0.032011	132
MAX.dA.dT	<b>0.001549</b>	Yes	<b>0.000014</b>	Yes	25.22511	9.069926	90	19.5603	6.647057	132	64.31333	24.77673	90	51.24644	18.95255	132
MIN.dA.dT	0.979063	No	0.119243	No	6.588111	2.658642	90	5.764015	2.269378	132	12.05456	5.245177	90	10.95538	5.069048	132
Tau.Propulsion	0.203884	No	0.253295	No			90			132	0.150978	0.103392	90	0.138298	0.06125	132
Overlap.Distance	0.039565	No	<b>0.001549</b>	Yes	1.749778	0.686131	90	1.463712	0.629242	132	1.749778	0.686131	90	1.463712	0.629242	132
Paw.Placement.Positioning.PPP	<b>0.000293</b>	Yes	0.979063	No	0.443222	0.221435	90	0.442424	0.222697	132	0.443222	0.221435	90	0.442424	0.222697	132
Ataxia.Coefficient	0.055735	No	0.38151	No	0.794889	0.295526	90	0.845379	0.285901	132	0.546444	0.277777	90	0.579848	0.279277	132
Midline.Distance	0.998012	No	<b>0.000029</b>	Yes	2.572	0.38345	90	2.450985	0.455068	132	1.539222	0.641965	90	1.190758	0.564684	132
Axis.Distance	0.836286	No	0.015682	No	0.838222	0.176753	90	0.752045	0.167454	132	1.299111	0.261708	90	1.220076	0.219397	132
Paw.Drag			<b>0.00008</b>	Yes	1	0	90	1	0	132	7.0439	3.321218	90	5.45697	2.551102	132

## Supplemental Table 2-6. Benchling off-target list for Gnao1 G203 gRNA

Feng *et al* Table S5 Benchling off-target list for Gnao1 G203 gRNA

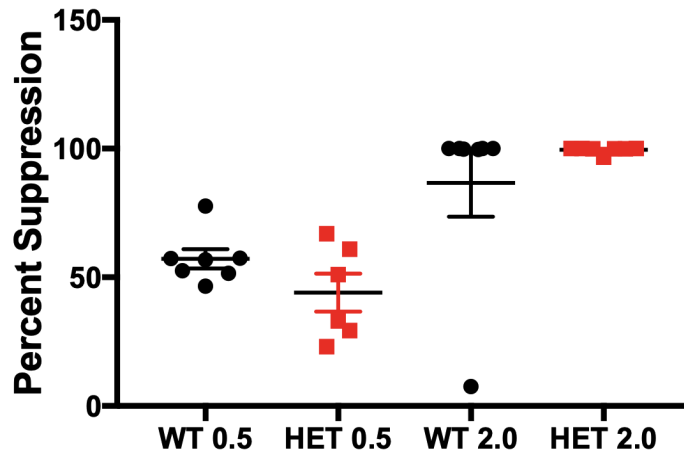
Sequence	PAM	Score	Gene	Chromosome	Mismatches
TGCAGGCTGTTTGACGTCGG	GGG	100	ENSMUSG00000031748	chr8	0
GGCAAGCTGATTGACGTCCTG	TAG	0.6189		chr18	4
TGGATGGTGTGGACGTCGG	AAG	0.5200	ENSMUSG00000041390	chr6	4
TGCAGGCTGTTGAAGTCTG	CAG	0.5076		chr3	2
GGTGGGCTGTTGACGTGGG	AGG	0.3804		chr1	4
TTCAGGCTGAGTGACGTCAG	TGG	0.3169	ENSMUSG00000032497	chr9	4
AGCAGGCACTTTGAAGTCGG	AAG	0.2931		chr3	4
TTCAGTCTGTTAGACGTCCTG	TAG	0.1953		chr1	4
TGCATGGGGTTTGACTTCGG	AGG	0.1929		chr13	4
TGCTGGCTGTTGAGGTGGG	AAG	0.1923		chr1	3
TCCAGGCTGGTGGACGTGGG	CAG	0.1710		chr1	4
TGATGGCTGTTGACTTCGG	GAG	0.1556	ENSMUSG00000086805	chr8	4
TACAGAATGTTTGACGTGGG	AGG	0.1543	ENSMUSG00000057614	chr5	4
TTCAGTCTGTTGAGGTCGT	TGG	0.1515		chrX	4
AGCAGGCTGCTGACATCGA	GAG	0.1480		chr4	4
TGCAAGCTGGTTGAGGTCAG	GGG	0.1450		chr17	4
TCCAGGATGTTGATGCCGG	AAG	0.1403		chr18	4
TGCAGGCTGTCTGAAGTCTG	GGG	0.1343	ENSMUSG00000026413	chr1	3
GGCTGGCTGTTGACCTCAG	AGG	0.1262		chrX	4
AGCAGCCTGTTGAAGTCTG	TGG	0.1144		chr11	4
GGCAGGCTGTATGAAGCGG	AGG	0.1127		chr5	4
TGGAGGCTGTACACGTCAG	CAG	0.1127		chr1	4
TGCTGGCTATTTGAAGTCTG	AGG	0.1004		chr10	4
TGCTGGTTATTTGTCGTCGG	GAG	0.1002		chr11	4
TCCAGGCTGTCTGATGTCAG	GAG	0.0954		chrX	4
TTCAGGATGTTGACGTATG	CAG	0.0933		chr3	4
TGCACGCTGAGACGTGGG	CGG	0.0930	ENSMUSG00000020015	chr10	4
TGCATGCTGTCTGAAGTCAG	AAG	0.0865		chrX	4
TGCAGGCTGTATGACCTCTG	GGG	0.0862		chr2	3
TGCAGTCTCTTGACGACAG	TGG	0.0836		chr11	4



Supplemental Figure 2-6. GABA and glutamate show no significant differences between *Gnao1*<sup>+/R209H</sup> and wildtype littermates. HPLC analysis of a second cohort of *Gnao1*<sup>+/G203R</sup> mice, there was no significant difference in GABA or glutamate within the left hemisphere. Student's unpaired T-test: nonsignificant.

## **APPENDIX B**

### **Chapter 3**



**Supplemental Figure 3-1. WT and *Gnao1<sup>+ / R209H</sup>* mice show no difference in percent suppression of locomotion after oxotremorine treatment *Gnao1<sup>+ / R209H</sup>* mice show similar sensitivity to risperidone treatment at 2.0 mg/kg or 0.5 mg/kg compared to WT treated mice, Student t-test.**

## REFERENCES

## REFERENCES

1. Worley PF, Baraban JM, Van Dop C, Neer EJ, Snyder SH. Go, a guanine nucleotide-binding protein: immunohistochemical localization in rat brain resembles distribution of second messenger systems. *Proc Natl Acad Sci U S A*. 1986;83(12):4561-5. PubMed PMID: 3086888; PubMed Central PMCID: PMCPMC323774.
2. Sternweis PC, Robishaw JD. Isolation of two proteins with high affinity for guanine nucleotides from membranes of bovine brain. *J Biol Chem*. 1984;259(22):13806-13. PubMed PMID: 6438083.
3. Neer EJ, Lok JM, Wolf LG. Purification and properties of the inhibitory guanine nucleotide regulatory unit of brain adenylate cyclase. *J Biol Chem*. 1984;259(22):14222-9. PubMed PMID: 6150041.
4. Huff RM, Axton JM, Neer EJ. Physical and immunological characterization of a guanine nucleotide-binding protein purified from bovine cerebral cortex. *J Biol Chem*. 1985;260(19):10864-71. PubMed PMID: 3928624.
5. Jiang M, Bajpayee NS. Molecular mechanisms of go signaling. *Neurosignals*. 2009;17(1):23-41. Epub 2009/02/12. doi: 10.1159/000186688. PubMed PMID: 19212138; PubMed Central PMCID: PMCPMC2836949.
6. Colecraft HM, Brody DL, Yue DT. G-protein inhibition of N- and P/Q-type calcium channels: distinctive elementary mechanisms and their functional impact. *J Neurosci*. 2001;21(4):1137-47. PubMed PMID: 11160384.
7. Adele S, Jie H, Rory F. RGS Proteins in heart: Brakes on the Vagus. *Frontiers in physiology*. 2012;3:95. doi: 10.3389/fphys.2012.00095. PubMed PMID: article.
8. Fu Y, Zhong H, Nanamori M, Mortensen RM, Huang X, Lan K, et al. RGS-insensitive G-protein mutations to study the role of endogenous RGS proteins. *Methods Enzymol*. 2004;389:229-43. doi: 10.1016/S0076-6879(04)89014-1. PubMed PMID: 15313569.
9. Goldenstein BL, Nelson BW, Xu K, Luger EJ, Pribula JA, Wald JM, et al. Regulator of G protein signaling protein suppression of Galphao protein-mediated alpha2A adrenergic receptor inhibition of mouse hippocampal CA3 epileptiform activity. *Mol Pharmacol*. 2009;75(5):1222-30. Epub 2009/02/18. doi: 10.1124/mol.108.054296. PubMed PMID: 19225179; PubMed Central PMCID: PMCPMC2672807.
10. Nakamura K, Kodera H, Akita T, Shiina M, Kato M, Hoshino H, et al. De Novo mutations in GNAO1, encoding a G $\alpha$ o subunit of heterotrimeric G proteins, cause epileptic encephalopathy. *Am J Hum Genet*. 2013;93(3):496-505. Epub 2013/08/29. doi: 10.1016/j.ajhg.2013.07.014.

PubMed PMID: 23993195; PubMed Central PMCID: PMCPMC3769919.

11. M. KJ, Sahaya K, Dalton HM, Charbeneau RA, Kohut KT, Gilbert K, et al. Gain-of-function mutation in *Gnao1*: a murine model of epileptiform encephalopathy (EIEE17)? *Mamm Genome*. 2014;25(5-6):202-10. Epub 2014/04/05. doi: 10.1007/s00335-014-9509-z. PubMed PMID: 24700286; PubMed Central PMCID: PMCPMC4042023.
12. Shimada T, Yamagata K. Pentylentetrazole-Induced Kindling Mouse Model. *J Vis Exp*. 2018;(136). Epub 2018/06/12. doi: 10.3791/56573. PubMed PMID: 29985308; PubMed Central PMCID: PMCPMC6101698.
13. Meredith K, Meredith P, Ivana M, Anne R, Marie G, Eduardo P-P, et al. Spectrum of neurodevelopmental disease associated with the *GNAO1* guanosine triphosphate-binding region. *Epilepsia*. 2019. doi: 10.1111/epi.14653. PubMed PMID: kelly\_2019.
14. Gawlinski P, Renata P, Tomasz G, Danuta S, Monika C, Beata N, et al. PEHO Syndrome May Represent Phenotypic Expansion at the Severe End of the Early-Onset Encephalopathies. *Pediatr Neurol*. 2016;60:83-7. doi: 10.1016/j.pediatrneurol.2016.03.011. PubMed PMID: gawlinski\_2016.
15. Law C-Y, Tzu-Lun CS, Young CS, Kin-Cheong YE, Sui-Fun NG, Nai-Chung F, et al. Clinical whole-exome sequencing reveals a novel missense pathogenic variant of *GNAO1* in a patient with infantile-onset epilepsy. *Clin Chim Acta*. 2015;451(Pt B):292-6. doi: 10.1016/j.cca.2015.10.011. PubMed PMID: law\_2015.
16. Marcé-Grau A, James D, Javier L-P, Concepción G-JM, Lorena M-G, Ester C-L, et al. *GNAO1* encephalopathy: further delineation of a severe neurodevelopmental syndrome affecting females. *Orphanet J Rare Dis*. 2016;11:38. doi: 10.1186/s13023-016-0416-0. PubMed PMID: marcgrau\_2016.
17. Saitsu H, Ryoko F, Bruria B-Z, Yasunari S, Masakazu M, Nobuhiko O, et al. Phenotypic spectrum of *GNAO1* variants: epileptic encephalopathy to involuntary movements with severe developmental delay. *Eur J Hum Genet*. 2016;24(1):129-34. doi: 10.1038/ejhg.2015.92. PubMed PMID: saitsu\_2016.
18. Kulkarni N, Sha T, Ratan B, Saunder B, A. GT. Progressive movement disorder in brothers carrying a *GNAO1* mutation responsive to deep brain stimulation. *J Child Neurol*. 2016;31(2):211-4. doi: 10.1177/0883073815587945. PubMed PMID: kulkarni\_2016.
19. Feng H, Sjögren B, Karaj B, Shaw V, Gezer A, Neubig RR. Movement disorder in. *Neurology*. 2017;89(8):762-70. Epub 2017/07/26. doi: 10.1212/WNL.0000000000004262. PubMed PMID: 28747448; PubMed Central PMCID: PMCPMC5580866.
20. (CDC) CfDCaP. Epilepsy in adults and access to care--United States, 2010. *MMWR Morb Mortal Wkly Rep*. 2012;61(45):909-13. PubMed PMID: 23151949.

21. McTague A, Howell KB, Cross JH, Kurian MA, Scheffer IE. The genetic landscape of the epileptic encephalopathies of infancy and childhood. *Lancet Neurol.* 2016;15(3):304-16. Epub 2015/11/17. doi: 10.1016/S1474-4422(15)00250-1. PubMed PMID: 26597089.
22. Subramony SH, Schott K, Raike RS, Callahan J, Langford LR, Christova PS, et al. Novel CACNA1A mutation causes febrile episodic ataxia with interictal cerebellar deficits. *Ann Neurol.* 2003;54(6):725-31. doi: 10.1002/ana.10756. PubMed PMID: 14681882.
23. Ananth AL, Robichaux-Viehoever, Young-Min A, Young-Min K, Andrea H-K, Rachel C, et al. Clinical Course of Six Children With GNAO1 Mutations Causing a Severe and Distinctive Movement Disorder. *Pediatr Neurol.* 2016;59:81-4. doi: 10.1016/j.pediatrneurol.2016.02.018. PubMed PMID: ananth\_2016.
24. Schirinzi T, Giacomo G, Lorena T, Gessica V, Serena G, Loreto R, et al. Phenomenology and clinical course of movement disorder in GNAO1 variants: Results from an analytical review. *Parkinsonism Relat Disord.* 2018. doi: 10.1016/j.parkreldis.2018.11.019. PubMed PMID: schirinzi\_2018.
25. Chen YZ, Matsushita MM, Robertson P, Rieder M, Girirajan S, Antonacci F, et al. Autosomal dominant familial dyskinesia and facial myokymia: single exome sequencing identifies a mutation in adenylyl cyclase 5. *Arch Neurol.* 2012;69(5):630-5. doi: 10.1001/archneurol.2012.54. PubMed PMID: 22782511; PubMed Central PMCID: PMC3508680.
26. Carecchio, Miryam, E. MN. Emerging monogenic complex hyperkinetic disorders. *Curr Neurol Neurosci Rep.* 2017;17(12):97. doi: 10.1007/s11910-017-0806-2. PubMed PMID: carecchio\_2017.
27. Fryxell KJ, Moon WJ. CpG mutation rates in the human genome are highly dependent on local GC content. *Mol Biol Evol.* 2005;22(3):650-8. Epub 2004/11/10. doi: 10.1093/molbev/msi043. PubMed PMID: 15537806.
28. Jang HS, Shin WJ, Lee JE, Do JT. CpG and Non-CpG Methylation in Epigenetic Gene Regulation and Brain Function. *Genes (Basel).* 2017;8(6). Epub 2017/05/23. doi: 10.3390/genes8060148. PubMed PMID: 28545252; PubMed Central PMCID: PMC5485512.
29. Messé LA, Aronoff J, Wilson JP. Motivation as a mediator of the mechanisms underlying role assignments in small groups. *J Pers Soc Psychol.* 1972;24(1):84-90. PubMed PMID: 5079558.
30. Kong A, Frigge ML, Masson G, Besenbacher S, Sulem P, Magnusson G, et al. Rate of de novo mutations and the importance of father's age to disease risk. *Nature.* 2012;488(7412):471-5. doi: 10.1038/nature11396. PubMed PMID: 22914163; PubMed Central PMCID: PMC3548427.
31. Panchin AY, Makeev VJ, Medvedeva YA. Preservation of methylated CpG dinucleotides in

human CpG islands. *Biol Direct*. 2016;11(1):11. Epub 2016/03/22. doi: 10.1186/s13062-016-0113-x. PubMed PMID: 27005429; PubMed Central PMCID: PMC4804638.

32. Urdinguio RG, Sanchez-Mut JV, Esteller M. Epigenetic mechanisms in neurological diseases: genes, syndromes, and therapies. *Lancet Neurol*. 2009;8(11):1056-72. doi: 10.1016/S1474-4422(09)70262-5. PubMed PMID: 19833297.

33. Schorling DC, Tobias D, Christina E, Katrin H, Rudolf K, Daniel E, et al. Expanding phenotype of de novo mutations in GNAO1 : four new cases and review of literature. *Neuropediatrics*. 2017;48(5):371-7. doi: 10.1055/s-0037-1603977. PubMed PMID: schorling\_2017.

34. Feng H, Suad K, R. NR, Christos S. A mechanistic review on GNAO1 -associated movement disorder. *Neurobiol Dis*. 2018;116:131-41. doi: 10.1016/j.nbd.2018.05.005. PubMed PMID: feng\_2018.

35. Gazi L, Nickolls SA, Strange PG. Functional coupling of the human dopamine D2 receptor with G alpha i1, G alpha i2, G alpha i3 and G alpha o G proteins: evidence for agonist regulation of G protein selectivity. *Br J Pharmacol*. 2003;138(5):775-86. doi: 10.1038/sj.bjp.0705116. PubMed PMID: 12642378; PubMed Central PMCID: PMC1573727.

36. Zhang Q, Pacheco MA, Doupnik CA. Gating properties of GIRK channels activated by Galpha(o)- and Galpha(i)-coupled muscarinic m2 receptors in *Xenopus* oocytes: the role of receptor precoupling in RGS modulation. *J Physiol*. 2002;545(2):355-73. PubMed PMID: 12456817; PubMed Central PMCID: PMC2290703.

37. Li Q, Lau A, Morris TJ, Guo L, Fordyce CB, Stanley EF. A syntaxin 1, Galpha(o), and N-type calcium channel complex at a presynaptic nerve terminal: analysis by quantitative immunocolocalization. *J Neurosci*. 2004;24(16):4070-81. doi: 10.1523/JNEUROSCI.0346-04.2004. PubMed PMID: 15102922.

38. Strittmatter SM, Fishman MC, Zhu XP. Activated mutants of the alpha subunit of G(o) promote an increased number of neurites per cell. *J Neurosci*. 1994;14(4):2327-38. PubMed PMID: 8158271.

39. Bromberg KD, Iyengar R, He JC. Regulation of neurite outgrowth by G(i/o) signaling pathways. *Front Biosci*. 2008;13:4544-57. Epub 2008/05/01. PubMed PMID: 18508528; PubMed Central PMCID: PMC3068557.

40. Lan KL, Sarvazyan NA, Taussig R, Mackenzie RG, DiBello PR, Dohlman HG, et al. A point mutation in Galphao and Galphai1 blocks interaction with regulator of G protein signaling proteins. *J Biol Chem*. 1998;273(21):12794-7. PubMed PMID: 9582306.

41. Kehrl JM, Sahaya K, Dalton HM, Charbeneau RA, Kohut KT, Gilbert K, et al. Gain-of-function mutation in Gnao1: a murine model of epileptiform encephalopathy (EIEE17)? *Mamm Genome*. 2014;25(5-6):202-10. Epub 2014/04/05. doi: 10.1007/s00335-014-9509-z. PubMed PMID:

24700286; PubMed Central PMCID: PMC4042023.

42. Arya R, Christine S, L. GD, L. LJ, D. HK. GNAO1 -associated epileptic encephalopathy and movement disorders: c. 607G>A variant represents a probable mutation hotspot with a distinct phenotype. *Epileptic Disord.* 2017;19(1):67-75. doi: 10.1684/epd.2017.0888. PubMed PMID: arya\_2017.
43. Xiong J, Jing P, Hao-Lin D, Chen C, Xiao-Le W, Shi-Meng C, et al. Recurrent convulsion and pulmonary infection complicated by psychomotor retardation in an infant . *Zhongguo Dang Dai Er Ke Za Zhi.* 2018;20(2):154-7. doi: 10.7499/j.issn.1008-8830.2018.02.014. PubMed PMID: xiong\_2018.
44. Qin W, Dion SL, Kutny PM, Zhang Y, Cheng AW, Jillette NL, et al. Efficient CRISPR/Cas9-Mediated Genome Editing in Mice by Zygote Electroporation of Nuclease. *Genetics.* 2015;200(2):423-30. Epub 2015/03/27. doi: 10.1534/genetics.115.176594. PubMed PMID: 25819794; PubMed Central PMCID: PMC4492369.
45. Doench JG, Fusi N, Sullender M, Hegde M, Vaimberg EW, Donovan KF, et al. Optimized sgRNA design to maximize activity and minimize off-target effects of CRISPR-Cas9. *Nat Biotechnol.* 2016;34(2):184-91. Epub 2016/01/18. doi: 10.1038/nbt.3437. PubMed PMID: 26780180; PubMed Central PMCID: PMC4744125.
46. Haeussler M, Schönig K, Eckert H, Eschstruth A, Mianné J, Renaud JB, et al. Evaluation of off-target and on-target scoring algorithms and integration into the guide RNA selection tool CRISPOR. *Genome Biol.* 2016;17(1):148. Epub 2016/07/05. doi: 10.1186/s13059-016-1012-2. PubMed PMID: 27380939; PubMed Central PMCID: PMC4934014.
47. Hsu PD, Scott DA, Weinstein JA, Ran FA, Konermann S, Agarwala V, et al. DNA targeting specificity of RNA-guided Cas9 nucleases. *Nat Biotechnol.* 2013;31(9):827-32. Epub 2013/07/21. doi: 10.1038/nbt.2647. PubMed PMID: 23873081; PubMed Central PMCID: PMC3969858.
48. Iyer V, Boroviak K, Thomas M, Doe B, Riva L, Ryder E, et al. No unexpected CRISPR-Cas9 off-target activity revealed by trio sequencing of gene-edited mice. *PLoS Genet.* 2018;14(7):e1007503. Epub 2018/07/09. doi: 10.1371/journal.pgen.1007503. PubMed PMID: 29985941; PubMed Central PMCID: PMC6057650.
49. Truett GE, Heeger P, Mynatt RL, Truett AA, Walker JA, Warman ML. Preparation of PCR-quality mouse genomic DNA with hot sodium hydroxide and tris (HotSHOT). *Biotechniques.* 2000;29(1):52, 4. doi: 10.2144/00291bm09. PubMed PMID: 10907076.
50. Hirata H, Takahashi A, Shimoda Y, Koide T. Caspr3-Deficient Mice Exhibit Low Motor Learning during the Early Phase of the Accelerated Rotarod Task. *PLoS One.* 2016;11(1):e0147887. Epub 2016/01/25. doi: 10.1371/journal.pone.0147887. PubMed PMID: 26807827; PubMed Central PMCID: PMC4726695.

51. Deacon RM, Nielsen S, Leung S, Rivas G, Cubitt T, Monds LA, et al. Alprazolam use and related harm among opioid substitution treatment clients - 12 months follow up after regulatory rescheduling. *Int J Drug Policy*. 2016;36:104-11. Epub 2016/06/11. doi: 10.1016/j.drugpo.2016.06.006. PubMed PMID: 27453147.
52. Hansen ST, Pulst SM. Response to ethanol induced ataxia between C57BL/6J and 129X1/SvJ mouse strains using a treadmill based assay. *Pharmacol Biochem Behav*. 2013;103(3):582-8. Epub 2012/10/24. doi: 10.1016/j.pbb.2012.10.010. PubMed PMID: 23103202; PubMed Central PMCID: PMC4900535.
53. Franco-Pons N, Torrente M, Colomina MT, Vilella E. Behavioral deficits in the cuprizone-induced murine model of demyelination/remyelination. *Toxicol Lett*. 2007;169(3):205-13. Epub 2007/02/02. doi: 10.1016/j.toxlet.2007.01.010. PubMed PMID: 17317045.
54. DiBello PR, Garrison TR, Apanovitch DM, Hoffman G, Shuey DJ, Mason K, et al. Selective uncoupling of RGS action by a single point mutation in the G protein alpha-subunit. *J Biol Chem*. 1998;273(10):5780-4. PubMed PMID: 9488712.
55. Grecksch G, Becker A, Schroeder H, Kraus J, Loh H, Höllt V. Accelerated kindling development in mu-opioid receptor deficient mice. *Naunyn Schmiedebergs Arch Pharmacol*. 2004;369(3):287-93. Epub 2004/02/12. doi: 10.1007/s00210-004-0870-4. PubMed PMID: 14963640.
56. Wilczynski GM, Konopacki FA, Wilczek E, Lasiecka Z, Gorlewicz A, Michaluk P, et al. Important role of matrix metalloproteinase 9 in epileptogenesis. *J Cell Biol*. 2008;180(5):1021-35. doi: 10.1083/jcb.200708213. PubMed PMID: 18332222; PubMed Central PMCID: PMC2265409.
57. Ahmad MF, Ferland D, Ayala-Lopez N, Contreras GA, Darios E, Thompson J, et al. Perivascular Adipocytes Store Norepinephrine by Vesicular Transport. *Arterioscler Thromb Vasc Biol*. 2019;39(2):188-99. doi: 10.1161/ATVBAHA.118.311720. PubMed PMID: 30567483; PubMed Central PMCID: PMC6344267.
58. Donzanti BA, Yamamoto BK. An improved and rapid HPLC-EC method for the isocratic separation of amino acid neurotransmitters from brain tissue and microdialysis perfusates. *Life Sci*. 1988;43(11):913-22. PubMed PMID: 2901021.
59. Gillies GE, Murray HE, Dexter D, McArthur S. Sex dimorphisms in the neuroprotective effects of estrogen in an animal model of Parkinson's disease. *Pharmacol Biochem Behav*. 2004;78(3):513-22. doi: 10.1016/j.pbb.2004.04.022. PubMed PMID: 15251260.
60. J. BTU, DesRoches CL, Wilson D, Chau V, Nakagawa T, Yamasaki M, et al. Prospective cohort study for identification of underlying genetic causes in neonatal encephalopathy using whole-exome sequencing. *Genet Med*. 2018;20(5):486-94. Epub 2017/08/17. doi:

10.1038/gim.2017.129. PubMed PMID: 28817111.

61. Danti FR, Serena G, Marta R, Martino M, J. CK, Lucy RF, et al. GNAO1 encephalopathy: Broadening the phenotype and evaluating treatment and outcome. *Neurol Genet.* 2017;3(2):e143. doi: 10.1212/NXG.000000000000143. PubMed PMID: danti\_2017.

62. Menke LA, Marc E, Mariel A, J. OVJ, Frank B, M. CJ. Recurrent GNAO1 mutations associated with developmental delay and a movement disorder. *J Child Neurol.* 2016;31(14):1598-601. doi: 10.1177/0883073816666474. PubMed PMID: menke\_2016.

63. Honey CM, K. MA, Maja T-G, M. vKCD, Gabriella H, Adi S. GNAO1 Mutation-Induced Pediatric Dystonic Storm Rescue With Pallidal Deep Brain Stimulation. *J Child Neurol.* 2018;33(6):413-6. doi: 10.1177/0883073818756134. PubMed PMID: honey\_2018.

64. Waak M, S. MS, David C, Kate S, Lisa C, Peter S, et al. GNAO1 -related movement disorder with life-threatening exacerbations: movement phenomenology and response to DBS . *J Neurol Neurosurg Psychiatr.* 2018;89(2):221-2. doi: 10.1136/jnnp-2017-315653. PubMed PMID: waak\_2018.

65. Sanem Y, Tuncer T, Serdar C, Sarenur G, Hasan T, Gul S. Excellent response to deep brain stimulation in a young girl with GNAO1 -related progressive choreoathetosis. *Childs Nerv Syst.* 2016;32(9):1567-8. doi: 10.1007/s00381-016-3139-6. PubMed PMID: yilmaz\_2016.

66. Consortium E-R, Project EPG, Consortium EK. De novo mutations in synaptic transmission genes including DNM1 cause epileptic encephalopathies. *Am J Hum Genet.* 2014;95(4):360-70. doi: 10.1016/j.ajhg.2014.08.013. PubMed PMID: euroepinomicsresconsortium\_2014.

67. Zhu X, Petrovski S, Xie P, Ruzzo EK, Lu YF, McSweeney KM, et al. Whole-exome sequencing in undiagnosed genetic diseases: interpreting 119 trios. *Genet Med.* 2015;17(10):774-81. Epub 2015/01/15. doi: 10.1038/gim.2014.191. PubMed PMID: 25590979; PubMed Central PMCID: PMC4791490.

68. Tatem KS, Quinn JL, Phadke A, Yu Q, Gordish-Dressman H, Nagaraju K. Behavioral and locomotor measurements using an open field activity monitoring system for skeletal muscle diseases. *J Vis Exp.* 2014;(91):51785. Epub 2014/09/29. doi: 10.3791/51785. PubMed PMID: 25286313; PubMed Central PMCID: PMC4672952.

69. Parr T, Friston KJ. Working memory, attention, and salience in active inference. *Sci Rep.* 2017;7(1):14678. Epub 2017/11/07. doi: 10.1038/s41598-017-15249-0. PubMed PMID: 29116142; PubMed Central PMCID: PMC5676961.

70. Stroobants S, Gantois I, Pooters T, D'Hooge R. Increased gait variability in mice with small cerebellar cortex lesions and normal rotarod performance. *Behav Brain Res.* 2013;241:32-7. Epub 2012/12/03. doi: 10.1016/j.bbr.2012.11.034. PubMed PMID: 23219967.

71. Song CH, Fan X, Exeter CJ, Hess EJ, Jinnah HA. Functional analysis of dopaminergic systems in a DYT1 knock-in mouse model of dystonia. *Neurobiol Dis.* 2012;48(1):66-78. Epub 2012/05/31. doi: 10.1016/j.nbd.2012.05.009. PubMed PMID: 22659308; PubMed Central PMCID: PMC3498628.
72. Dhir A. Pentylentetrazol (PTZ) kindling model of epilepsy. *Curr Protoc Neurosci.* 2012;Chapter 9:Unit9.37. doi: 10.1002/0471142301.ns0937s58. PubMed PMID: 23042503.
73. Pelosi A, Menardy F, Popa D, Girault JA, Hervé D. Heterozygous Gnal Mice Are a Novel Animal Model with Which to Study Dystonia Pathophysiology. *J Neurosci.* 2017;37(26):6253-67. Epub 2017/05/25. doi: 10.1523/JNEUROSCI.1529-16.2017. PubMed PMID: 28546310.
74. Korchounov AM. Role of D1 and D2 receptors in the regulation of voluntary movements. *Bull Exp Biol Med.* 2008;146(1):14-7. PubMed PMID: 19145338.
75. Raike RS, Jinnah HA, Hess EJ. Animal models of generalized dystonia. *NeuroRx.* 2005;2(3):504-12. doi: 10.1602/neurorx.2.3.504. PubMed PMID: 16389314; PubMed Central PMCID: PMC1144494.
76. Oleas J, Yokoi F, DeAndrade MP, Pisani A, Li Y. Engineering animal models of dystonia. *Mov Disord.* 2013;28(7):990-1000. doi: 10.1002/mds.25583. PubMed PMID: 23893455; PubMed Central PMCID: PMC3800691.
77. Wettshureck N, Offermanns S. Mammalian G proteins and their cell type specific functions. *Physiol Rev.* 2005;85(4):1159-204. doi: 10.1152/physrev.00003.2005. PubMed PMID: 16183910.
78. Solis GP, Katanaev VL. Gao (*Oncotarget.* 2018;9(35):23846-7. Epub 2017/10/25. doi: 10.18632/oncotarget.22067. PubMed PMID: 29844856; PubMed Central PMCID: PMC5963625.
79. Smith KM, Dahodwala N. Sex differences in Parkinson's disease and other movement disorders. *Exp Neurol.* 2014;259:44-56. Epub 2014/03/28. doi: 10.1016/j.expneurol.2014.03.010. PubMed PMID: 24681088.
80. Revankar CM, Cimino DF, Sklar LA, Arterburn JB, Prossnitz ER. A transmembrane intracellular estrogen receptor mediates rapid cell signaling. *Science.* 2005;307(5715):1625-30. Epub 2005/02/10. doi: 10.1126/science.1106943. PubMed PMID: 15705806.
81. Wooten GF, Currie LJ, Bovbjerg VE, Lee JK, Patrie J. Are men at greater risk for Parkinson's disease than women? *J Neurol Neurosurg Psychiatry.* 2004;75(4):637-9. PubMed PMID: 15026515; PubMed Central PMCID: PMC1739032.
82. Kompoliti K. Estrogen and movement disorders. *Clin Neuropharmacol.* 1999;22(6):318-26.

PubMed PMID: 10626091.

83. Madalan A, Yang X, Ferris J, Zhang S, Roman G. G(o) activation is required for both appetitive and aversive memory acquisition in *Drosophila*. *Learn Mem.* 2012;19(1):26-34. Epub 2011/12/21. doi: 10.1101/lm.024802.111. PubMed PMID: 22190729.

84. Schutsky K, Ouyang M, Thomas SA. Xamoterol impairs hippocampus-dependent emotional memory retrieval via Gi/o-coupled  $\beta$ 2-adrenergic signaling. *Learn Mem.* 2011;18(9):598-604. Epub 2011/08/30. doi: 10.1101/lm.2302811. PubMed PMID: 21878527; PubMed Central PMCID: PMC3166789.

85. Fitzgerald PJ. Is elevated norepinephrine an etiological factor in some cases of epilepsy? *Seizure.* 2010;19(6):311-8. Epub 2010/05/20. doi: 10.1016/j.seizure.2010.04.011. PubMed PMID: 20493725.

86. Consortium G. The Genotype-Tissue Expression (GTEx) project. *Nat Genet.* 2013;45(6):580-5. doi: 10.1038/ng.2653. PubMed PMID: 23715323; PubMed Central PMCID: PMC4010069.

87. Nakamura K, Hirofumi K, Tenpei A, Masaaki S, Mitsuhiro K, Hideki H, et al. De Novo mutations in GNAO1, encoding a G $\alpha$  subunit of heterotrimeric G proteins, cause epileptic encephalopathy. *Am J Hum Genet.* 2013;93(3):496-505. doi: 10.1016/j.ajhg.2013.07.014. PubMed PMID: nakamura\_2013.

88. Blumkin L, Tally L-S, Ana W, Hilla B-P, Ayelet Z, Keren Y, et al. Multiple Causes of Pediatric Early Onset Chorea-Clinical and Genetic Approach. *Neuropediatrics.* 2018;49(4):246-55. doi: 10.1055/s-0038-1645884. PubMed PMID: blumkin\_2018.

89. Sakamoto S, Yukifumi M, Ryoko F, Noriko M, Hiroshi S, Akihiko M, et al. A case of severe movement disorder with GNAO1 mutation responsive to topiramate. *Brain Dev.* 2017;39(5):439-43. doi: 10.1016/j.braindev.2016.11.009. PubMed PMID: sakamoto\_2017.

90. Rim JH, Hee KS, Sik HI, Sung KS, Jieun K, Woo KH, et al. Efficient strategy for the molecular diagnosis of intractable early-onset epilepsy using targeted gene sequencing. *BMC Med Genomics.* 2018;11(1):6. doi: 10.1186/s12920-018-0320-7. PubMed PMID: rim\_2018.

91. Marecos C, S. D, I. A, E. C, A. M. GNAO1 : a new gene to consider on early-onset childhood dystonia . *Rev Neurol.* 2018;66(9):321-2. PubMed PMID: marecos\_2018.

92. Koy A, Sebahattin C, Victoria G, Kerstin B, Thomas R, Christophe M, et al. Deep brain stimulation is effective in pediatric patients with GNAO1 associated severe hyperkinesia. *J Neurol Sci.* 2018;391:31-9. doi: 10.1016/j.jns.2018.05.018. PubMed PMID: koy\_2018.

93. Dhamija R, W. MJ, B. SB, P. GH. GNAO1 -Associated Movement Disorder. *Mov Disord Clin*

Pract. 2016;3(6):615-7. doi: 10.1002/mdc3.12344. PubMed PMID: dhamija\_2016.

94. Consortium. De novo mutations in SLC1A2 and CACNA1A are important causes of epileptic encephalopathies. *Am J Hum Genet.* 2016;99(2):287-98. doi: 10.1016/j.ajhg.2016.06.003. PubMed PMID: epi4kconsortium\_2016.

95. Talvik I, S. MoR, Merilin V, Ulvi V, Hg LL, A. DH, et al. Clinical phenotype of de novo GNAO1 mutation: case report and review of literature. *Child Neurology Open.* 2015;2(2):2329048X15583717. doi: 10.1177/ 2329048X15583717. PubMed PMID: talvik\_2015.

96. Consortium, Epilepsy Phenome/Genome Project and C. De novo mutations in synaptic transmission genes including DNMT1 cause epileptic encephalopathies. *Am J Hum Genet.* 2014;95(4):360-70. doi: 10.1016/j.ajhg.2014.08.013. PubMed PMID: euroepinomicsresconsortium\_2014.

97. Gerald B, Keri R, Newell B, Szabolcs S, L. SA, Chris B, et al. Neonatal epileptic encephalopathy caused by de novo GNAO1 mutation misdiagnosed as atypical Rett syndrome: Cautions in interpretation of genomic test results. *Semin Pediatr Neurol.* 2018;26:28-32. doi: 10.1016/j.spen.2017.08.008. PubMed PMID: gerald\_2018.

98. Bruun TUJa. Prospective cohort study for identification of underlying genetic causes in neonatal encephalopathy using whole-exome sequencing. *Genet Med.* 2018;20(5):486-94. doi: 10.1038/gim.2017.129. PubMed PMID: bruun\_2018.

99. Takezawa Y, Atsuo K, Kazuhiro H, Tetsuya N, Yurika N-U, Takehiko I, et al. Genomic analysis identifies masqueraders of full-term cerebral palsy. *Ann Clin Transl Neurol.* 2018;5(5):538-51. doi: 10.1002/acn3.551. PubMed PMID: takezawa\_2018.

100. Okumura A, Koichi M, Mami S, Hirokazu K, Atsushi I, Shingo N, et al. A patient with a GNAO1 mutation with decreased spontaneous movements, hypotonia, and dystonic features. *Brain Dev.* 2018;40(10):926-30. doi: 10.1016/j.braindev.2018.06.005. PubMed PMID: okumura\_2018.

101. Consortium EK. De novo mutations in SLC1A2 and CACNA1A are important causes of epileptic encephalopathies. *Am J Hum Genet.* 2016;99(2):287-98. doi: 10.1016/j.ajhg.2016.06.003. PubMed PMID: epi4kconsortium\_2016.

102. Feather-Schussler DN, Ferguson TS. A Battery of Motor Tests in a Neonatal Mouse Model of Cerebral Palsy. *J Vis Exp.* 2016;(117). Epub 2016/11/03. doi: 10.3791/53569. PubMed PMID: 27842358; PubMed Central PMCID: PMC5226120.

103. Feng H, L. LC, Y. DE, Huirong X, R. LJ, R. NR. Mouse models of GNAO1 -associated movement disorder: Allele- and sex-specific differences in phenotypes. *PLoS ONE.* 2019;14(1):e0211066. doi: 10.1371/journal.pone.0211066. PubMed PMID: feng\_2019.

104. Seibenhener ML, Wooten MC. Use of the Open Field Maze to measure locomotor and anxiety-like behavior in mice. *J Vis Exp.* 2015;(96):e52434. Epub 2015/02/06. doi: 10.3791/52434. PubMed PMID: 25742564; PubMed Central PMCID: PMC4354627.
105. Carvalho RC, Silva RH, Abílio VC, Barbosa PN, Frussa-Filho R. Antidyskinetic effects of risperidone on animal models of tardive dyskinesia in mice. *Brain Res Bull.* 2003;60(1-2):115-24. PubMed PMID: 12725899.
106. Neve KA, Seamans JK, Trantham-Davidson H. Dopamine receptor signaling. *J Recept Signal Transduct Res.* 2004;24(3):165-205. PubMed PMID: 15521361.
107. Alkufri F, Shaag A, Abu-Libdeh B, Elpeleg O. Deleterious mutation in GPR88 is associated with chorea, speech delay, and learning disabilities. *Neurol Genet.* 2016;2(3):e64. Epub 2016/03/09. doi: 10.1212/NXG.0000000000000064. PubMed PMID: 27123486; PubMed Central PMCID: PMC4830197.
108. Eunson LH, Graves TD, Hanna MG. New calcium channel mutations predict aberrant RNA splicing in episodic ataxia. *Neurology.* 2005;65(2):308-10. doi: 10.1212/01.wnl.0000169020.82223.dd. PubMed PMID: 16043807.
109. Betke KM, Wells CA, Hamm HE. GPCR mediated regulation of synaptic transmission. *Prog Neurobiol.* 2012;96(3):304-21. Epub 2012/01/28. doi: 10.1016/j.pneurobio.2012.01.009. PubMed PMID: 22307060; PubMed Central PMCID: PMC3319362.